Outlining a balance-point model of homeostasis in the small intestine of broiler chickens

By

Sara Elizabeth Cloft

Dissertation submitted to the faculty of the Virginia Polytechnic Institute and State University in partial fulfillment of the requirements for the degree of

Doctor of Philosophy

In
Animal and Poultry Sciences

Eric A. Wong, Chair

Michael E. Persia

John J. Maurer

Katarzyna B. Miska

June 10th 2022

Blacksburg, VA

Keywords: Homeostasis, Small intestine, Broiler, In situ hybridization, quantitative PCR

Copyright 2022, Sara Cloft

Outlining a balance-point model of homeostasis in the small intestine of broiler chickens

Sara Cloft

GENERAL AUDIENCE ABSTRACT

In healthy birds, the small intestine absorbs nutrients while preventing the free passage of microbes or toxic chemicals into the body. The two functions: absorption and barrier exclusion seem contradictory, but a balance is struck to ensure both functions continue. This balance-point, homeostasis, persists until an event disturbs it. Once disturbed the balance-point is changed and the intestine is unable to maintain both functions, until a new balance is found following recovery. The objective of the dissertation is to better understand intestinal homeostasis, through four different research projects. Experiment 1 characterized the intestinal cell population changes in broiler chickens during Runting Stunting Syndrome, a viral infection. The major finding of this chapter was that a stem cell gene, that is normally robustly expressed was not expressed in some groups of infected chicks but not all. Experiment 2 investigated the intestinal response of broiler chickens to *Eimeria acervulina*, an intestinal parasitic infection. *Eimeria*, which infects intestinal enterocytes, caused a decrease in defensive genes during the peak of infection. Then after the peak the intestine began to recover, as indicated by increased cell proliferation. Experiment 3 profiled changes in the expression patterns of stem cell and proliferation genes in the small intestine during the last days before hatch and the first week post-hatch. Pre-hatch stem and proliferative gene expression occurred in the crypt and villus, but became restricted to the crypt early during the post-hatch period. Experiment 4 assessed the effect of feeding probiotics to embryos before hatching on

intestinal gene expression. Embryos fed probiotics had increased Mucin-2 and Peptide Transporter 1 gene expression in the last segment of the intestine, the ileum compared to non-fed embryos 48 hours after feeding. Additionally, treatments fed saline also showed increased gene expression, though to a lesser extent. Together these projects illustrate various disturbances to intestinal homeostasis and how intestinal cells change and respond during the disturbance and recovery periods.

Outlining a balance-point model of homeostasis in the small intestine of broiler chickens

Sara Cloft

TECHNICAL ABSTRACT

Since the removal of in feed antibiotics in the past few years commercial poultry production is especially sensitive to the health of the small intestine. Healthy small intestines balance nutrient absorption and defensive barrier functions to ensure the chicken is able to meet the whole-body nutritional needs and is able to help prevent internalization of pathogens or potentially toxic components. This balance can only be maintained under stable conditions. When a disturbance event occurs the intestine imbalances until a new, and less efficient, balance can be achieved. The objective of this dissertation is to propose a novel model to understanding intestinal homeostasis in the face of various disturbance events. Chapter 2 investigated the effects of Runting Stunting Syndrome on broiler chickens in four different groups of chicks displaying clinical symptoms. The major finding in this study was that in two of the four groups the expression of stem cell gene Olfactomedin 4 was absent from the crypt though other functional genes were found to still be expressed there. Chapter 3 characterized intestinal gene expression following a single challenge of *Eimeria acervulina* in broiler chickens. During *Eimeria* infection gene expression of multiple host defense peptide genes were decreased compared to uninfected chickens. Further, *Eimeria* infected chickens increased cell proliferation within the crypt and post-peak infection showed signs of intestinal recovery. Additionally, chapter 3 developed a novel method for visualizing *Eimeria* as it infects the intestine. In chapters 4 and 5 cell type population changes during the peri-

hatch intestinal maturation process were evaluated. Peri-hatch intestinal maturation is critical for the successful transition from embryonic to post-hatch life. Chapter 4 profiled changes in proliferative cells and gene expression of various stem cell marker genes during the peri-hatch period: the last three days of embryogenesis and the first week post-hatch. The stem cell marker gene Leucine Rich Repeat Containing G Protein-Coupled Receptor 5 (Lgr5) decreased during the post-hatch period while Olfactomedin 4 increased post-hatch. Both stem cell genes were expressed within the intestinal crypt, though prior to hatch Lgr5 was expressed in the lamina propria and villi as well. Additionally, the marker of proliferation Ki67 gene was expressed in cells throughout the intestine prior to hatch but became restricted to the crypts and along the center of the villi. Chapter 5 assessed the effect of providing probiotics to late term embryos via *in ovo* feeding (IOF). The effects of IOF were primarily observed on embryonic day 20 (e20), roughly 48 hours after IOF. On e20 the embryos *in ovo* fed probiotics in saline had increased expression in the ileum of Peptide Transporter 1 (PepT1) a marker gene for enterocytes and Mucin-2 (Muc2) a marker gene for goblet cells compared to non-injected control embryos. Also, on e20 the embryos *in ovo* fed saline only had numerically increased PepT1 and Muc2 compared to non-injected control embryos. The difference in responses between the probiotic and saline fed embryos on e20 suggests different routes of stimulation. These investigations illustrate various possible scenarios and means of investigating intestinal homeostasis during disturbance events.

ACKNOWLEDGEMENTS

This dissertation is the result of the past four years of work during my PhD. I have had the pleasure to work with many collaborators and have the assistance of many undergraduate and graduate students during this time. In particular I would like to acknowledge the contributions of Sydney Kinstler, Kaitlyn Reno, Maeve Davis, Johanna Heller, Emily Meluch, and Meiting Jia for their assistance with the studies and lab work. I would also like to thank the Persia and Dalloul research lab members at Virginia Tech and UGA for their many discussions and brainstorming sessions they participated in.

I am forever indebted to Dr. Eric Wong, my committee chair and advisor for his confidence in me and the inspiration he regularly bestows. I would also like to acknowledge his support in all of my extracurricular endeavors and hare-brained ideas that have been a crucial part of my PhD program. I am also very sorry for how much glassware I broke.

Additionally, I would like to thank my committee Dr. Mike Persia, Dr. John Maurer, and Dr. Kate Miska for the time they have put in over the past four years for me through committee meetings, reading documents, and answering questions. I would also like to thank all of them for challenging me and pushing me to develop into the Poultry scientist I am today. I look forward to continuing to make you all proud through the rest of my career.

And finally, the Balance-Point model would not be complete without Dominic my fiancé. Your patience and willingness to debate this model with me over the past years has been essential and a joy, even when we both said things we regret. Without your support and love I would not have finished.

Table of Contents

List of Abbreviations x

List of Figures xii

List of Tables xiv

1. Introduction and Literature Review 1

Intestinal homeostasis 2

Establishment of the intestine 9

Disruptions of intestinal homeostasis 10

Disturbances faced in commercial poultry production 12

Objectives 15

References 17

Figure Captions 24

2. Runting Stunting Syndrome in broiler chickens is associated with altered intestinal stem cell morphology and gene expression 29

Introduction 30

Materials and Methods 32

Results 37

Discussion 40

References 48

Figure Captions 55

3. A temporal investigation of genes associated with intestinal homeostasis in broiler chickens following a single infection with *Eimeria acervulina* 67

Introduction 68

Materials and Methods 70

Results 75

Discussion 79

References 86

Figure Captions 92

4. Profiling intestinal proliferative cells in the small intestine of broiler chickens via in situ hybridization during the peri-hatch period 104

Introduction 104

Materials and Methods 106

Results 109

Discussion 111

References 115

Figure Captions 119

5. In ovo feeding of probiotics alters gene expression patterns in the small intestine during the first week post-hatch in broiler chicks 126

Introduction 127

Materials and Methods 129

Results 132

Discussion 138

References 144

Figure Captions 148

6. Discussion and Conclusions 160

Defining the Balance-Point Model 160

Investigating the balance point model with novel and expected disturbances 164

Limitations and opportunities of the proposed model 169

References 172

Figure Captions 173

List of Abbreviations

Ascl2- Achaete-scute complex homolog 2- stem cell master regulator gene

Atoh1- Atonal homolog 1 (Drosophila)- Notch signaling gene, associated with secretory lineage cells

AvBDs- Avian Beta defensins- class of host defense peptides

BW- Body weight

Col3a1- Collagen Type III Alpha 1 Chain - collagen gene expressed in the intestine

CD- crypt depth

d- day (days) post hatch

DAMPS- danger associated molecular patterns- recognize surface antigens from microorganisms

DLL1- Delta Like Canonical Notch Ligand 1- Notch signaling receptor

dpi- day post infection

Ea-SAG- Eimeria acervulina sporozoite surface antigen- parasite life stage gene

e17- embryonic day 17- number of days of incubation

GALT- Gut Associated Lymphoid Tissue- the innate immune system within the intestine

Hes1- Hes Family BHLH Transcription Factor 1- Notch signaling factor in absorptive lineage cells

IgA- Immunoglobulin A- antibody subtype present within the mucosal surfaces of the intestine

IOF- in ovo feeding- injection of solution to embryonic amnion fluid prior to hatch

ISH- in situ hybridization- mRNA visualization methodology

Ki67- marker of proliferation Ki67- gene expressed in proliferating cells, marks stem and precursor cells that are still capable of dividing

LEAP2- Liver enriched antimicrobial peptide 2- host defense peptide

Lgr5- Leucine Rich Repeat Containing G Protein-Coupled Receptor 5- stem cell marker gene

MAS- Malabsorption Syndromes- diseases characterized by diarrhea, decreased feed intake, and dehydration

Muc2- Mucin 2- secreted mucus layer protein, goblet cell marker gene

Notch 1- Neurogenic locus notch homolog protein 1- gene associated with cell differentiation

Olfm4- Olfactomedin 4- stem cell marker gene

PepT1- Peptide Transporter 1- di and tri-peptide transporter, enterocyte marker gene

qPCR or RT-qPCR- real-time quantitative polymerase chain reaction- mRNA quantitative method

RSS- Runting Stunting Syndrome- viral malabsorption disease of young chicks, unknown causative agent

RPLP0 & RPLP1 & RPL4- Ribosomal protein large subunit P0 & P1 & 4- Reference genes used for qPCR analysis

SGLT1- sodium glucose cotransporter 1- glucose transporter

USWL- unstirred water layer- mucus layer overlying the lumen of the intestine

VH- Villus Height

Wnt3a- Wnt family member 3A- gene associated with maintaining the stem cell niche in the intestinal crypt

List of Figures

Figure 1-1. Chicken small intestine model 26

Figure 1-2. The intestinal enterocyte 27

Figure 1-3. A simplified diagram of intestinal cell differentiation in the intestine 28

Figure 2-1. Cells expressing Olfm4, proliferation marker Ki67, PepT1, SGLT1, and Muc2 mRNA in Control and RSS chicks 62

Figure 2-2. Cells expressing Olfm4, proliferation marker Ki67, Muc2, and SGLT1 mRNA in cystic and normal crypts of RSS chicks 63

Figure 2-3. Cells expressing Olfm4, PepT1, and Muc2 mRNA in Control and RSS chicks challenged with astrovirus 64

Figure 2-4. Cells expressing Olfm4, proliferation marker Ki67, PepT1, SGLT1, and Muc2 mRNA in chicks displaying clinical signs of RSS 65

Figure 2-5. Cells expressing Olfm4, PepT1, and Muc2 mRNA in chicks from farms in Brazil that showed clinical signs of RSS 66

Figure 3-1. Plasma carotenoids concentration in uninfected and *Eimeria acervulina* infected chickens 98

Figure 3-2. Crypt elongation following infection with *Eimeria acervulina* 99

Figure 3-3. Avian beta defensins (AvBD), Liver enriched antimicrobial peptide 2 (LEAP2), and Mucin 2 (Muc2) mRNA profiles following infection with *Eimeria acervulina* 100

Figure 3-4. Collagen 3a1 (Col3a1), Marker of proliferation Ki67, Olfactomedin 4 (Olfm4) and Notch 1 mRNA profiles following infection with *Eimeria acervulina* 101

Figure 3-5. In situ hybridization analysis of *Eimeria acervulina* sporozoite surface antigen (Ea-SAG) mRNA following infection with *E. acervulina*.....102

Figure 3-6. In situ hybridization analysis of *Eimeria acervulina* sporozoite surface antigen (Ea-SAG) and Mucin 2 (Muc2) mRNA following infection with *E. acervulina* 103

Figure 4-1. Relative mRNA abundance of Olfm4, Lgr5, and Ki67 mRNA in the small intestine during the peri-hatch period 122

Figure 4-2. Expression of Olfm4 mRNA in the intestine from late embryogenesis to early post hatch using in situ hybridization 123

Figure 4-3. Expression of Lgr5 mRNA in the intestine from late embryogenesis to early post hatch using in situ hybridization 124

Figure 4-4. Expression of Ki67 mRNA in the intestine from late embryogenesis to early post hatch using in situ hybridization 126

Figure 5-1. mRNA abundance of stem cell related genes: Expression of Achaete-scute complex homolog 2 (Acsl2), Leucine rich repeat containing G protein-coupled receptor 5 (Lgr5), Olfactomedin 4 (Olfm4), and Wnt family member 3a (Wnt3a) mRNA in each intestinal segment from embryonic day (e) 20 to 7 days post-hatch (d).....154

Figure 5-2. mRNA abundance of stem cell related genes: Expression of Achaete-scute complex homolog 2 (Acsl2), Leucine rich repeat containing G protein-coupled receptor 5 (Lgr5), Olfactomedin 4 (Olfm4), and Wnt family member 3a (Wnt3a) mRNA on embryonic day (e) 20 to 7 days post-hatch (d) in each intestinal segment 155

Figure 5-3. mRNA abundance of differentiated cell marker genes: Expression of marker genes for precursor cells - marker of proliferation Ki67, enterocytes - Peptide transporter 1 (PepT1), goblet cells - Mucin-2 (Muc2), and enteroendocrine cells - Chromogranin A in each intestinal segment from embryonic day (e) 20 to 7 days post-hatch (d) 156

Figure 5-4. mRNA abundance of differentiated cell marker genes: Expression of marker genes for precursor cells - marker of proliferation Ki67, enterocytes - Peptide transporter 1 (PepT1), goblet cells - Mucin-2 (Muc2), and enteroendocrine cells - Chromogranin A on embryonic day (e) 20 to 7 days post-hatch (d) in each intestinal segment 157

Figure 5-5. mRNA abundance of Notch pathway genes associated with intestinal cell differentiation: Expression of Notch 1, Delta-Like Ligand 1 (DLL1), Hairy and enhancer of split-1 (Hes1), and Atonal BHLH Transcription Factor 1 (Atoh1) in each intestinal segment from embryonic day (e) 20 to 7 days post-hatch (d) 158

Figure 5-6. mRNA abundance of Notch pathway genes associated with intestinal cell differentiation: Notch 1, Delta-Like Ligand 1 (DLL1), Hairy and enhancer of split-1 (Hes1), and Atonal BHLH Transcription Factor 1 (Atoh1) on embryonic day (e) 20 to 7 days post-hatch (d) in each intestinal segment 159

Figure 6-1. A graphical representation of the Balance-Point Model 174

List of Tables

Table 2-1. Morphological changes in chickens with RSS induced by exposure to poultry litter from RSS affected flocks in Georgia 58

Table 2-2. Morphological changes in chickens with RSS induced by astrovirus 59

Table 2-3. Morphological changes in chickens showing clinical RSS signs in Georgia ..60

Table 2-4. Morphological changes in chickens from a flock testing positive for RSS in Brazil.....61

Table 3-1. Primers for quantitative PCR.....95

Table 3-2. Growth performance data of infected and uninfected broiler chickens.....96

Table 3-3. Comparison of crypt depth measures between Olfm4-stained crypts and hematoxylin and eosin-stained crypts.....97

Table 4-1. Primers for quantitative PCR.....121

Table 5-1. Primers for quantitative PCR.....151

Table 5-2. Hatch rate following in ovo feeding at embryonic day 17.5 152

Table 5-3. Body weights at hatch and post-hatch following in ovo feeding at embryonic day 17.5.....153

Chapter 1 Introduction and Literature Review

The function of the small intestine is to internalize essential nutrients from the external world while simultaneously protecting the body from the dangers. These contradicting requirements have pushed the intestine to develop control mechanisms designed to preserve a homeostatic state where absorption and defense are balanced. At a system level, homeostasis is the maintenance of an internal environment sufficient for the continued proper functioning of the system by responding systematically to disturbances with the goal of retaining functionality. Disruptions force the system to change to maintain or return to functionality. Intestinal functions are highly robust and have been optimized to respond to some disturbances, such as the post-hatch intestinal transition or responses to stable microbiome shifts. The responses to these disturbances seem coordinated and orderly; however, when disturbances are novel, such as disease, the fragility of the homeostatic balance is exposed. Compensatory mechanisms activated to respond to novel disruptions may cause long term consequences typically resulting in an overall less efficient functional state, the allostatic state. Understanding the compensatory mechanisms that trigger allostasis requires investigating instances of disruption.

In recent years, the United States (U.S.) poultry industry has moved to remove antibiotics from their diets due to consumer demand. Currently, about 50% of broiler chickens are produced in antibiotic free programs (Smith, 2019). Most major food companies and poultry producers have committed to raising poultry without antibiotics. A major challenge facing U.S. producers is controlling gut health in broilers. Previously, low levels of in-feed antibiotics kept the intestine stable by knocking down populations of microorganisms both beneficial and pathogenic (Niewold, 2007). With in-feed

antibiotics broiler producers were able to increase the economies of scale by increasing stocking density, reducing downtime between flocks, and utilizing built up litter systems (Catry, 2017). Removal of these antibiotics predispose broilers to intestinal disruptions, as broiler chickens have weakened immune systems. Removal of in-feed antibiotics resulted in increased incidences of enteric diseases, reduced feed conversion, and in some instances early life mortality; reducing profits and bird welfare (Salois, 2017). U.S. poultry producers need new management strategies that mitigate the incidence and impact of intestinal disruptions. Development of such strategies requires an understanding of how the intestine and poultry respond to intestinal disruptions. Thus, the purpose of this dissertation is to propose a model for understanding the response of the small intestine to various disruptions.

Intestinal homeostasis

Intestinal homeostasis is a balance of multiple underlying components that contribute to the overall functionality of the intestine. The intestine has two key functions that are essential to life. First, the intestine is responsible for internalizing essential nutrients and basic elements that the body is unable to manufacture on its own. Second, the intestine is responsible for protecting the body from the harmful parts of the external world and to minimize the risk of damage from internalization of potentially harmful molecules. These two functions compete for resources and can interfere with one another. Optimal functioning of the intestine requires the competing functions to find a balanced state where the interference between the two functions is minimized.

Intestine Structure

The small intestine features two major functional structures (Fig. 1-1): **villi**, which are fingerlike structures that project into the lumen to make direct contact with digesta moving through the intestine, and **crypts**, which contain a population of stem cells that maintain villi structure. Both villi and crypts are supported by underlying mucosa tissue and crosslinked collagens and actin proteins that reinforce their unique structures. Collagens, such as Collagen Type III Alpha 1 Chain (Col3a1), have been shown to support increased villi height following positive dietary stimulation (Brautigan et al., 2017).

The villi are composed of differentiated cells, mainly absorptive enterocytes, that bring nutrients into circulation by use of transporter proteins that bind specific molecules in the brush border membrane but also secretory epithelial cell types, which support nutrient absorption by regulating the digestive process or secreting lubricating mucus. Once inside the cell, nutrients move to the basolateral membrane where specialized transporters move nutrients to underlying blood vessels that will carry nutrients to the liver and then to the rest of the body (Gilbert et al., 2008; Fig. 1-2). In chickens, enterocytes can be visualized in tissue using in situ hybridization (ISH) of the gene peptide transporter 1 (PepT1) (Zhang and Wong, 2017). In situ hybridization is a molecular technique where a specific mRNA transcript is highlighted by chromogens or fluorophores that creates a signal that can be seen in the tissue. PepT1 mRNA can be quantified using real-time quantitative polymerase chain reaction (RT-qPCR). Enterocytes migrate up the villi over time and are lost from extrusion zones at the top of the villi, requiring continuous replacement. Enterocytes and secretory lineage epithelial cells are lost by two mechanisms: shedding and apoptosis. The majority of cells are lost

by apoptosis, which occurs in terminally differentiated cells along the villi (Hall et al., 1994). Some epithelial cells are lost by shedding or due to damage from contact with moving digesta or invasion by microorganisms. Replacement cells migrate up from the crypt located at the base of the villi, taking approximately 48 hours to reach the upper villi (Imondi and Bird, 1966). The entire mucosa surface is turned over roughly every 3 to 5 days (Barker et al., 2008).

The crypt maintains a population of intestinal stem cells to serve as replacement cells that will maintain intestinal functionality and can rapidly respond to villi damage (Fig. 1-1). Stem cells in the chicken intestine can be visualized with ISH using a few different genes. Olfactomedin 4 (Olfm4) is a secreted glycoprotein that is expressed in the bottom of the crypt in mammals (Itzkovitz et al., 2012; Muñoz et al., 2012) and highlights the entire crypt in chickens (Zhang and Wong, 2018). Leucine Rich Repeat Containing G Protein-Coupled Receptor 5 (Lgr5) is a stem cell gene that regulates Wnt expression. In mammalian crypts Lgr5 is a robust marker of stem cells (Muñoz et al., 2012). In chickens Lgr5 is more of a general stem cell marker gene so in the early post-hatch period it is expressed beyond the crypt region (Zhang and Wong, 2018). The proliferation marker antigen Ki67 (Ki67 or MKi67) highlights stem cells but also any cell that is proliferating within the intestine. Intestinal stem cells will continually divide in the presence of crypt niche factors such as Notch and Wnt signals (Tian et al., 2015). Wnt signals are primary influential factors within the crypt (Hou et al., 2017). Achaete-scute complex homolog 2 (Ascl2) and Wnt family member 3a (Wnt3a) maintain stem cell populations in the crypt through direct interaction with Lgr5-expressing cells (van der Flier et al., 2009). Notch signals also influence the stem cell niche in the crypt, and are

directly responsible for Olfm4 expression (Carulli et al., 2015). Daughter cells, produced from dividing stem cells, maintain the crypt population. However, crypt size is fixed, causing some daughter cells to be pushed up out of the crypt (Itzkovitz et al., 2012; Beumer and Clevers, 2016).

Daughter cells that move up out of the crypt lose their stemness, becoming transit-amplifying or progenitor cells which differentiate into either absorptive-enterocytes or secretory cell types such as goblet, Paneth, enteroendocrine, or tuft cells based on Notch signals that control cell differentiation (Fig. 1-3). Progenitor cells differentiate into absorptive or secretory lineages based on the expression of Atoh1(Notch pathway), without Atoh1, progenitor cells become absorptive precursors (Hou et al., 2017). The balance of absorptive and secretory cell types is important for proper functioning of the intestine. Secretory cell types produce mucins, hormones, and other molecules that contribute to the effectiveness of enterocytes but do not absorb nutrients themselves. A majority of epithelial cells must be enterocytes to facilitate optimal absorption. The secretory and secretory precursor cells themselves maintain this balance by ensuring neighboring cells are on the absorptive lineage through the Notch Delta like ligand 1 (DLL1) and Notch receptors expressed on the shared border (Fre et al., 2005). Activation of the Notch receptor triggers the expression of Hairy enhancer of split 1 (Hes1), which commits the cell to the absorptive lineage (Hou et al., 2017).

Cells that remain on the secretory lineage differentiate into goblet, Paneth, enteroendocrine, or tuft cells which connect the intestine to the immune, endocrine, and nervous systems. Goblet cells secrete mucins that form the mucus layer (described further below) which creates an initial defensive barrier for the intestine. In chickens,

goblet cells can be viewed in tissue sections through histology stains (Alcian blue and Periodic acid-Schiff reagents) or ISH (Mucin-2, Muc2). Individual cells can be seen along the villi and in the crypt (Reynolds et al., 2020). Paneth cells secrete antimicrobial peptides and Wnt niche factors. In mammals, Paneth cells reside only in the crypt and specifically lie between stem cells (Beumer and Clevers, 2016). In chickens the presence of Paneth cells is controversial in terms of their location (Zhang et al., 2019). In mammals Paneth cells are only present in the crypt in an alternating pattern amongst stem cells. This fits with their function of secreting niche factors that maintain the stem cell niche. Studies in chickens however have found Lysozyme C positive cells (a marker of Paneth cells) both in the crypt and along the villi, but not in a clear alternating pattern with stem cells, potentially contradicting the function described in mammals (Nile et al., 2007; Wang et al., 2016; Bar Shira and Friedman, 2018; Yu et al., 20121). Enteroendocrine cells and Tuft cells are less common in the intestine and they have chemosensory functions (May and Kaestner, 2010; Gerbe and Jay, 2016; Gribble and Reimann, 2016). Neither cell type has been extensively studied in chickens, as in mammals. Chromogranin A is used in ISH as a cell marker for enteroendocrine cells and has been measured in chickens before (Zhao et al., 2022).

Intestine Function

Efficient absorption of nutrients is the primary function of the small intestine. Birds have evolved a unique shortened gastrointestinal tract that accommodates flight. To compensate for its short length, chickens employ contractile waves which pass along the small intestine to mix and move digesta through the intestinal tract; as well as segment-specific morphological and transporter adaptations, enabling specialized functions,

increasing overall efficiency (Moran, 2014). The unstirred water layer (USWL; Fig. 1-2) further prolongs the contact time of digesta material. The USWL is composed of a mucus layer anchored to the surface of villi, trapping digesta that is enzymatically digested, releasing smaller particles that pass through pores in the mucus layer to be absorbed by underlying enterocytes (Moran 2017). The USWL is also a niche biome for commensal microbial species colonizing the small intestine. These communities compete with the host for nutrients but also contribute to host nutrition by digesting particles the host is not otherwise equipped to digest and by synthesizing beneficial biomolecules (Maki et al., 2019).

The other essential function of the intestine is the maintenance of a defensive barrier to mitigate the risks of internalization of potentially harmful molecules. To facilitate efficient nutrient absorption, the intestinal villi are limited to a single cell layer thickness allowing direct absorption to the underlying circulation through enterocytes. There is an inherent risk that microbial organisms will be able to cross into the circulation. To minimize the risk of microorganisms bypassing enterocytes, the mucin layer restricts immediate access to the villi surface by trapping microorganisms (Moran 2014; 2017). The mucin layer is also colonized by commensal organisms that help defend the intestine by secreting antimicrobials that directly act on invading microorganisms or by creating niche environments that exclude invaders (Kogut, 2019). To prevent microorganisms from bypassing enterocytes and moving between cells, tight junction proteins cross link neighboring epithelial cells, blocking access and maintaining integrity (Fig. 3; Awad et al., 2017). Together these adaptations restrict access to the circulatory system, leaving only access through the enterocytes. Enterocytes synthesize host defense

peptides such as liver enriched antimicrobial peptide-2 (LEAP-2) and Avian beta defensins (AvBD), which destroy microorganisms before they can pass into the circulation (Cuperus et al., 2013). The variety of mechanisms employed by the intestine to prevent translocation of bacteria into the circulatory system work collaboratively to mitigate the risks associated with maintaining robust intestinal microbiota populations.

Besides colonizing the mucin layer, the gut microbiota also exists along the entire gastrointestinal tract from beak to vent and influences the microflora of the environment of the bird (Broom and Kogut, 2018). Microorganisms colonize the intestinal lumen, the mucin layer, the deep mucus area associated with crypts, and the surface of villus epithelial cells (Dibner et al., 2008). As discussed above, the mucin layer and host defense peptides control microbial proliferation in the lumen and mucosal layers of the small intestine. Below that, epithelial cells contain pattern recognition receptors which signal to the underlying gut-associated lymphoid tissue (GALT) in the lamina propria through cytokine and chemokines (Dibner et al., 2008). Additionally, specialized epithelial cells, intraepithelial lymphocytes, residing along the villi sample the surrounding microbiome for the GALT. The GALT contains many different cell types of the immune system that respond to pathogenic organisms (Dibner et al., 2008). In addition to cell-associated receptors, secreted Immunoglobulin A (IgA) interacts with the gut microbiome and neutralizes harmful microorganisms. The immune system of the bird is tolerant of the commensal species of the microbiome. Immunological sensitization to the microbiome develops post-hatch, when cells appear in the bursa that are able to trap antigens from the microbiome passing through the cloaca (Bar-Shira et al., 2005; Dibner et al., 2008). Host IgA secretion is dependent upon microbiome colonization, as the gut

lymphoid tissue of germ-free animals does not contain IgA+ cells (Dibner et al., 2008). Contact between IgA, epithelial cell pattern recognition receptors, and commensal microbial species trigger necessary cytokine expressions that shore up the barrier integrity of the mucin and tight junctions, reinforcing the defensive functions of the small intestine and preserving homeostasis (Allaire et al., 2018).

Establishment of the intestine

Chicken embryos rely on nutrients within the yolk but, like all precocial avian species, hatch ready to utilize complex feedstuffs without the need for parental aid. This is achieved by an essential disruption of intestinal homeostasis during the hatching process. In the egg, embryos rely upon the proteins in the albumen and the lipoproteins in the yolk for their nutrition; however, after hatching, chicks are fed a carbohydrate based diet. This change requires the intestine to undergo a maturation process where the villi lengthen and the crypt increases in size to support the increase in surface area (Uni et al., 2000).

Prior to the formation of the intestines in the embryo, the yolk sac tissue functions in its place (Wong and Uni, 2021). The yolk sac tissue forms villi like structures lined by endodermal epithelial cells which are multi-functional, capable of both absorption and secretion of various products. By mid-incubation, the yolk sac tissue is taking up nutrients to supply the rapid embryonic growth prior to hatch. The intestine develops in the chicken embryo during late incubation but is not functional until hatching begins. At embryonic day (e) 18, embryos swallow the amniotic fluid, initiating the hatching process and jumpstarting the maturation of the intestine (Moran, 2007). Between e18 and day of hatch the villi lengthen and crypts develop rapidly approximately tripling the weight and

absorptive surface area of the intestine (Uni et al., 2003). Enterocytes present along the villi in embryos are rapidly replaced by mature enterocytes in the first 48 hours post-hatch (Uni et al., 1998a). The morphological changes are accompanied by increases in enzyme secretion and nutrient transporter expression (Uni et al., 1998b; 2003). This period of rapid change during the first 7 days post-hatch is accompanied by an establishment of immunocompetence within the gastrointestinal tract (Bar-Shira et al., 2003) and a metabolic transition in the liver from utilizing predominately lipids to majorly starch nutrients (Richards et al., 2010), and increased satellite cell mitotic activity (Nierobisz et al., 2007). The intestine continues to transition from embryonic to mature cells during the first 16 days of age (Sklan, 2001), facilitating the 10-fold increase in body weight occurring in the first 3 weeks post-hatch. The post-hatch intestinal maturation is an evolutionary disruption of intestinal homeostasis that is essential to adapt hatchlings to their environment and to facilitate their survival.

Disruptions of intestinal homeostasis

Frequently intestinal homeostasis is disrupted by something in the external environment. In response to disruptions of homeostasis, the intestine changes to preserve overall functionality, albeit in a way that previously was inefficient. Some disturbances have evolved concurrent with the homeostatic balance of the small intestine. The response to these disturbances has been optimized to the point that the disturbances appear to be essential aspects of intestinal development. Similarly, some disruptions are a regular part of life, such as the hatching process or the establishment of the mature microbiome, resulting in well-coordinated and orderly responses that minimize the long-term consequences. However, novel disturbances produce responses that seem

disordered, exposing the fragility of the homeostatic balance between absorption and defense. The compensatory mechanisms that are activated to respond to novel disruptions have long term consequences and typically result in the intestine entering an allostatic state instead of returning to the previous homeostatic balance. This new state is not a true homeostatic state, the optimal balance between absorption and defense cannot be returned to because inflammation is diverting nutrients and altering interactions with the microbiome (Ramsay and Woods, 2014).

Allostasis is commonly defined as an overactive response that continues after the trigger signal ceases (Ramsay and Woods, 2014). A true homeostatic balance is a dynamic state that achieves optimal functioning while minimizing associated costs (Woods and Wilson, 2013). In an allostatic state, the intestine maintains an overactive response and is thus distinct from the homeostatic balance. When disruptions occur often in the life history of a species, distinct mechanisms evolve to optimize the responses, keeping them from becoming overly active and persistent. At that point, a disturbance is no longer considered novel. This can be seen in the response of broilers to the post-hatch intestinal maturation process as the bird does not display any signs of disease associated with a novel homeostatic disruption, despite clear changes in the intestinal balance. In contrast, when broilers experience chronic inflammation or infection, a compensatory response, such as pathological inflammation and villi hypertrophy, is activated to push the intestine back towards the homeostatic balance of nutrient absorption and defense. This results in a performance drop as the intestinal homeostatic balance is shifted to prioritize defense while maintaining an efficient enough state to maintain intestinal functionality and therefore survival. Understanding how the small intestine responds to

novel disruptions will lead to a better understanding of intestinal function and the homeostatic balance it maintains, as well as contribute to the growing research area of gut health in the antibiotic free era.

Disturbances faced in commercial poultry production

The modern broiler is prone to chronic inflammation resulting from their rapid growth rate, high stocking density, modern poultry diets (ingredients, feed changes, nutrient excesses), and from the challenge of maintaining a stable microbiome while being continuously exposed to more microorganisms. As discussed earlier, the microbiome and the immune system reinforce the integrity of intestinal barriers through inflammatory cytokines. This inflammatory response is essential and beneficial to intestinal homeostasis and is characterized as physiological inflammation (Kogut et al., 2018). However, physiological inflammation can shift to a chronic and damaging process through activation of damage associated molecular patterns (DAMPS) by excess stress. Stressors often arise as unintended results of modern management practices such as the inclusion of non-starch polysaccharide ingredients into diets, phase feeding programs that involve routine feed changes, dietary nutrient excesses, increased litter nitrogen, and heat stresses (Kogut et al., 2018). The harmful inflammation will become chronic as the inflammation will not clear the stressor. Additionally, the inflammation will likely further damage cells, increasing DAMP signals and perpetuating the inflammatory state. As mentioned at the beginning of this chapter, in-feed antibiotics dampened the effect of stressors; with their removal, intestinal homeostasis is precariously balanced and all too often tips into an allostatic state resulting in decreased feed efficiency. The first disturbance the small intestine experiences is the transition from embryonic to post-hatch,

known as the intestinal maturation process. This was described in detail in earlier sections but briefly, the consumption of the amniotic fluid on e18 supplies nutrients that stimulate the formation of crypts and mature villi. Uni and Ferket pioneered a technique to supplement the amniotic fluid with nutrients just prior to consumption by the embryo in a process called in ovo feeding (Uni et al., 2005). In ovo feeding has been shown to improve the post-hatch intestinal maturation process by improving the growth of the small intestine (Roto et al., 2016). The administration of probiotic species in ovo seeds the gastrointestinal tract early with beneficial bacteria (Ducatelle et al., 2014; Hou and Tako, 2018), that enhance cellular and immune development of the intestine. Administration of probiotics (~0.1 ml) to broiler embryos does not adversely affect hatchability and produces positive post-hatch immune responses. However, in ovo feeding typically uses larger volumes (0.3- 0.6 ml) to supplement the amniotic fluid. There has been no research investigating the responses to larger volumes. Since previous research has established that in ovo feeding promotes intestinal maturation, we expect that in ovo feeding of a probiotic would synergize with the expected intestinal maturation process.

During the intestinal maturation process, chicks are placed on farms. In the U.S. that usually is on built-up litter re-used from previous flocks with clean shavings added on top. Used litter contains a unique microbial population that will transfer to the new chicks and colonize their intestinal tract. In most cases this is not problematic; however, it can result in disease as pathogenic organisms colonize the intestine and over proliferate. One disease seen in early life that may be associated with the microbial transfer is Runting Stunting Syndrome (RSS), a malabsorption syndrome of broiler chickens that

causes afflicted birds to decrease their feed efficiency and suffer from diarrhea (Johnson et al., 2020). Afflicted birds have wider variations in body weight than birds in healthy flocks, with individuals that recovered from infection remaining stunted. The exact etiology of RSS is debated but it is likely the result of a viral infection in young chicks that interacts with the microbiome (Devaney et al., 2016; Kang et al., 2018; de Oliveria et al., 2021). Similar to other intestinal disturbances histopathological evaluation reveals signs of inflammation: blunted and broken villi and dilated cystic crypts (Kang et al., 2018). RSS is unique in that birds remain stunted following viral clearance. Investigation into the mechanisms causing the stunting at the intestinal level have been sparsely undertaken. We expect that an alteration in the cell turnover process would explain the persistent symptoms following viral clearance.

Poultry houses around the world are infested with a protozoan parasite: *Eimeria spp.* which cause coccidiosis in chickens (Conway and Mckenzie, 2007). Coccidiosis is a major economically damaging disease worldwide in broiler chicken production and is characterized by consecutive infection and reinfection of multiple *Eimeria spp*. Chickens consume sporulated oocysts in the litter or feces and their digestion process releases sporozoites which invade individual epithelial cells along the villi. Invasion by the sporozoite is aided by their surface antigens which alter epithelial cell defenses (Liu et al., 2018). Inside infected epithelial cells, *Eimeria* sporozoites multiply asexually, increasing in number until the epithelial cell ruptures, releasing parasites out to surrounding tissue where they invade nearby epithelial cells to continue the cycle. Eventually the parasite transitions to sexual reproduction, forming gametes that combine to form a fertilized oocyst that ruptures out and is shed in feces to infect another bird or

reinfect the host (Conway and McKenzie, 2007). The infection-multiplication cycle repeats and culminates in widespread tissue damage impairing the functionality of the intestine and reducing the performance of the bird. In contrast with RSS, infected broilers recover from coccidiosis and enter into a compensatory growth phase (Henken et al., 1994). Infection with *Eimeria spp*. is known to trigger tissue hyperplasia and alter cellular renewal rates (Fernando and McCraw, 1973) which likely shifts the intestine into an allostatic state. Researchers have not tracked the biological response of the host defense peptides over the course of coccidiosis infection, nor changes in genes associated with intestinal homeostasis to assess this disturbance response.

Objectives

The objective of this dissertation is to introduce the balance-point model of intestinal homeostasis as a proposed model for understanding the response of the small intestine to various disruptions. This is accomplished through investigations of distinct intestinal disruptions over the course of four independent research chapters including both novel and expected disruptions. The first research chapter (**Chapter 2**) examined intestinal morphology and the mRNA expression of various stem (Olfm4), proliferative (Ki67), absorptive (PepT1, SGLT1), and secretory (Muc2) cell markers in the small intestine of chickens showing clinical signs of RSS arising from experimentally induced and natural infections. The second research chapter (**Chapter 3**) characterized the change in intestinal homeostasis over time following a single challenge with *Eimeria acervulina* in naïve broiler chickens by looking at gene expression and mucosal morphology. An additional objective of this chapter was to localize *E. acervulina* in duodenal cells of infected broilers utilizing ISH of a sporozoite surface antigen. The third research chapter

(**Chapter 4**) profiled the changes in proliferative cells across the small intestine focusing on the development of the intestinal crypt during the last 4 days in ovo and first 7 days post-hatch using ISH and RT-qPCR analysis of stem (Olfm4 and Lgr5) and proliferative cell marker (Ki67) genes. The fourth research chapter (**Chapter 5**) assessed the ability of a commercial mixed-species probiotic provided via in ovo feeding on e17.5 to modulate the small intestinal maturation process during the final days of incubation and the first week post-hatch. The last two research chapters examine the intestinal maturation process occurring during the peri-hatch period. Throughout the research chapters there was an effort to evaluate responses over time following a disturbance as compensatory and maladaptive responses are not likely to be fixed or static changes but likely fluctuate over time and between individual birds. The final chapter of the dissertation (**Chapter 6**) continued to define the proposed balance-point model of intestinal homeostasis using the conclusions of the research chapters.

References

Allaire, J.M., S.M. Crowley, H.T. Law, S.Y. Chang, H.J. Ko, and B.A. Vallance. 2018. The intestinal epithelium: central coordinator of mucosal immunity. Trends. Immunol. 39:677-696.

Awad, W.A., C. Hess, and M. Hess. 2017. Enteric pathogens and their toxin-induced disruption of the intestinal barrier through alteration of tight junctions in chickens. Toxins. 9:60.

Barker, N., M. van de Wetering, and H. Clevers. 2008. The intestinal stem cell. Genes Dev. 22:1856-1864.

Bar-Shira, E., D. Sklan, and A. Friedman. 2005. Impaired immune responses in broiler hatchling hindgut following delayed access to feed. Vet. Immunol. Immunopathol. 105:33-45.

Bar Shira, E., and A. Friedman. 2018. Innate immune functions of avian intestinal epithelial cells: Response to bacterial stimuli and localization of responding cells in the developing avian digestive tract. PLoS One 13:e0200393.

Beumer, J., and H. Clevers. 2016. Regulation and plasticity of intestinal stem cells during homeostasis and regeneration. Development 143:3639-3649.

Broom, L.J. and M.H. Kogut. 2018. The role of the gut microbiome in shaping the immune system of chicks. Vet Immunol. Immunopathol. 204:44-551.

Carulli, A.J., T.M. Keeley, E.S. Demitrack, J. Chung, I. Maillard, and L.C. Samuelson. 2015. Notch receptor regulation of intestinal stem cell homeostasis and crypt regeneration. Dev. Bio. 402:98-108.

Catry, B. 2017. Antimicrobial policies in animals and human health. Arch. Public Health 75:62.

Conway, D.P. and M.E. Mckenzie. 2007. Poultry Coccidiosis: Diagnostic and Testing Procedures. 3rd ed. Blackwell Publishing Ltd, Oxford, UK

Cuperus, T., M. Coorens, A. van Dijk, and H.P. Haagsman. 2013. Avian host defense peptides. Dev. Comp. Immunol. 41:352–369.

de Oliveira L.B., J.B. Stanton, J. Zhang, C. Brown, S.L. Butt, K. Dimitrov, C.L. Afonso, J.D. Volkening, L. Lara, C. de Oliveira, and R. Ecco. 2021. Runting and stunting syndrome in broiler chickens: histopathology and association with a novel picornavirus. Vet Pathol. 58:123–135.

Devaney, R., J. Trudgett, A. Trudgett, C. Meharg, and V. Smyth. 2016. A metagenomic comparison of endemic viruses from broiler chickens with runting-stunting syndrome and from normal birds. Avian Pathol. 45:616-629.

Dibner, J.J., J.D. Richards, and C.D. Knight. 2008. Microbial imprinting in gut development and health. J. Appl. Poult. Res. 17:174-188.

Ducatelle, R., V. Eeckhaut, F. Haesebrouck, and F. Van Immerseel. 2015. A review on prebiotics and probiotics for the control of dysbiosis: present status and future perspectives. Animal 9:43-48.

Fernando, M.A., and B.M. McCraw. 1973. Mucosal morphology and cellular renewal in the intestine of chickens following a single infection of *Eimeria acervulina*. J. Parasitol. 59:493-501.

Fre, S., M. Huyghe, P. Mourikis, S. Robine, D. Louvard, and S. Artavanis-Tsakonas. 2005. Notch signals control the fate of immature progenitor cells in the intestine. Nature 435:964-968.

Gerbe, F., and P. Jay. 2016. Intestinal tuft cells: epithelial sentinels linking luminal cues to the immune system. Mucosal Immunol. 9:1353-1359.

Gilbert, E.R., E.A. Wong, and K.E. Webb Jr. 2008. Board-invited review: peptide absorption and utilization: implications for animal nutrition and health. J. Anim. Sci. 86:2135-2155.

Gribble, F. M., and F. Reimann. 2016. Enteroendocrine cells: chemosensors in the intestinal epithelium. Annu. Rev. Physiol. 78:277-299.

Hall, P.A., P.J. Coates, B. Ansari, and D. Hopwood. 1994. Regulation of cell number in the mammalian gastrointestinal tract: the importance of apoptosis. J. Cell Sci. 107:3569-3577.

Henken, A.M., E.A.M. Graat, H.W. Ploeger, and T.E. Carpenter. 1994. Description of a model to simulate effects of *Eimeria acervulina* infection on broiler production. Parasitology, 108:513-518.

Hou Q, Ye L, Huang L, Yu Q. 2017. The research progress on intestinal stem cells and its relationship with intestinal microbiota. Front Immunol 8:599.

Hou, T., and E. Tako. 2018. The in ovo feeding administration (Gallus gallus)—An emerging in vivo approach to assess bioactive compounds with potential nutritional benefits. Nutrients. 10:418.

Imondi, A.R., and Bird, F. H. 1966. The turnover of intestinal epithelium in the chick. Poultry Sci. 45:142-147.

Itzkovitz, S., A. Lyubimova, I.C. Blat, M. Maynard, J. Van Es, J. Lees, T. Jacks, H. Cleavers and A. Van Oudenaarden. 2012. Single-molecule transcript counting of stem-cell markers in the mouse intestine. Nat. Cell Biol. 14:106-114.

Johnson T., and M. Day. 2020. Multicausal enteric diseases. In: Swayne D, M. Boulianne, C. Logue, L. McDougald, V. Nair, and D. Suarez, editors. Diseases of Poultry. 14th ed. Ames (IA): Wiley-Blackwell. p. 1390–1393.

Kang, K., E. Linnemann, A.H. Icard, V. Durairaj, E. Mundt and H. Sellers. 2018. Chicken astrovirus as an aetiological agent of runting-stunting syndrome in broiler chickens. J. Gen. Virology. 99:512-524.

Kogut, M.H., K.J. Genovese, C.L. Swaggerty, H. He, and L. Broom. 2018. Inflammatory phenotypes in the intestine of poultry: not all inflammation is created equal. Poult. Sci. 97:2339-2346.

Kogut, M.H. 2019. The effect of microbiome modulation on the intestinal health of poultry. Anim. Feed Sci. Tech. 250:32-40.

Liu, T., J. Huang, Y. Li, M. Ehsan, S. Wang, Z. Zhou, X. Song, R. Yan, L. Xu and X. Li. 2018. Molecular characterization and the protective immunity evaluation of Eimeria maxima surface antigen gene. Parasites Vectors 11:1-12.

Maki J.J, C.L. Klima, M.J. Sylte, and T. Looft. 2019. The microbial pecking order: Utilization of intestinal microbiota for poultry health. Microorganisms. 7:376.

May, C. L., and K.H. Kaestner. 2010. Gut endocrine cell development. Mol. Cell. Endocrinol. 323:70.

Moran, E.T. 2007. Nutrition of the developing embryo and hatchling. Poult. Sci. 86:1043-1049.

Moran Jr, E.T. 2014. Intestinal events and nutritional dynamics predispose *Clostridium perfringens* virulence in broilers. Poult. Sci. 93:3028-3036.

Moran Jr, E.T. 2017. Nutrients central to maintaining intestinal absorptive efficiency and barrier integrity in fowl. Poult. Sci. 96:1348-1363.

Muñoz, J., D.E. Stange, A.G. Schepers, M.Van De Wetering, B.K. Koo, S. Itzkovitz, R. Volckmann, K.S. Kuang, J. Koster, S. Radulescu, K. Myant, R. Versteeg, O.J. Sansom, J. H. van Es, N. Barker, A. van Oudenaarden, S. Mohammad, A.J.R. Heck, and H. Clevers. 2012. The Lgr5 intestinal stem cell signature: robust expression of proposed quiescent '+ 4'cell markers. EMBO J. 31:3079-3091.

Niewold, T. A. 2007. The nonantibiotic anti-inflammatory effect of antimicrobial growth promoters, the real mode of action? A hypothesis. Poult. Sci. 86:605-609.

Nile, C.J., C.L. Townes, G. Michailidis, B.H. Hirst, and J. Hall. 2004. Identification of chicken lysozyme g2 and its expression in the intestine. Cell. Mol. Life Sci. 61:2760-2766.

Ramsay, D.S. and S.C. Woods. 2014. Clarifying the roles of homeostasis and allostasis in physiological regulation. Psychol. Rev. 121:225-247.

Reynolds, K.L., Cloft, S.E., and Wong, E.A. 2020. Changes with age in density of goblet cells in the small intestine of broiler chicks. Poult. Sci. 99:2342-2348.

Reicher, N., T. Melkman-Zehavi, J. Dayan, E.A. Wong, and Z. Uni. 2022. Intra-amniotic administration of L-glutamine promotes intestinal maturation and enteroendocrine stimulation in chick embryos. Sci. Rep. 12:1-13.

Roto, S.A., Kwon, Y.M., and Ricke, S.C. 2016. Applications of in ovo technique for the optimal development of the gastrointestinal tract and the potential influence on the establishment of its microbiome in poultry. Front. Vet. Sci. 3:63.

Salois, M. 2017. The cost of broiler welfare standard. Chicken Marketing Summit. 2017 Elanco.

Smith, J. 2019. Broiler production without antibiotics: United States field perspectives. Anim. Feed Sci. Tech. 250:93-98.

Tian, H., B. Biehs, C. Chiu, C.W. Siebel, Y. Wu, M. Costa, F.J. de Sauvage, and O.D. Klein. 2015. Opposing activities of Notch and Wnt signaling regulate intestinal stem cells and gut homeostasis. Cell Rep. 11:33-42.

Uni, Z., S. Ganot, and D. Sklan. 1998a. Posthatch development of mucosal function in the broiler small intestine. Poult. Sci. 77:75–82.

Uni, Z., R. Platin, and D. Sklan. 1998b. Cell proliferation in chicken intestinal epithelium occurs both in the crypt and along the villus. J. Comp. Phsiol. B 168:241-247.

Uni, Z., A. Geyra, H. Ben-Hur, and D. Sklan. 2000. Small intestinal development in the young chick: crypt formation and enterocyte proliferation and migration. Br. Poult. Sci. 41:544-551.

Uni, Z., E. Tako, O. Gal-Garber, and D. Sklan. 2003. Morphological, molecular, and functional changes in the chicken small intestine of the late-term embryo. Poult. Sci. 82:1747-1754.

Uni, Z., P.R. Ferket, E. Tako, O. Kedar. 2005. In ovo feeding improves energy status of late-term chicken embryos. Poult. Sci. 84:764-770.

van der Flier, L.G., M.E. van Gijn, P. Hatzis, P. Kujala, A. Haegebarth, D.E. Stange, H. Begthel, M. van den Born, V. Guryev, I. Oving, and J.H. van Es. 2009. Transcription factor Achaete scute-like 2 controls intestinal stem cell fate. Cell 136:903–912.

Wang, L., J. Li, J. Li, R.X. Li, C.F. Lv, S. Li, Y.L. Mi, and C.Q. Zhang. 2016. Identification of the Paneth cells in chicken small intestine. Poult. Sci. 95:1631–1635.

Wong, E.A., and Z. Uni. 2021. Centennial Review: The chicken yolk sac is a multifunctional organ. Poult. Sci. 100:100821.

Woods H. and J. Wilson. 2013. An information hypothesis for the evolution of homeostasis. Trends Ecol. Evol. 28:283-289.

Zhang, H., and E.A. Wong. 2017. Spatial transcriptional profile of PepT1 mRNA in the yolk sac and small intestine in broiler chickens. Poult. Sci. 96:2871-2876.

Zhang, H. and E.A. Wong, 2018. Identification of cells expressing *OLFM4* and *LGR5* mRNA by in situ hybridization in the yolk sac and small intestine of embryonic and early post-hatch chicks. Poult. Sci. 97:628-633.

Zhao, D., M.B. Farnell, M.H. Kogut, K.J. Genovese, R.S. Chapkin, L.A. Davidson, L.R. Berghman and Y.Z. Farnell. 2022. From crypts to enteroids: establishment and characterization of avian intestinal organoids. Poult. Sci. 101:101642.

Figure Captions

Figure 1-1. Chicken small intestine model. The small intestine is composed of villi and crypts which function together to maintain efficient intestinal functioning. The crypt (A) is composed of stem cells that continuously divide giving rise to precursor cells which eventually differentiate into mature absorptive or secretory cells along the villus. At the tip of the villi (B) epithelial cells are shed due to apoptosis and sloughing off into the digesta. Cells at the villi tip that are lost are replaced by cells produced in the crypt. Figure 1-1 was created by S. Cloft.

Figure 1-2. The intestinal enterocyte. Absorptive enterocytes are responsible for absorbing nutrients from the intestinal lumen and transporting them into the bloodstream. To facilitate absorption the enterocyte at the apical or brush border membrane extends microvilli into the Unstirred Water Layer increasing the absorptive surface area available. Enterocytes also participate in the defensive barrier function by expressing antimicrobial peptides such as defensins or Liver enriched antimicrobial peptide 2. They also control access to the underlying bloodstream by blocking paracellular transport between cells by expressing tight junction proteins: occludin, claudin, and Junctional adhesion molecules (JAM). Figure 1-2 was created by S. Cloft.

Figure 1-3. A simplified diagram of intestinal cell differentiation in the intestine. Cell marker genes established for each cell type are listed in the legend. 1. Intestinal stem cells continuously divide producing daughter cells which migrate out of the intestinal crypt towards the villi. 2. A small subset of daughter cells remain in the crypt to ensure a stable

population of intestinal stem cells. Niche genes such as the regulatory factor Achaete-scute complex homolog 2 (Ascl2) and Wnt family member 3a (Wnt3a) maintain stem cell populations in the crypt. 3. Precursor cells exiting the crypt begin to differentiate into absorptive or secretory lineages based on Notch pathway signaling. Absorptive precursor cells express Notch1 which stimulates Hairy enhancer of split 1 (Hes1). Secretory precursors express the lineage switch transcription factor Atonal BHLH Transcription Factor 1 (Atoh1). 4. Secretory lineage cells comprise a small proportion of the intestine. They self-regulate their population by ensuring that all neighboring cells are on the absorptive lineage through cell-to-cell signals between Notch1 and Delta-Like Ligand 1 (DLL1). 5. There are 4 different mature secretory cell types: Goblet cells, Enteroendocrine cells, Tuft cells, and Paneth cells. Figure 1-3 was created by S. Cloft.

FIGURES

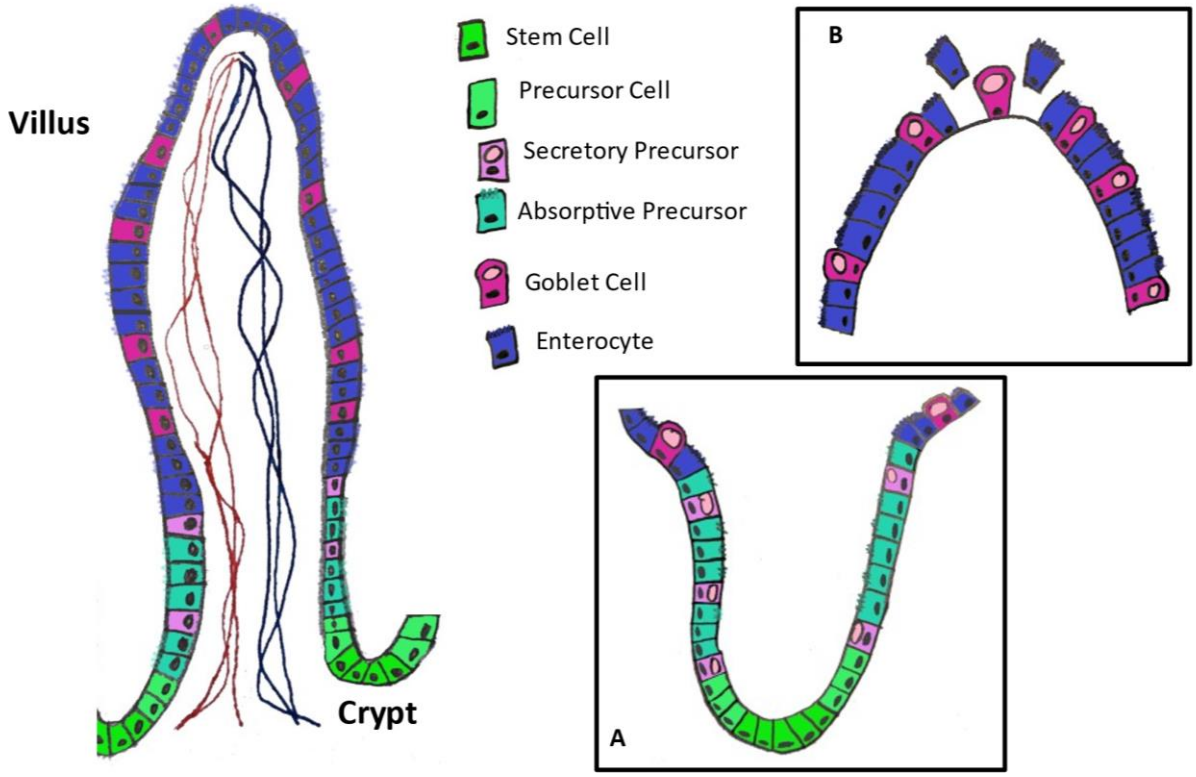

Figure 1-1.

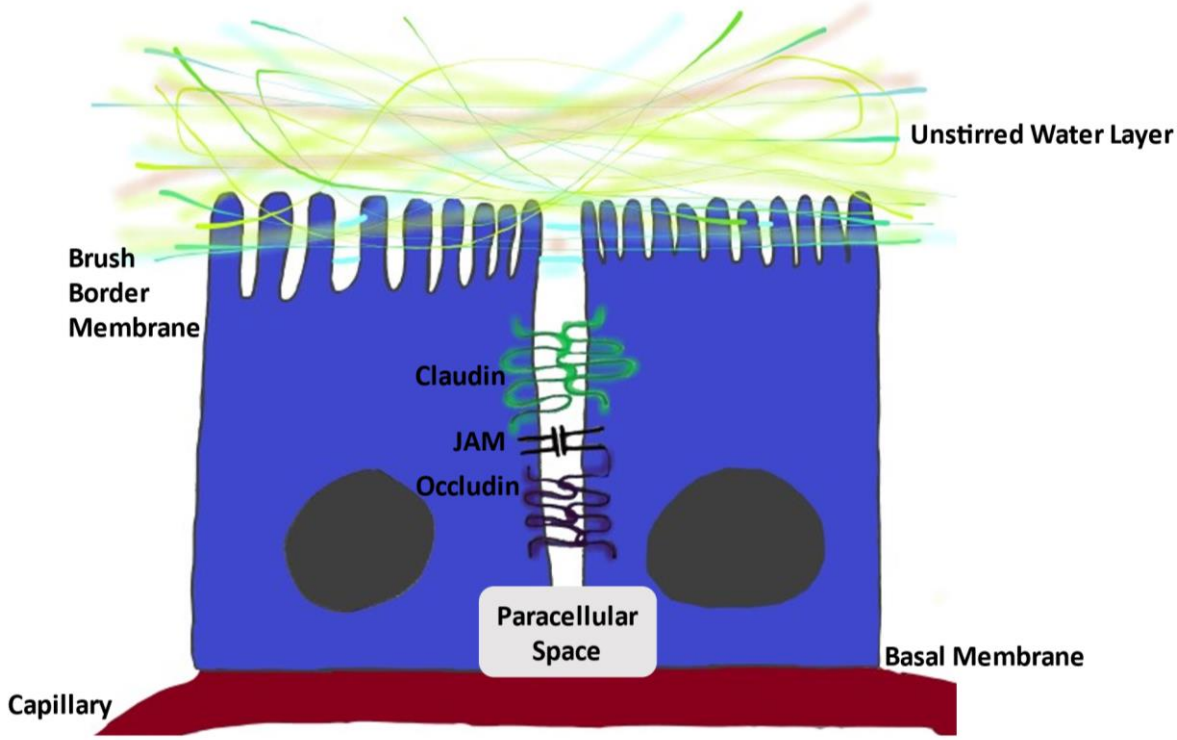
Unstirred Water Layer
Brush
Border
Membrane
Claudin
JAM
Occludin
Paracellular
Space
Basal Membrane
Capillary

Figure 1-2.

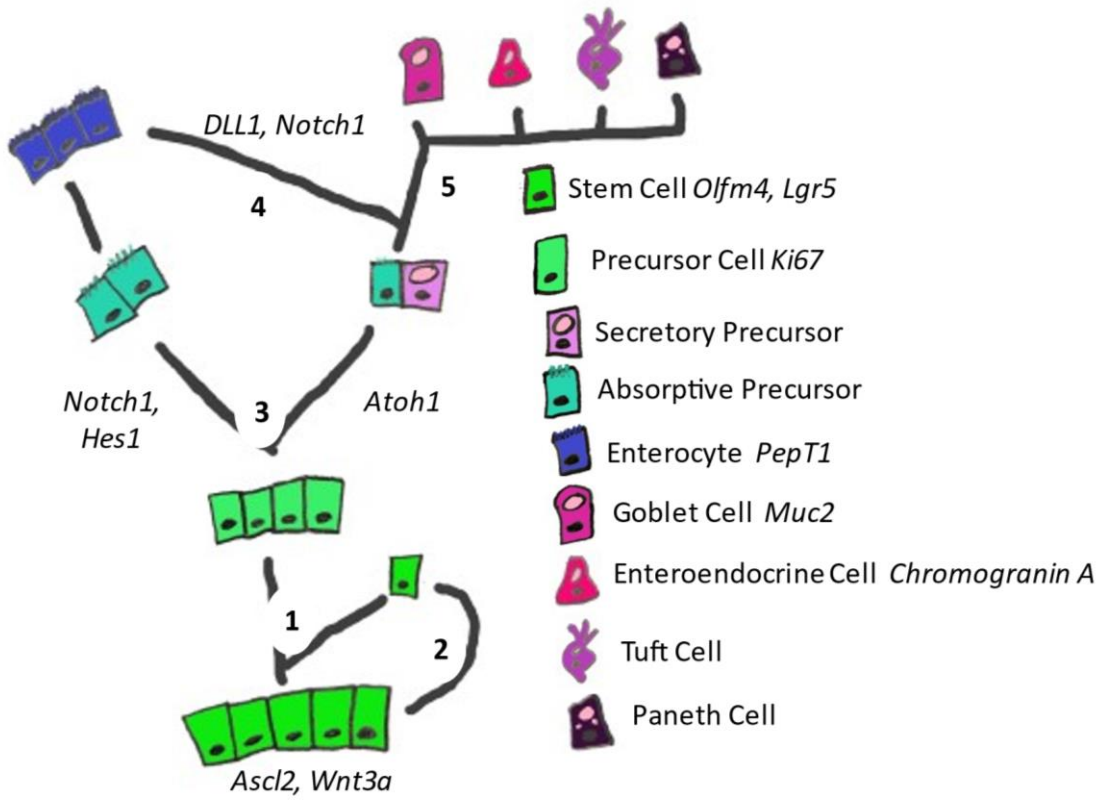
DLL1, Notch1
4
5
Notch1,
Hes1
3
Atoh1
1
2
Ascl2, Wnt3a
Stem Cell Olfm4, Lgr5
Precursor Cell Ki67
Secretory Precursor
Absorptive Precursor
Enterocyte PepT1
Goblet Cell Muc2
Enteroendocrine Cell Chromogranin A
Tuft Cell
Paneth Cell

Figure 1-3.

Chapter 2: Runting Stunting Syndrome in Broiler Chickens Is Associated with Altered Intestinal Stem Cell Morphology and Gene Expression*

*This chapter has been published in Avian Diseases February 2022 and reprinted with permission of copyright holders S.E. Cloft and E.A. Wong. DOI: 10.1637/aviandiseases-D-21-00109

ABSTRACT. Runting stunting syndrome (RSS) in broiler chickens is characterized by altered intestinal morphology and gene expression and stunted growth. The objective of this study was to conduct a retrospective study of gene expression in stem and differentiated cells in the small intestine of RSS chicks. Two different models of RSS were analyzed: broiler chicks that were experimentally infected and broiler chicks that were naturally infected. Experimentally infected chicks were exposed to litter from infected flocks (RSS-litter chicks) or infected with astrovirus (RSS-astrovirus chicks). Intestinal samples from naturally infected chicks showing clinical signs of RSS were acquired from commercial farms in Georgia and were brought into a poultry diagnostic lab (RSS-clinical-GA) and from farms in Brazil that had a history of RSS (RSS-clinical-BR). The RSS-clinical-BR chicks were separated into those that were positive or negative for gallivirus based on DNA sequencing. Intestinal morphology and intestinal cell type were identified in archived formalin-fixed, paraffin-embedded tissues. *In situ* hybridization for cell-specific mRNA was used to identify intestinal stem cells expressing olfactomedin 4 (Olfm4), proliferating cells expressing Ki67, absorptive cells expressing sodium glucose cotransporter 1 (SGLT1) and peptide transporter 1 (PepT1), and goblet cells expressing mucin 2 (Muc2). RSS-litter and RSS-clinical-GA chicks showed 4% to 7.5% cystic crypts, while gallivirus-positive RSS-clinical-BR chicks showed 11.7%

cystic crypts. RSS-astrovirus and gallivirus-negative RSS-clinical-BR chicks showed few cystic crypts. RSS-litter and gallivirus-positive RSS-clinical-BR chicks showed an increase in crypt depth compared to control or gallivirus-negative chicks, respectively. There was no expression of Olfm4 mRNA in the stem cells of RSS-litter and RSS-clinical-GA chicks, in contrast to the normal expression of Olfm4 mRNA in RSS-astrovirus and RSS-clinical-BR chicks. All chicks regardless of infection status showed normal expression of Ki67 mRNA in crypt cells, Muc2 mRNA in goblet cells, and SGLT1 or PepT1 mRNA in enterocytes. These results demonstrate that RSS, which can be induced by different etiologies, can show differences in the expression of the stem cell marker Olfm4.

Key words: runting stunting syndrome, Olfm4, PepT1, mucin-2, Ki67, cystic crypts, broiler

INTRODUCTION

Malabsorption syndromes (MASs) are transmissible, multifactorial enteric diseases that affect young poultry and cause high economic losses to the poultry industry (Rebel et al., 2006; Johnson et al., 2020). Several intestinal MASs are recognized in chickens and turkey poults, such as runting stunting syndrome (RSS) in chickens (Songserm et al., 2000) and poult enteritis complex in turkeys (Barnes et al., 2000). Clinically, these malabsorption syndromes include diarrhea, decreased feed intake, dehydration, poor feathering, marked growth depression, and a marked unevenness in size uniformity. Secondary leg problems such as rickets or brittle bones have been observed (Rebel et al., 2006). Necropsied birds have paler small intestines containing watery and frothy contents and undigested feed in the large intestine (Zavala and Sellers,

2005; Pantin-Jackwood, 2013) indicating lack of absorptive capability of the small intestine. At the morphological level, chicks have blunted and fused villi and dilated intestinal crypts, which is often referred to as cystic enteropathy (Reece and Frazier, 1990; Goodwin et al., 1993; Kang et al., 2012; Pantin-Jackwood, 2013). The lamina propria shows infiltrates of heterophils, macrophages, and lymphocytes (Rebel et al., 2006; Pantin-Jackwood, 2013 de Oliveria et al., 2021). The diarrhea caused by MAS often decreases following disease onset, but stunted birds do not recover, and poor uniformity usually remains for the life of the flock (Barnes et al., 200; Zavala and Sellers, 2005).

Clinical signs of RSS can be reproduced by inoculating young chicks with intestinal homogenates or by placing them on litter from affected flocks (Montgomery et al., 1997; Songserm et al., 2000; Songserm et al., 2002a; Kang et al., 2012). A number of viruses have been implicated as possible etiologic agents of RSS. Some clinical signs of RSS have been induced by infection with coronavirus (Hauck et al., 2016), astrovirus (Kang et al., 2018), parvovirus (Zsak et al., 2013), and an entero-like virus (Decaesstecker et al., 1986). Kim *et al.* (2020) reported that in four analyzed RSS flocks all contained astroviruses, which suggested that astroviruses play a key role in RSS. Furthermore, de Oliveira *et al.* (2021) showed that gallivirus was associated with the presence or absence of RSS lesions. Using a metagenomic analysis, Devaney *et al.* (2016) identified 20 DNA and RNA viral families in RSS-affected chickens. Lima *et al.* (2019), however, found that there were no statistically significant differences in the intestinal viromes of RSS and healthy chickens, which indicated a lack of association

between MAS and enteric viruses. Thus, there appear to be multiple etiological agents that can cause clinical signs of RSS.

Optimal nutrient absorption requires a functioning small intestine, which consists of stem cells in the crypts that differentiate into the absorptive and secretory cells lining the villi. Replicating stem cells express Ki67, a marker for cell proliferation. In chickens, intestinal stem cells express low mRNA levels of leucine-rich repeat-containing G protein coupled receptor 5 (Lgr5) and high levels of olfactomedin 4 (Olfm4) (Zhang and Wong, 2018). Olfm4 is a glycoprotein that is closely associated with many digestive diseases in humans (Wang et al., 2018). Absorptive enterocytes express a number of amino acid, peptide, mineral, and monosaccharide transporters (Wong et al., 2017). The mRNA for peptide transporter a (PepT1) and sodium glucose cotransporter 1 (SGLT1) have been localized to enterocytes in chickens using *in situ* hybridization (ISH) (Zhang and Wong, 2017; Zhang et al., 2019). Secretory cells such as goblet cells that express mucin 2 (Muc2) have been localized along the villi as well as in the crypts of chickens using ISH (Liu et al., 2020; Reynolds et al., 2020).

The pathogenesis of RSS may be due to a failure of intestinal stem cells to proliferate and differentiate into the enterocytes needed for nutrient absorption. To investigate this hypothesis, a retrospective study was performed on archived RSS tissues to characterize intestinal stem, absorptive, and secretory cells. The objective of this study was to examine intestinal morphology and the mRNA expression of various stem (Olfm4), proliferative (Ki67), absorptive (PepT1, SGLT1), and secretory (Muc2) cell markers in the small intestine of chickens showing clinical signs of RSS arising from experimentally induced and natural infections.

MATERIALS AND METHODS

Animals and tissue samples

Tissue samples were obtained from four previous studies of broiler chicks exposed experimentally to litter from RSS-affected flocks or challenged with astrovirus and chicks that exhibited clinical signs of RSS due to natural infections. All intestinal samples were fixed in formalin, embedded in paraffin, and stored. Although cystic crypts were observed in the duodenum, jejunum, and ileum of RSS chicks (de Oliveria et al., 2021), the analysis was limited to duodenum and jejunum because those were the only available archived samples.

Study 1. RSS was induced in broiler chicks (RSS-litter chicks) using contaminated litter from a commercial broiler farm with a history of clinical RSS as described by Kang *et al.* (2012). For the RSS challenge, 1-day-old chicks were placed on litter material obtained from a local commercial broiler farm with a history of clinical RSS. One-day-old control chicks were placed on fresh pine shavings as bedding material. Chicks were euthanatized at 5, 8, and 12 days postchallenge (dpc). The duodenal loop (n = 4–6) was collected from RSS-litter and control chicks. Chicks were shown to be positive for astrovirus using ISH.

Study 2. One-day-old chicks were challenged with an astrovirus isolated in cultured Leghorn male hepatoma (LMH) chicken hepatocellular carcinoma epithelial cells and back-passaged five times in chickens to induce RSS (RSS-astrovirus chicks) as described by Kang *et al.* (2018). Control chicks were challenged with tissue culture media. The duodenum was collected from RSS-astrovirus and control chicks at 1 to 5 dpc. Samples from 2 dpc to 5 dpc were analyzed (n = 4–6) in this study.

Study 3. Intestinal tissues collected from chicks that were from poultry houses suspected of RSS (RSS-clinical-GA chicks) were submitted to the Poultry Diagnostic and Research Center (PDRC) at the University of Georgia for analysis. These tissues were submitted as a container of fixed intestinal tissue from multiple chicks. Three different clinical cases were analyzed. For Clinical Case GA-1, the duodenum and jejunum of 11 chicks of unknown genetic breed at 15 days of age were submitted. Gross lesions were observed in five of 11 chicks. Histologic lesions were seen in 11 of 14 intestinal sections. For Clinical Case GA-2, eight samples of jejunum from chicks of unknown genetic breed at 11 days of age were submitted. RSS lesions were seen in the jejunum (four of eight). Intestines from this case were positive for astrovirus and reovirus. For Clinical Case GA-3, nine jejunal samples from Ross broiler chicks at 11 days of age were submitted, of which seven had RSS lesions. Reovirus and astrovirus were isolated from the intestines. The astrovirus was genetically similar to viruses isolated from chicks with white chick syndrome. Four to seven replicates were analyzed per case.

Study 4. Seven-day-old chicks that showed clinical signs of RSS (e.g., small size or low body weight) were collected from farms and flocks that had a previous history of RSS in the state of Minas Gerais, Brazil. Duodenal and jejunal tissue were examined for histopathology and for the presence of viruses by next generation sequencing as described by de Oliveira *et al.* (2021). Only duodenal tissue was examined in this study. The duodenal samples were separated into two groups: chicks without RSS lesions and negative for gallivirus (RSS^{-}-clinical-BR chicks, $n = 3$) and chicks with RSS lesions and positive for gallivirus (RSS^{+}-clinical-BR chicks, $n = 3$). All samples analyzed were positive for astrovirus.

Identification of cell types with ISH

Formalin-fixed paraffin-embedded intestinal samples were sectioned at PDRC, placed on slides, and then shipped to Virginia Tech (Blacksburg, VA). For ISH, the RNAscope 2.5 HD detection reagent kit (Brown; Advanced Cell Diagnostics, Newark, CA) and probes for the intestinal stem cell marker olfactomedin 4 (Olfm4, accession no. NM_001040463.1) (20), oligopeptide transporter (PepT1, accession no. KF366603.1) (Zhang and Wong, 2017), sodium-glucose transporter (SGLT1, accession no. NM_001293240.1) (Zhang et al., 2019), mucus component mucin 2 (Muc2, accession no. JX284122.1 (Liu et al., 2020; Reynolds et al., 2020), and proliferating cell marker Ki67 (accession no. XM_004942359.3) were used. For studies 1 and 3 all five genes were examined by ISH, whereas for studies 2 and 4 only Olfm4, PepT1, and Muc2 were examined. Tissue sections were counterstained with 50% Gill's hematoxylin no. 1 (Sigma-Aldrich, St. Louis, MO), rinsed in water, and then placed in 0.02% ammonia water to turn the purple stain to blue. The slides were dehydrated in a graded series of ethanol (70%, 95%, 95%) and a final xylene wash. Slides were sealed with clear mount solution (American Master Tech Scientific, Inc., Lodi, CA) and a glass coverslip. In all cases, control and RSS samples were processed simultaneously during the RNAscope procedure. Images were captured under bright field using a Nikon Eclipse 80i microscope and a DS-Ri1 digital camera (Nikon Instruments, Inc., Melville, NY).

Image analysis

Villus height (VH) and crypt depth (CD) were measured on slides processed with ISH for Olfm4 mRNA using ImageJ (Schindelin et al., 2012). Olfm4 mRNA is a marker for intestinal stem cells and was used to delineate the functional crypt (Zhang and Wong,

2018; Liu et al., 2020). Crypt depth was measured from the base of the crypt to the top of the cells staining for Olfm4 mRNA. Only normal crypts were measured for calculating CD. Villus height was measured from the top of the region staining for Olfm4 mRNA to the tip of the villus. In the case of samples from RSS-litter and RSS-clinical chicks where there was no expression of Olfm4 mRNA, the crypt region was delineated from the villus by morphological differences between the base of the villi and the top of the crypt. Approximately 60 normal crypts and 20 intact villi per section were measured for each replicate chick.

Cystic crypts were differentiated from normal crypts by the presence of flattened epithelial cells lining the cystic crypt as previously described (Kang et al., 2012). For each sample, rectangular regions were randomly drawn on Olfm4 stained images using the ImageJ drawing tool from the top, left, right, and bottom areas of the section. Within each region, the total number of normal and cystic crypts were counted. The frequency of cystic crypts was then calculated based on the average number of cystic crypts divided by the average total number of crypts per region. For statistical analysis all frequencies were transformed using square-root arcsine to address non-normality of the data.

All cystic crypts were measured along the central diameters in micrometers, top to bottom and left to right using the drawing tool on ImageJ. The two-dimensional images of cystic crypts were determined to be multifoci ellipses with the majority being the traditional two-foci ellipse. The estimated area of each cystic crypt was calculated using the formula $A_{ellipse} = \pi ab$, where a = the radius of the major vertex and b = the radius of the minor vertex. The area measures of the cystic crypts were lognormally distributed so

data were transformed with a log10 transformation to conform to normality for statistical analysis.

Statistical analysis

All data were analyzed using JMP Pro v15.0 (SAS Institute Cary, NC). Morphological measurements and counts of Muc2 mRNA-expressing cells were non-normally distributed with unequal variances, so the nonparametric Welch test was used to analyze the RSS-astrovirus, RSS-litter, and sham infected control chicks, based on dpc and infection status. RSS-clinical-GA samples were analyzed as three different case submissions. RSS-clinical-BR chicks were analyzed based on the presence or absence of gallivirus by DNA sequencing. In instances of statistical significance ($P \leq 0.05$) the Steel-Dwass test was used for mean separation. When evaluating cystic crypts, samples from RSS-litter, RSS-astrovirus, RSS-clinical-GA, and RSS-clinical-BR chicks were evaluated separate from the control chicks using a *t*-test, as well as a one-way ANOVA following data transformation to evaluate differences between individual samples or submissions.

RESULTS

Intestinal morphology, stem, and differentiated cells in experimentally infected chicks reared on litter from RSS- affected flocks in Georgia

Chicks reared on litter from a farm with a history of clinical RSS (RSS-litter) showed increased CD at 5, 8 and 12 dpc; however, VH and the villus height to crypt depth ratio (VH/CD) were not different at any time point compared to control chicks reared on fresh pine shavings (Table 2-1). The frequency of cystic crypts in the duodenum of RSS-litter chicks at 5, 8, and 12 dpc ranged between 3.2% and 4.4% of the

total number of crypts. The average area of the cystic crypts ranged between 3899.1 ± 1033.2 and 5685.2 ± 956.5 μm^2. There were no cystic crypts observed in samples from control chicks.

RSS-litter chicks showed a complete absence of Olfm4 mRNA in the crypts of the duodenum at 5, 8 and 12 dpc, while the control chicks showed the expected strong expression of Olfm4 mRNA in the crypts (Fig. 2-1). The crypt cells for RSS-litter chicks were still proliferating because expression of Ki67 was similar to crypt cells from control chicks. Enterocytes of RSS-litter chicks expressed both PepT1 and SGLT1 mRNA. and goblet cells expressed Muc2 mRNA, similar to intestinal cells of control chicks. Fig. 2-2 shows higher magnification images of cells staining for Olfm4, Ki67, Muc2, and SGLT1 mRNA as well as examples of cystic crypts from RSS-litter chicks. Some cystic crypts were surrounded by a thin layer of cells that expressed mRNA for the proliferation cell marker Ki67, goblet cell marker Muc2, and enterocyte marker SGLT1.

Intestinal morphology and stem and differentiated cells in experimentally infected chicks challenged with astrovirus.

Astrovirus has been proposed as an etiological agent for RSS and thus represents another model for experimentally induced RSS. For astrovirus-infected chicks (RSS-astrovirus), there was no difference in VH, CD, or VH/CD at 2, 3, 4, and 5 dpc compared to control chicks (Table 2-2). One cystic crypt was detected at 4 dpc in the duodenum of one RSS-astrovirus chick.

In contrast to the RSS-litter chicks, astrovirus challenged chicks showed normal expression of Olfm4 mRNA in the crypt, PepT1 mRNA in enterocytes, and Muc2 mRNA in goblet cells similar to control chicks (Fig. 2-3). Because these tissue samples showed

normal expression of Olfm4 mRNA, they were not analyzed further for Ki67 and SGLT1 mRNA expression.

Intestinal morphology and stem and differentiated cells in three clinical cases of RSS submitted to the Poultry Diagnostic and Research Center at the University of Georgia.

Because only intestinal samples from chicks showing clinical signs of RSS were submitted to the PDRC for diagnosis, no control chicks from these three flocks were available for analysis. Thus, only a comparison was made among the three clinical cases of RSS in Georgia. RSS-clinical sample GA1 had the greatest VH and VH/CD compared to RSS-clinical samples GA2 and GA3 (Table 2-3). There was no difference in CD among the three samples. There was no difference in frequency of cystic crypts and cystic crypt area for the three RSS-clinical-GA samples.

Similar to the results with chicks experimentally infected with RSS-litter, the intestines from RSS clinical cases GAl, GA2, and GA3 showed a total absence of Olfm4 mRNA in the crypts but a normal mRNA expression pattern of Ki67 in crypt cells, PepT1 and SGLT1 in enterocytes, and Muc2 in goblet cells (Fig. 2-4).

Intestinal morphology and stem and differentiated cells in clinical cases of RSS in Brazil.

Intestinal samples from chicks that showed clinical signs of RSS from farms in Brazil with a previous history of RSS were collected and analyzed for the presence of viruses using DNA sequencing. These clinical samples were separated into chicks with cystic crypts and positive for gallivirus (RSS^{+}-clinical-BR) and chicks without cystic crypts and negative for gallivirus (RSS^{-}-clinical-BR). The gallivirus-negative RSS^{-}-

clinical-BR chicks showed only a single cystic crypt in one of the analyzed samples, whereas gallivirus-positive RSS^{+}-clinical-BR chicks showed a mean of 11.7% cystic crypts with a cystic crypt area of 5930.5 ± 584.3 um^{2} for the three analyzed samples (Table 2-4). The gallivirus-positive RSS^{+}-clinical-BR chicks had increased CD but no change in VH, resulting in a decreased VH/CD compared to gallivirus-negative RSS^{-}-clinical-BR chicks.

The duodenal samples for both the gallivirus-negative RSS^{-}-clinical-BR and gallivirus-positive RSS^{+}-clinical-BR chicks expressed Olfm4 mRNA in stem cells, PepT1 mRNA in enterocytes, and Muc2 mRNA in goblet cells (Fig. 2-5). Because these samples also showed normal expression of Olfm4 mRNA, they were not analyzed further for Ki67 and SGLT1 mRNA expression.

DISCUSSION

Runting stunting syndrome is characterized by persistent stunted growth accompanied by abnormal intestinal morphology, mainly the presence of cystic crypts. In the RSS-litter chicks and RSS-clinical-BR chicks, which both showed a high percentage of cystic crypts, there was an increase in CD compared to the respective controls. By contrast, the presence of a single cystic crypt in the RSS-astrovirus samples did not affect CD. The observed increase in CD, as determined by an increase in mean measurement of CD based on morphology (RSS-litter chicks, Study 1) or cells stained for Olfm4 (RSS^{+}-clinical-BR, Study 4), suggested that there was an expansion of the population of stem cells, which would be needed to replace any lost or damaged intestinal villus cells. Fernando and McCraw (1973) had previously speculated that the crypt deepens in response to intestinal disease (e.g., coccidiosis) to maintain intestinal functionality.

Increased CD or crypt hyperplasia has been observed following a variety of intestinal infections. Research into the intestinal response to *Eimeria acervulina* infection reported that the crypt hyperplasia was accompanied by an increased proliferation rate of crypt cells to promote a rapid regeneration of the villus (Fernando and McCraw, 1973; 1977). Further, crypt hyperplasia has been described as a compensatory mechanism following the development of cystic crypts, which do not adequately provide the villus with replacement absorptive and secretory cells (Stringer et al., 2012). It is possible that the greater CD found in our study for RSS chicks is a compensatory response to try to maintain intestinal functionality.

Villus height following RSS, either experimentally infected or from field studies, was inconsistently affected. De Oliveira *et al.* (2021) reported an increase in VH in the duodenum of sick (RSS) chicks compared to healthy (control) chicks. While Montgomery *et al.* (1997) and Songserm *et al.* (2000) reported that VH varied throughout their RSS-infected population but the overall group mean was not different from control birds. Otto *et al.* (2006) reported significant shortening of villi in association with crypt hyperplasia in RSS-affected broilers. Similarly, Songserm *et al.* (2002b) reported a loss of overall absorptive surface area due to villi fusion and decreased VH. Overall, studies agree that VH/CD changes after RSS infection were mostly due to increased CD rather than significant VH changes. Our results agree with this finding as we consistently found increased CD in RSS-litter and RSS^{+}-clinical-BR chicks compared to their respective controls with no change in VH. There was, however, no morphological difference observed between RSS-astrovirus chicks and their controls. We also observed villi fusion occurring in all groups of RSS-infected chicks, with an increased prevalence of fusion

occurring near cystic crypts. The loss of VH, reduction in villi number from fusion, and occurrence of cystic crypts creates a less functional intestine in RSS-infected chicks. While the observed crypt hyperplasia is an attempt to compensate for the loss of functionality, it is likely that RSS-infected chicks are unable to overcome the intestinal damage enough to recover from the effects of RSS infection.

Cystic crypts are described as a hallmark lesion of RSS. The formation of cystic crypts occurs as epithelial cells lining the crypt degenerate, causing crypts to dilate and seal off from the rest of the intestinal tissue (Kang et al., 2012; de Oliveira et al., 2021). RSS chicks also had multifocal necrotic and dilated crypts, and some of these crypts had the lumen filled with cellular debris and heterophils (de Oliveira et al., 2021). In our study we observed with ISH some positive Muc2, Ki67, and SGLT1 mRNA signals inside the flattened epithelial cells lining the cystic crypts from the RSS-litter, RSS-clinical-GA, and RSS-clinical-BR chicks (only Muc2 expression was investigated in the last group). The expression level, however, was much less than in a normal crypt. For example, in normal chicken crypts Muc2 is expressed in an alternating cell pattern along the entire crypt (Liu et al., 2020; Reynolds et al., 2020), although in our study we observed sporadic numbers of cells staining for Muc2 or just one or two signals in a cystic crypt. It is unclear what the positive signals observed in cystic crypts mean. It could be that the signals coming from cystic crypts are mRNA remnants from when the crypt was functioning normally, or the cystic crypt may retain some limited functionality. In a mouse study, knockout of the intestinal homeostasis regulator gene *Cdx2* resulted in the development of long-lasting cystic crypts that retained limited proliferation functionality based on Ki67 expression (Stringer et al., 2012). It seems that until the

epithelial cells completely degrade away inside the cystic crypt, some gene expression will be detected, although no other study has investigated this phenomenon. Regardless of the exact mechanism behind the positive signals observed, the cystic crypts are likely not contributing replacement cells for the villi.

The most striking finding in the current study was the variable mRNA expression of the stem cell marker gene Olfm4 in the crypts of RSS chicks. Zhang and Wong (2018) had previously shown that all cells in the intestinal crypt strongly express Olfm4 mRNA. In this study, there was no association between expression of Olfm4 mRNA in crypt cells with mode of RSS induction. Olfm4 mRNA was not expressed in the experimentally infected RSS-litter chicks and naturally infected RSS-clinical-GA chicks but was expressed in the experimentally infected RSS-astrovirus chicks and the naturally infected RSS-clinical-BR chicks. Van Hemert *et al.* (2004) reported a transcriptome analysis of chicks experimentally infected with a homogenate from MAS chicks and found that Olfm4 was not one of the downregulated genes, which suggests that there was normal expression of Olfm4 mRNA in these MAS chicks. In our study, the crypt cells that did not express Olfm4 mRNA still expressed normal levels of mRNA for the proliferative cell marker Ki67 and Muc2 mRNA. Furthermore, all RSS samples tested showed the expected patterns of expression for SGLT1 (Zhang et al., 2019) or PepT1 (Zhang and Wong, 2017) mRNA in enterocytes and Muc2 mRNA in goblet cells (Liu et al., 2020; Reynolds et al., 2020). Together, these results suggest that the differentiation pathways from stem cells to enterocytes and goblet cells was not affected in spite of loss of Olfm4 mRNA.

Loss of Olfm4 mRNA expression was not associated with presence of virus in the intestinal crypts. Both astrovirus (Kang et al., 2018) and gallivirus (de Oliveira et al., 2021) were shown by ISH to be present in stem cells of RSS-astrovirus and RSS-clinical-BR samples, respectively, but in neither case was Olfm4 mRNA inhibited. Thus, it does not appear that suppression of Olfm4 mRNA is directly viral mediated. A more complete analysis of the virome of experimentally infected and naturally infected chicks may reveal a correlation between Olfm4 expression and the presence of specific viruses. It is also possible that the timing of sample collection and viral titer may play important roles in the suppression of Olfm4 mRNA expression.

It is likely that the initial viral infection caused a disruption of development of the normal chick microbiome. In normal chicks, the anaerobic portion of the microbiome is gaining in abundance at this age, and even mild inflammation would result in unfavorable conditions for their survival. De Oliveira *et al.* (2021) had previously reported a mild inflammation during RSS. In this case the lamina propria was expanded by a mild to moderate quantity of vacuolated macrophages, lymphocytes, plasmacytes, and some heterophils, with macrophages predominantly located close to the necrotic and dilated crypts. The gassy nature of the intestinal contents would likely result from the birds' malabsorption allowing bacterial growth on simple carbohydrates. Therefore, loss of the beneficial activity of the microbiome would contribute to the symptoms, and we have partly demonstrated this (Mundt et al., 2015). However, the mechanism of impairment and resolution of RSS elicited by the litter model has never been demonstrated.

Disruption of the Notch signaling pathway or knockout of selected genes in mice has resulted in loss of *Olfm4* expression in intestinal stem cells. Notch signaling is an

evolutionarily conserved process that is involved in determining cell fate and is essential for proliferation, differentiation, and maintenance of intestinal stem cells (Demitrack and Samuelson, 2016; Liang et al., 2019). The intestinal epithelium is continuously renewing itself by actively cycling stem and progenitor cells. Regulation of these processes is needed to balance proliferation and stem cell renewal with differentiation to ensure tissue homeostasis. The Notch receptor-ligand pathway consists of transmembrane Notch receptors (Notch1–4) and transmembrane ligands such as Delta-like (DLL)1, 3, and 4. The Notch receptor and its ligands are transmembrane proteins with large extracellular domains. Ligand binding results in proteolytic cleavage in the Notch receptor that releases the Notch intracellular domain (NICD). The NICD translocates to the nucleus to regulate transcription of Notch target genes. These genes include hairy and enhancer of split 1 (Hes1) and Olfm4, which promote proliferation and differentiation of intestinal stem cells towards the absorptive lineage, resulting in enterocyte development. In mammals, expression of Olfm4 in stem cells was directly dependent upon Notch signaling, with transcription activated through binding sites in the Olfm4 promoter (VanDussen et al., 2012). Inhibition of Notch signaling in mice with dibenzazepine, resulted in loss of Olfm4 mRNA in crypt stem cells (VanDussen et al., 2012). Knockout of the Notch 1 receptor or DLL1 and DLL4 in mice resulted in loss of Olfm4 mRNA expression in the crypt (Pellegrinet et al., 2011; Carulii et al., 2015). Further, loss of Olfm4 expression did not fully recover after 60 days even though the expression of other Notch pathway genes returned to normal levels (Carulli et al., 2015). Interestingly, knockout of the tight junction protein Claudin-7, which is not a member of the Notch pathway, in mice resulted in an almost complete loss of Olfm4-expressing stem cells and

disruption of intestinal epithelial cell differentiation (Xing et al., 2020). It is unclear exactly what role Olfm4 plays in intestinal stem cells. Some studies have suggested that it participates in the regulation of cell proliferation and apoptosis (Kobayashi et al., 2007). Related to that suggestion, Carulli *et al.* (2015) found that the number of intestinal stem cells was reduced following Notch1 knockout and reduction of Olfm4. Much less is known about the Notch pathway and its role in stem cell maintenance and differentiation in avian species (Zhang et al., 2019). Based on results from mammalian studies, however, we speculate that in the case of RSS-litter and RSS-clinical-GA chicks there may be a disruption in the Notch signaling pathway, resulting in loss of Olfm4 mRNA in crypt cells and possibly a reduction in the population of intestinal stem cells, which may contribute to the pathogenesis of RSS.

There is precedent for Notch pathway disruption from an intestinal infection. Infection with transmissible gastroenteritis virus in pigs targets the crypt intestinal stem cells and niche regulator Paneth cells. This resulted in inhibition of Notch signaling leading to a decrease in the number of Paneth cells and Olfm4-expressing stem cells and increase in the proliferation of goblet cells at the expense of enterocytes (Wu et al., 2020). Additionally, infection of pig intestinal crypts by *Lawsonia intracellularis*, the causative agent of proliferative enteropathy, triggered crypt hyperplasia by simultaneous induction of Notch signaling and inhibition of Wnt signaling. However, in this study, there was no change in Olfm4 expression, which suggests that the population of cells undergoing proliferation are not intestinal stem cells but rather progenitor or transit-amplifying cells that have yet to differentiate (Huan et al., 2020).

In summary, experimentally infected RSS-litter chicks and naturally infected RSS-clinical-GA chicks showed no expression of the stem cell marker Olfm4, but normal expression of Ki67 and Muc2 in the crypt. By contrast, the experimentally infected RSS-astrovirus chicks and naturally infected RSS-clinical-BR chicks expressed normal levels of Olfm4 in the crypt. All RSS samples showed normal expression of Muc2 in the goblet cells and SGLT1 and PepT1 in enterocytes, which shows that loss of Olfm4 mRNA in the crypt cells did not affect the production of goblet cells and enterocytes along the villi. These results demonstrate that RSS, which can be induced by different etiologies, can show differences in the molecular and cellular responses.

REFERENCES

Barnes H.J., J.S. Guy, and J.P. Vaillancourt. 2000. Poult enteritis complex. Rev Sci Tech. 19:565–588.

Carulli A.J., T.M. Keeley, E.S. Demitrack, J. Chung, I. Maillard, and L.C. Samuelson. 2015. Notch receptor regulation of intestinal stem cell homeostasis and crypt regeneration. Develop Biol. 402:98–108.

de Oliveira L.B., J.B. Stanton, J. Zhang, C. Brown, S.L. Butt, K. Dimitrov, C.L. Afonso, J.D. Volkening, L. Lara, C. de Oliveira, and R. Ecco. 2021. Runting and stunting syndrome in broiler chickens: histopathology and association with a novel picornavirus. Vet Pathol. 58:123–135.

Decaesstecker M., G. Charlier, and G. Meulemans. 1986. Significance of parvoviruses, entero-like viruses and reoviruses in the aetiology of the chicken malabsorption syndrome. Avian Pathol. 5:769–782.

Demitrack E.S., and L.C. Samuelson. 2016. Notch regulation of gastrointestinal stem cells. J Physiol. 594:4791–4803.

Devaney R., J. Trudgett, A. Trudgett, C. Meharg, V.A. Smyth. 2016. Metagenomic comparison of endemic viruses from broiler chickens with runting-stunting syndrome and from normal birds. Avian Pathol. 45:616–629.

Fernando M.A., and B.M. McCraw. 1973. Mucosal morphology and cellular renewal in the intestine of chickens following a single infection of Eimeria acervulina. J. Parasitol. 59:493–501.

Fernando M.A. and B.M. McCraw. 1977. Changes in the generation cycle of duodenal crypt cells in chickens infected with Eimeria acervulina. Z Parasitenkd. 52:213–218.

Goodwin M.A., J.F. Davis, M.S. McNulty, J. Brown, and E.C. Player. 1993. Enteritis (so-called runting stunting syndrome) in Georgia broiler chicks. Avian Dis. 37:451–458.

Hauck R., R.A. Gallardo, P.R. Woolcock, and H.L. Shivaprasad. 2016. A coronavirus associated with runting stunting syndrome in broiler chickens. Avian Dis. 60:528–534.

Huan Y.W., R.J. Bengtsson, N. MacIntyre, J. Guthrie, H. Finlayson, S.H. Smith, A.L. Archibald, and T. Ait-Ali. 2017. Lawsonia intracellularis exploits β-catenin/Wnt and Notch signalling pathways during infection of intestinal crypt to alter cell homeostasis and promote cell proliferation. PloS ONE 12:e0173782.

Johnson T., and M. Day. 2020. Multicausal enteric diseases. In: Swayne D, M. Boulianne, C. Logue, L. McDougald, V. Nair, and D. Suarez, editors. Diseases of poultry. 14th ed. Ames (IA): Wiley-Blackwell. p. 1390–1393.

JMP, version 15.0. 1989-2021. SAS Institue Inc, Cary (NC): JMP Statistical Discovery. https://www.jmp.com/support/notes/35/282.html.

Kang K.I., M. El-Gazzar, H.S. Sellers, F. Dorea, S.M. Williams, T. Kim, S. Collett, and E. Mundt. 2012. Investigation into the aetiology of runting and stunting syndrome in chickens. Avian Pathol. 41:41–50.

Kang K., E. Linnemann, A.H. Icard, V. Durairaj, E. Mundt, and H.S. Sellers. 2018. Chicken astrovirus as an aetiological agent of runting-stunting syndrome in broiler chickens. J Gen Virol. 99:512–524.

Kim H.R., Y.K. Kwon, I. Jang, and Y.C. Bae. 2020. Viral metagenomic analysis of chickens with runting-stunting syndrome in the Republic of Korea. Virol J. 17:53.

Kobayashi D, S. Koshida, R. Moriai, N. Tsuji, and N. Watanabe. 2007. Olfactomedin 4 promotes S-phase transition in proliferation of pancreatic cancer cells. Cancer Sci. 98:334–340.

Liang S.J., X.G. Li, and X.Q. Wang. 2019.. Notch signaling in mammalian intestinal stem cells: determining cell fate and maintaining homeostasis. Curr Stem Cell Res Ther. 14:583–590.

Lima D.A., S.P. Cibulski, C. Tochetto, A. Varela, F. Finkler, T.F. Teixeira, M.R. Loiko, C. Cerva, D.M. Junqueira, F.Q. Mayer, and P.M. Roehe. 2019.The intestinal virome of malabsorption syndrome-affected and unaffected broilers through shotgun metagenomics. Virus Res. 26:9–20.

Liu K., M. Jia, and E.A. Wong. 2020. Delayed access to feed affects broiler small intestinal morphology and intestinal cell ontogeny. Poult Sci. 99:5275–5285.

Montgomery R.D., C.R. Boyle, W.R. Maslin, and D.L. Magee. 1997. Attempts to reproduce a runting/stunting-type syndrome using infectious agents isolated from affected Mississippi broilers. Avian Dis. 41:80–92.

Mundt E., S.R. Collett, R. Berghaus, A.A. Pedroso, M.D. Lee, and J.J. Maurer. 2015. Can bacteriotherapy using commercially available probiotics, prebiotic, and organic

acids ameliorate the symptoms associated with runting stunting syndrome in broiler chickens? Avian Dis. 59:201–206.

Otto P., E.M. Liebler-Tenorio, M. Elschner, J. Reetz, U. Löhren, and R. Diller. 2006. Detection of rotaviruses and intestinal lesions in broiler chicks from flocks with runting and stunting syndrome (RSS). Avian Dis. 50:411–418.

Pantin-Jackwood M.J. 2013. Multicausal Enteric Diseases. In: Swayne D.E., J.R. Glisson, L.R. McDougald, L.K. Nolan, D.L. Suarez and V.L. Nair, editors. Diseases of poultry. 13th ed. Ames (IA): Wiley-Blackwell. p. 1322–1325.

Pellegrinet L., V. Rodilla, Z. Liu, S. Chen, U. Koch, L. Espinosa, K.H. Kaestner, R. Kopan, J. Lewis, and F. Radtke. 2011. Dll1- and dll4-mediated notch signaling are required for homeostasis of intestinal stem cells. Gastroenterology 140:1230–1240.

Rebel J.M.J., F.R.M. Balk, J. Post, S. van Hemert, B. Zekarias, and N. Stockhofe. 2006. Malabsorption syndrome in broilers. World's Poult Sci J. 62:17–29.

Reece R.L., and J.A. Frazier. 1990. Infectious stunting syndrome of chickens in Great Britain: field and experimental studies. Avian Pathol.19:723–758.

Reynolds K.L., S.E. Cloft, and E.A. Wong. 2020. Changes with age in density of goblet cells in the small intestine of broiler chicks. Poult Sci. 99:2342–2348.

Schindelin J., I. Arganda-Carreras, E. Frise, V. Kayning, M. Longair, T. Pietzsch, S. Preibisch, C. Ruden, S. Saalfeld, B. Schmid et al.. 2012. Fiji: an open-source platform for biological-image analysis. Nat Methods 9: 676-682.

Songserm T., J.M. Pol, D. van Roozelaar, G.L. Kok, F. Wagenaar, and A.A. ter Huurne 2000. A comparative study of the pathogenesis of malabsorption syndrome in broilers. Avian Dis. 44:556–567.

Songserm T., B. Engel, D.J. Van Roozelaar, G.L. Kok, A. Pijpers, J.M.A. Pol, and A.A.H.M. ter Huurne. 2002a Cellular immune response in the small intestine of two broiler chicken lines orally inoculated with malabsorption syndrome homogenates. Vet Immunol Immunopathol. 85:51–62.

Songserm T., B. Zekarias, D.J. van Roozelaar, R.S. Kok, J.M. Pol, A.A. Pijpers, and A.A. ter Huurne. 2002b. Experimental reproduction of malabsorption syndrome with different combinations of reovirus, Escherichia coli, and treated homogenates obtained from broilers. Avian Dis. 46:87–94.

Stringer E.J., I. Duluc, T. Saandi, I. Davidson, M. Bialecka, T. Sato, N. Barker, H. Clevers, C.A. Pritchard, D.J. Winton, N.A. Wright, J.N. Freund, J. Deschamps, and F. Beck. 2012. Cdx2 determines the fate of postnatal intestinal endoderm. Development 139:465–474.

van Hemert S., A.J. Hoekman, M.A. Smits, and J.M. Rebel. 2004. Differences in intestinal gene expression profiles in broiler lines varying in susceptibility to malabsorption syndrome. Poult Sci. 83:1675–1682.

VanDussen K.L., A.J. Carulli, T.M. Keeley, S.R. Patel, B.J. Puthoff, S.T. Magness, I.T. Tran, I. Maillard, C. Siebel, Å. Kolterud, A.S. Grosse, D.L. Gumucio, S.A. Ernst, Y.H. Tsai, P.J. Dempsey and L.C. Samuelson. 2012. Notch signaling modulates proliferation and differentiation of intestinal crypt base columnar stem cells. Development 139:488–497.

Wang X., S. Chen, Y. Zhang, and C. Xu. 2018. Olfactomedin-4 in digestive diseases: a mini review. World J Gastroenterol. 24:1881–1887.

Wong E., E.R. Gilbert, and K.B. Miska. 2017. Nutrient transporter gene expression in poultry, livestock and fish. In: Scanes C.G., and R.A. Hill, editors. Biology of domestic animals. Boca Raton (FL): CRC Press. p. 319–344.

Wu A., B. Yu, K. Zhang, Z. Xu, D. Wu, J. He, J. Luo, Y. Luo, J. Yu, P. Zheng, L. Che, X. Mao, Z. Huang, L. Wang, J. Zhao and D. Chen. 2020. Transmissible gastroenteritis virus targets Paneth cells to inhibit the self-renewal and differentiation of Lgr5 intestinal stem cells via Notch signaling. Cell Death Dis. 11:1–16.

Xing T., L.J. Benderman, S. Sabu, J. Parker, J. Yang, Q. Lu, L. Ding, and Y.H.Chen. 2020. Tight junction protein claudin-7 is essential for intestinal epithelial stem cell self-renewal and differentiation. Cell Molec Gastroenterol Hepatol. 9:641–659.

Zavala G., and H. Sellers. 2005. Runting-stunting syndrome. In: Poultry informed professional. p. 1–10. https://esploro.libs.uga.edu/esploro/outputs/newsletterArticle/Poultry-informed-professional/9949315884402959#files_and_links.

Zhang H., and E.A. Wong. 2017. Spatial transcriptional profile of PepT1 mRNA in the yolk sac and small intestine in broiler chickens. Poult Sci. 96:2871–2876.

Zhang H., and E.A. Wong. 2018. Identification of cells expressing OLFM4 and LGR5 mRNA by in situ hybridization in the yolk sac and small intestine of embryonic and early post-hatch chicks. Poult Sci. 97:628–633.

Zhang H., D. Li, L. Liu, L. Xu, M. Zhu, X. He, and Y. Liu. 2019. Cellular composition and differentiation signaling in chicken small intestinal epithelium. Animals 9:870.

Zhang H., H. Li, J. Kidrick, and E.A. Wong. 2019. Localization of cells expressing SGLT1 mRNA in the yolk sac and small intestine. Poult Sci. 98:984–990.

Zsak L., R.M. Cha, and J.M. Day. 2013. Chicken parvovirus-induced runting-stunting syndrome in young broilers. Avian Dis. 57:123–127.

ACKNOWLEDGMENTS

J.M. was supported by United States Department of Agriculture HATCH grant VA-160130. E.W. was supported in part by the Virginia Agricultural Experiment Station and the Hatch Program of the National Institute of Food and Agriculture, U.S. Department of Agriculture (NIFA-USDA). Sample collection for R.E. was supported by the Fundação de Amparo à Pesquisa do Estado de Minas Gerais (FAPEMIG), Project Grant Number APQ-04398-16 and 02714-18.

FIGURE CAPTIONS

Figure 2-1. Cells expressing Olfm4, proliferation marker Ki67, PepT1, SGLT1, and Muc2 mRNA in Control and RSS chicks. Intestinal samples for Study 1 were from chicks that were challenged with clean litter (Control) or litter from houses with clinical RSS cases (RSS-litter) (9). Cells expressing Olfm4, Ki67, PepT1, SGLT1, and Muc2 mRNA were detected in the duodenum of broiler chickens at 5, 8, and 12 days postchallenge (dpc) with ISH using the RNAscope 2.5 HD kit (Brown). mRNA expression of the target gene was revealed as brown staining. There was no expression of Olfm4 mRNA in RSS-litter chicks. Tissues were counterstained with 50% hematoxylin. Images were captured at 100× magnification. Insets in the Control and RSS-litter samples at 5 dpc show higher magnification images.

Figure 2-2. Cells expressing Olfm4, proliferation marker Ki67, Muc2, and SGLT1 mRNA in cystic and normal crypts of RSS chicks. Intestinal samples are from chicks 8 days post challenge with litter from houses with clinical RSS cases as shown in Fig. 1. Cells expressing Olfm4, Ki67, Muc2, and SGLT1 mRNA were detected with ISH using

the RNAscope 2.5 HD kit (Brown). mRNA expression of the target gene was revealed as brown staining. Cystic crypts are indicated with black arrows. Tissues were counterstained with 50% hematoxylin. Images were captured at 200× magnification.

Figure 2-3. Cells expressing Olfm4, PepT1, and Muc2 mRNA in Control and RSS chicks challenged with astrovirus. Intestinal samples for Study 2 were from chicks challenged with culture medium (Control) or astrovirus isolated in cultured LMH chicken hepatocellular carcinoma epithelial cells and serially passaged in chickens (14). Cells expressing Olfm4, PepT1, and Muc2 mRNA were detected in the duodenum of broiler chicks at 5 days postchallenge with ISH using the RNAscope 2.5 HD kit (Brown). mRNA expression of the target gene was revealed as brown staining. Tissues were counterstained with 50% hematoxylin. Images were captured at 100× magnification.

Figure 2-4. Cells expressing Olfm4, proliferation marker Ki67, PepT1, SGLT1, and Muc2 mRNA in chicks displaying clinical signs of RSS. Three sets of clinical isolates from multiple RSS chicks were submitted to the University of Georgia Poultry Diagnostic and Research Center from commercial broiler flocks (Study 3). RSS-clinical-GA1 consisted of duodenum and jejunum from chicks of unknown genetic breed at 15 days of age; RSS-clinical-GA2 consisted of jejunum from chicks of unknown genetic breed at 11 days of age; and RSS-clinical-GA3 consisted of jejunum from Ross broiler chicks at 11 days of age. Cells expressing Olfm4, Ki67, PepT1, SGLT1, and Muc2 mRNA were detected using the RNAscope 2.5 HD kit (Brown). mRNA expression of the

target gene was revealed as brown staining. All tissues were counterstained with 50% hematoxylin. Images were captured at 100× magnification.

Figure 2-5. Cells expressing Olfm4, PepT1, and Muc2 mRNA in chicks from farms in Brazil that showed clinical signs of RSS. Duodenal tissue for Study 4 was previously collected, assessed for morphological changes and for the presence of viruses using DNA sequencing, and separated into groups that were positive or negative for gallivirus (10). Intestinal samples from RSS^{-}-clinical-BR chicks had no cystic crypts and were positive for astrovirus but negative for gallivirus. Intestinal samples from RSS^{+}-clinical-BR chicks had cystic crypts and were positive for both astrovirus and gallivirus. Cells expressing Olfm4, PepT1, and Muc2 mRNA were detected in the duodenum of 7-day-old broiler chicks with ISH using the RNAscope 2.5 HD kit (Brown). mRNA expression of the target gene was revealed as brown staining. Tissues were counterstained with 50% hematoxylin. Images were captured at 100× magnification.

TABLES

Table 2-1. Morphological changes in chickens with RSS induced by exposure to poultry litter from RSS affected flocks in Georgia.[A]

Treatment[B]	Days post challenge	% Cystic crypts	Cystic crypt area (μm^2)	Villus height (μm)	Crypt depth (μm)	VH/CD
Control	5	0^{b}		587.7 ± 62.1^{bcd}	42.2 ± 1.8^{c}	13.9 ± 1.3
Control	8	0^{b}		573.7 ± 43.1^{cd}	38.4 ± 1.3^{c}	14.5 ± 0.9
Control	12	0^{b}		743.6 ± 46.4^{abc}	52.9 ± 1.4^{b}	15.2 ± 1.0
RSS-litter	5	4.4 ± 1.2^{a}	3899.1 ± 1033.2	667.9 ± 43.1^{bcd}	57.4 ± 1.3^{ab}	11.8 ± 0.9
RSS-litter	8	3.2 ± 1.2^{a}	5076.2 ± 800.3	723.3 ± 41.0^{abcd}	58.4 ± 1.2^{ab}	12.6 ± 0.9
RSS-litter	12	4.3 ± 1.2^{a}	5685.2 ± 956.5	810.5 ± 41.0^{ab}	61.0 ± 1.2^{a}	13.3 ± 0.9
P value[C]		<0.0001	0.286	<0.0001	<0.0001	0.166

[A]Each value represents the mean ± standard error of the mean of four to six replicate birds per treatment timepoint. Values within a column not sharing a common lowercase letter are significantly different ($P < 0.05$) based on Steel-Dwass mean separation.
[B]RSS litter = intestinal samples from chicks grown on litter from farms with a history of RSS; Control = intestinal samples from chicks grown on fresh pine shavings.
[C]Welch analysis of variance.

Table 2-2. Morphological changes in chickens with RSS induced by astrovirus.[A]

Treatment[B]	Days post challenge	% Cystic crypts	Cystic crypt area (μm^2)	Villus height (μm)	Crypt depth (μm)	VH/CD
Control	2	0		713.6 ± 18.7[ab]	52.3 ± 13.0	14.4 ± 3.2
Control	3	0		886.1 ± 70.4[ab]	79.7 ± 10.4	11.4 ± 2.4
Control	4	0		1099.0 ± 138.7[a]	80.2 ± 6.4	14.0 ± 2.8
Control	5	0		1112.0 ± 113.1[a]	75.2 ± 4.4	15.1 ± 2.5
RSS-astrovirus	2	0		615.5 ± 22.3[b]	59.8 ± 3.2	10.9 ± 1.4
RSS-astrovirus	3	0		828.8 ± 22.3[ab]	78.0 ± 3.2	11.0 ± 1.4
RSS-astrovirus	4	1.1	3805.8[C]	982.1 ± 30.7[ab]	104.0 ± 8.7	9.6 ± 0.6
RSS-astrovirus	5	0		976.1 ± 48.5[ab]	86.2	11.5
P value[D]				0.014	0.142	0.602

[A]Each value represents the mean ± standard error of the mean of four to six replicate birds per treatment timepoint. Values within a column not sharing a common lowercase letter are significantly different ($P < 0.05$) based on Steel-Dwass mean separation.
[B]RSS-astrovirus = intestinal samples from chicks challenged with astrovirus propagated in cell culture; Control = intestinal samples from chicks challenged with cell culture medium.
[C]Only a single cystic crypt was observed and measured for RSS-astrovirus 4 days postchallenge.
[D]Welch analysis of variance.

Table 2-3. Morphological changes in chickens showing clinical RSS signs in Georgia.[A]

Sample[B]	Age (days)	% Cystic crypts	Cystic crypt area (μm^2)	Villus height (µm)	Crypt depth (µm)	VH/CD
RSS-clinical-GA1	15	7.5 ± 2.8	5174.4 ± 1461.1	996.0 ± 68.7[a]	58.9 ± 1.9[ab]	16.9 ± 1.1[a]
RSS-clinical-GA2	11	2.5 ± 2.5	2868.9 ± 2530.7	492.1 ± 55.1[b]	56.5 ± 1.5[ab]	8.7 ± 0.9[b]
RSS-clinical-GA3	10	4.6 ± 2.5	9868.5 ± 1789.5	584.0 ± 53.2[b]	62.5 ± 1.4[a]	9.4 ± 0.9[b]
P value[C]		0.162	0.334	<0.0001	0.023	<0.0001

[A]Each value represents the mean ± standard error of the mean of four to seven replicate birds per sample. Values within a column not sharing a common lowercase letter are significantly different ($P < 0.05$) based on Steel-Dwass mean separation.
[B]RSS-clinical-GA = intestinal samples from chicks suspected of having RSS submitted to the Poultry Diagnostic and Research Center at the University of Georgia.
[C]Welch analysis of variance.

Table 2-4. Morphological changes in chickens from a flock testing positive for RSS in Brazil.[A]

Sample[B]	Astrovirus[C]	Gallivirus[C]	% Cystic crypts[D]	Cystic crypt area (μm^2)	Villus height (μm)	Crypt depth (μm)	VH/CD
RSS$^-$-clinical-BR	+	–	0[b]		1013.6 ± 45.8	113.2 ± 3.5[b]	8.3 ± 0.3[a]
RSS$^+$-clinical-BR	+	+	11.7 ± 0.1[a]	5930.5 ± 584.3	946.3 ± 39.6	161.0 ± 4.3[a]	6.4 ± 0.4[b]
P value[E]			<0.0001		0.273	<0.0001	0.0002

[A]Each value represents the mean ± standard error of the mean of three replicate birds per sample. Values within a column not sharing a common lowercase letter are significantly different ($P < 0.05$) based on Steel-Dwass mean separation.
[B]RSS-clinical-BR = intestinal samples from chicks from a flock in Brazil that showed clinical signs of RSS.
[C]Samples were analyzed by DNA sequencing to determine the presence or absence of astrovirus and gallivirus.
[D]Only a single cystic crypt was detected in the RSS−-clinical BR samples and was not included.
[E]Welch analysis of variance.

FIGURES

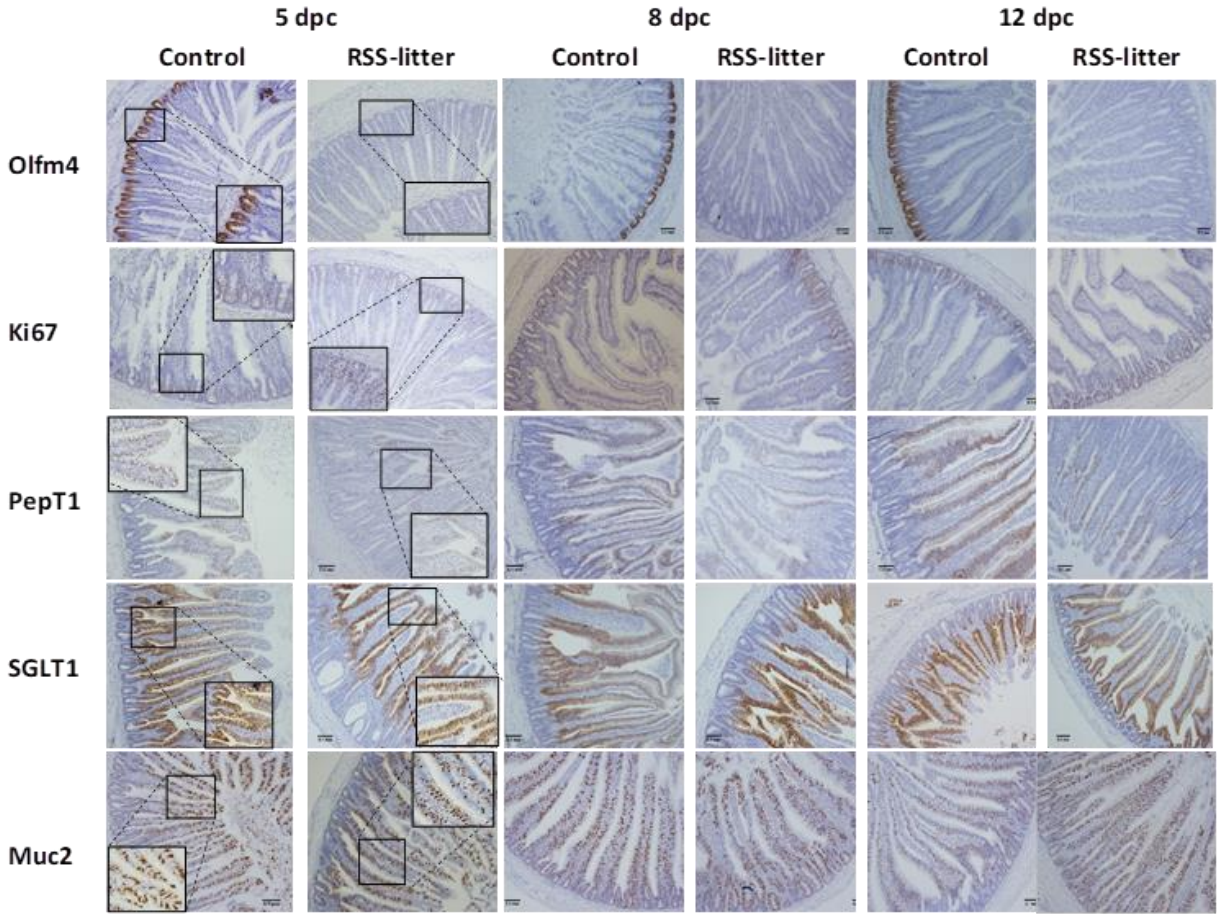

Figure 2-1.

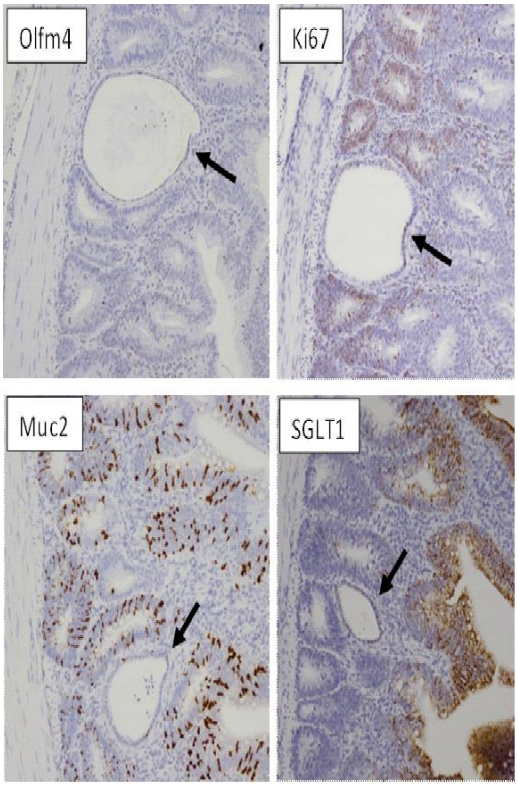

Figure 2-2.

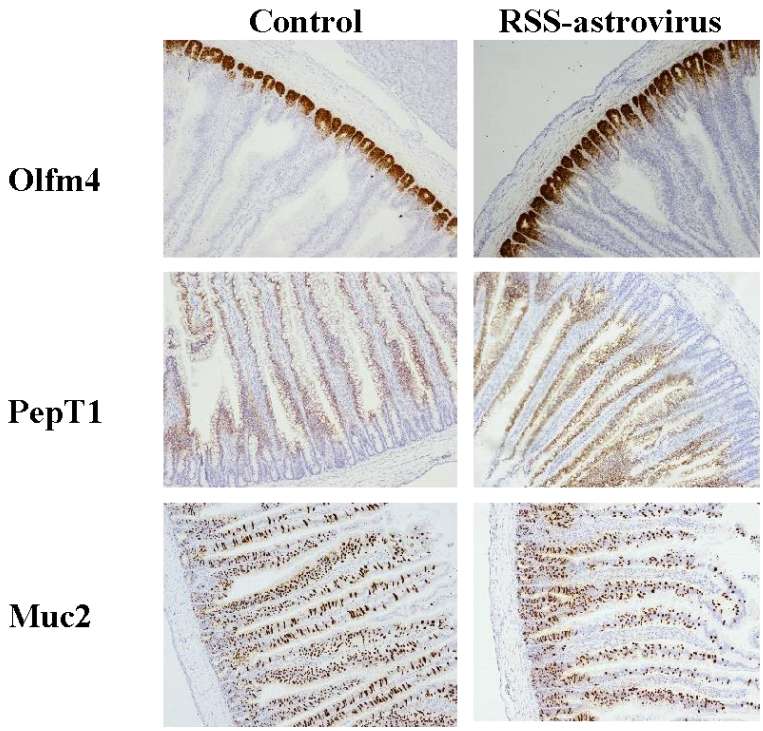

Figure 2-3.

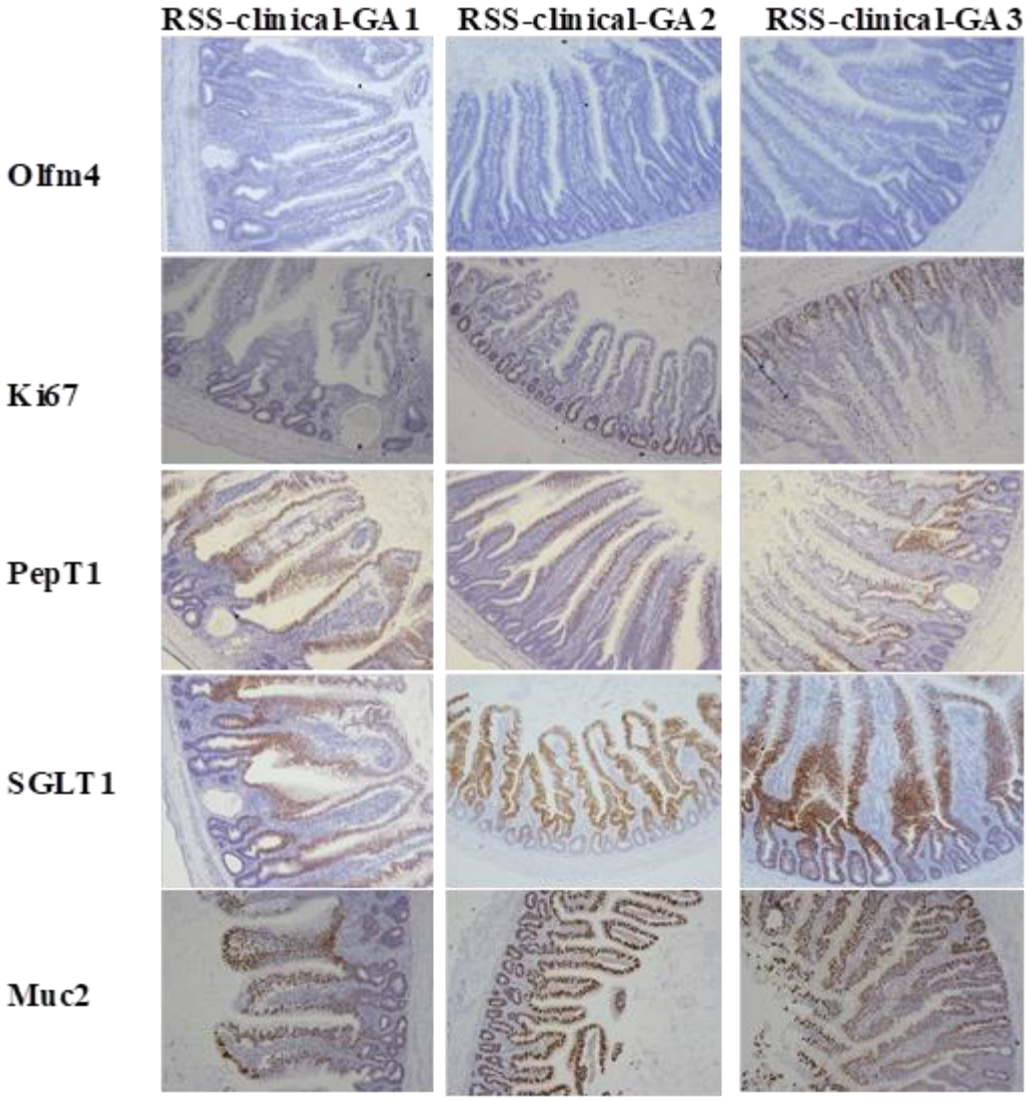
RSS-clinical-GA1
RSS-clinical-GA2
RSS-clinical-GA3
Olfm4
Ki67
PepT1
SGLT1
Muc2

Figure 2-4.

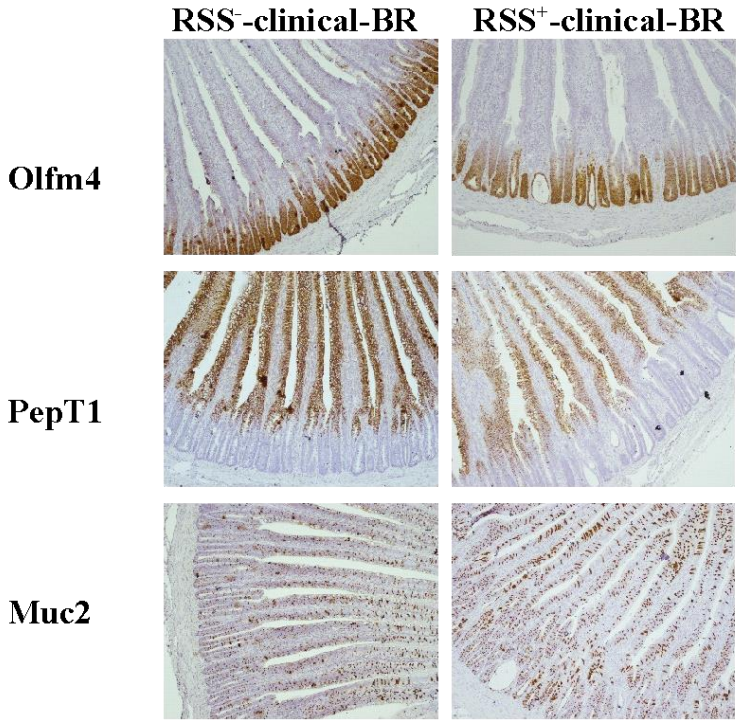

Figure 2-5.

Chapter 3: A temporal investigation of genes associated with intestinal homeostasis in broiler chickens following a single infection with *Eimeria acervulina*[*]

ABSTRACT Infection with the protozoan parasite *Eimeria* causes the economically devastating disease coccidiosis, which is characterized by gross tissue damage and inflammation resulting in blunted villi and altered intestinal homeostasis. Using quantitative PCR (qPCR) and in situ hybridization (ISH) methodology, changes in intestinal homeostasis following a single challenge with *Eimeria acervulina* in naïve broiler chickens were investigated. There were increased crypt depths for chickens infected with *E. acervulina* starting at 3 days post-infection (dpi) and continuing to the end of the study, 14 dpi. Accompanying these changes were increased mRNA abundance for collagen 3a1, Notch 1 and Ki67 cell proliferation in infected chickens compared to uninfected chickens after 7 dpi. Up to 7 dpi infected chickens had decreased Liver enriched antimicrobial peptide 2 (LEAP2), Mucin2 (Muc2), and Avian beta defensins 1 and 6 compared to uninfected chickens. LEAP2 mRNA continued being depressed through 14 dpi. *Eimeria* infection was visualized by in situ hybridization (ISH) with the *E. acervulina* sporozoite surface antigen gene (Ea-SAG), which was only detectable on 5 and 7 dpi by ISH and qPCR in *E. acervulina* infected chickens. The Muc2 ISH signal was decreased in regions where *E. acervulina* was present, suggesting that the decrease in Muc2 by qPCR may be from the loss of Mucin2 in the localized regions where the *Eimeria* had invaded the tissue.

Keyword: Crypt Depth, *Eimeria acervulina*, Intestinal Homeostasis, *In situ* hybridization, goblet cells

INTRODUCTION

One of the greatest health and management challenges faced in the poultry industry is the parasitic disease coccidiosis, caused by *Eimeria spp*. which invades epithelial cells along the villi. *Eimeria* is considered ubiquitous in the environment and different species infect a specific host species (Blake and Tomley, 2014) as well as affect different regions of the gastrointestinal tract. *Eimeria acervulina* is one of the most common species that infect chickens, preferentially invading the duodenum (Conway and Mckenzie, 2007). Inside infected epithelial cells, *Eimeria* sporozoites multiply asexually increasing in number until the epithelial cell ruptures releasing parasites out to surrounding tissue. The released first generation merozoites invade epithelial cells and undergo their own asexual multiplication, schizogony resulting in a large infectious burden on the intestine (Warren and Ball, 1967). Eventually sexual reproduction results in a fertilized oocyst that also ruptures from an epithelial cell and is shed in the feces to sporulate in the environment. Nearby birds can then be infected or reinfected, in the case of the original host, with *Eimeria* to start the cycle over again. The infection-multiplication cycle repeats until chickens develop immunity and culminates in widespread tissue damage impairing the functionality of the intestine and reducing the performance of the bird.

In general, few studies have tracked broiler intestinal cell changes via molecular characterization following *E. acervulina* infection over 2 weeks post-infection, most studies have limited sampling to peak infection, to around 7 days post-infection. Previous studies have reported changes in host defense peptides, such as avian beta-defensins (AvBD) and Liver enriched antimicrobial peptide 2 (LEAP2) (Paris and Wong, 2013; Su

et al., 2017) and in intestinal functioning via digestive enzymes and nutrient transporters (Su et al., 2014; Miska and Fetterer, 2017). These studies have shown that in response to *E. acervulina* invasion, LEAP2 is downregulated and brush border nutrient transporters are downregulated which may restrict the amount of glutamate and other critical amino acids that are brought into the cell. The nutrient transporter changes are postulated to be a response by the epithelial cell to starve out the parasite (Paris and Wong, 2013). However, many epithelial cells fail to starve out the parasite and end up destroyed by the parasite induced rupture or by the host immune response.

To date no research has investigated the change in intestinal homeostasis following *Eimeria* infection. Intestinal homeostasis is the ideal state where the intestine balances nutrient digestion and absorption with maintaining defensive barrier functions without tipping too far into one function that impairs the other. *Eimeria* infection disrupts intestinal homeostasis by invading absorptive enterocytes and redirecting absorbed nutrients as well as causing tissue damage that activates the immune system. Fernando and McCraw (1973) have previously shown that intestinal crypt depth increases and villi height decreases following infection, but no work has investigated molecular changes supporting this change in intestinal structure. The stem cell marker gene Olfactomedin 4 can be utilized to evaluate crypt depth as it clearly delineates stem cells in the crypt from those of the villi (Zhang and Wong, 2018; Liu et al., 2020). Increases in crypt depth are likely increases in cell proliferation, though no one has evaluated changes in the gene expression of Marker of proliferation Ki67 or other proliferation genes.

Following peak infection of *Eimeria* villi height rebounds, again likely due to increased replacement cells from the crypt. Previously, Brautigan et al. (2017) correlated

increased villi height with collagen mRNA increases and increased collagen deposition; though no research has assessed collagen gene expression following intestinal tissue destruction. Similarly, villi growth would likely be accompanied by increased expression of cell differentiation signaling genes such as Notch 1 which is associated with differentiation of crypt stem cells into absorptive enterocytes (Fre et al., 2005).

Identification of *Eimeria* within intestinal cells have relied upon visualization of hematoxylin and eosin stained sections, using the unique morphological structures of the parasite to differentiate it from host cell structures (Conway and Mckenzie, 2007). Detection of specific *Eimeria* species relied on the location of lesions but in the past decade molecular advances have allowed the creation of species-specific primers for PCR-based detection methods (Carvalho et al., 2011). There have been past attempts at in situ hybridization (ISH) for *Eimeria* and other protozoan species, but these have targeted viruses infecting the parasite (Lee and Fernando, 1998; Del Cacho et al., 2001) or 18S rRNA of the species (Liebhart et al., 2006). The images obtained from these studies confirm that the parasite is present in the tissue, but they do not provide information about infection dynamics or invasion cell-type preferences of *Eimeria sp*. in intestinal tissue.

The main objective of this research was to characterize the change in intestinal homeostasis over time following a single challenge with *Eimeria acervulina* in naïve broiler chickens by examining gene expression and mucosal morphology. A second objective was to localize *Eimeria acervulina* in duodenal cells of infected broilers utilizing ISH.

MATERIALS AND METHODS

Animals and Tissue Sampling

All studies were carried out under protocols approved by the Beltsville Research Center Animal Care and Use Committee and conducted at the Animal Parasitic Disease Laboratory (USDA Agricultural Research Service, Beltsville, MD). Ross 708 broilers (Longenecker's Hatchery, Elizabethtown, PA) were raised from day of hatch to 21 d of age in wire battery cages. Broilers were fed a corn-soybean meal diet that met the nutritional requirements as described by the National Research Council (NRC, 1994). At 21 d of age broilers were orally gavaged with 2 ml of either sterile water (uninfected) or with 100,000 *Eimeria acervulina* oocysts from USDA BARC stock (infected). After infection chickens were returned to their cages (4 per cage) on opposite sides of the room to prevent cross-contamination.

Approximately 3 hours after infection, d 0 post-infection (dpi) samples were collected from both infected and uninfected treatments. Six cages per treatment were randomly selected and 1 chicken per cage was euthanized by cervical dislocation for intestinal sampling. Following euthanasia, blood samples were collected by cardiac puncture and placed into EDTA containing tubes. Samples were centrifuged at 2,000 × g at 4 °C to collect plasma for carotenoid measurements using previously described methods (Allen, 1987). An intact 5 cm segment from the center of the duodenal loop was cut away and rinsed with sterile PBS and placed into neutral buffered formalin for later histological analysis. Twenty-four hours after collection, samples were moved to 70% ethanol until embedding in paraffin. Additional duodenal segments were diced and snap frozen in liquid nitrogen and stored at -80 °C for gene expression analysis. This process was repeated on d 3, 5, 7, 10, and 14 dpi. Chickens sampled at each timepoint were

housed in different cages. Both chickens and feed were weighed at each time point to calculate BW gain (calculated by subtracting weight at d 21 from final weight at either 7 or 10 dpi), feed intake (FI; the amount of feed consumed between day 21 of age and end of study), and feed conversion ratio (FCR; calculated by dividing the amount of feed consumed between day 21 of age and end of study by the amount of weight gain).

Identification of Stem Cells and Morphological Measurements

The segments collected for histological analysis were embedded in paraffin (StageBio, Mount Jackson, VA). Formalin-fixed, paraffin embedded tissues were sectioned (5 to 6 µm) using a microtome and mounted on Superfrost-Plus glass slides (Electron Microscopy Sciences, Hatfield, PA). *In situ* hybridization (ISH) was conducted using the RNAscope (Advanced Cell Diagnostics, Newark, CA) method with a singleplex olfactomedin 4 (Olfm4) probe (NM_001040463.1) detected using the RNAscope 2.5 HD Assay–BROWN detection kit (Advanced Cell Diagnostics). Slides were counterstained with 50% Gill's hematoxylin no. 1 (Sigma-Aldrich, St. Louis, MO), rinsed in distilled water, and placed in 0.02% ammonia water to turn the purple stain to blue. Slides were sealed with VectaMount (Vector Lab, Burlingame, CA) and a glass coverslip.

Brightfield microscopy images were captured using a Nikon Eclipse 80i microscope with a DS-Ri1 digital camera. Villus height (VH) and crypt depth (CD) were measured on 40x magnification images using Image J software from the National Institutes of Health (Bethesda, MD). Olfm4 is a marker of intestinal stem cells and was used to define the functional crypt for CD measurements on Olfm4 ISH images (Zhang & Wong, 2018). For hematoxylin and eosin-stained images, CD was determined based on

morphological differences between the crypt and villi structures. VH was measured from the top of the functional crypt to the tip of the villus. Approximately 75 CD measurements and 30 VH measurements were taken per sample (n = 6 chickens per treatment timepoint).

RNA extraction and Quantitative PCR

Snap frozen samples were homogenized with TriReagent using a tissue lyser and total RNA was extracted using the Directzol RNA mini prep columns (Zymo Research, Irvine, CA). RNA concentration and purity were determined using a Nanodrop 1000 spectrophotometer (Thermo Fisher Scientific, Waltham, MA). Complementary DNA was synthesized using the Applied Biosystems high capacity cDNA reverse transcription kit (Thermo-Fisher Scientific). Gene expression was determined by quantitative PCR (qPCR). The qPCR reactions consisted of 5 µL Fast SYBR Green Master Mix (Applied Biosystems), 1µL of forward primer (5µM), 1µL of reverse primer (5 µM), and 1.5 µL of cDNA (diluted 1:30). Duplicate qPCR reactions were performed using an Applied Biosystems 7500 Fast Real-time PCR system (Thermo Fisher Scientific). Primers were designed using Primer Express 3.0 (Applied Biosystems) and are listed in Table 1. The *Eimeria acervulina* major sporozoite surface antigen gene (Ea-SAG) was identified as a potential parasite marker because of its conserved domain (in the superfamily cl12617 Sporozoite TA4 surface antigen pfam11054) shared between *E. acervulina, E. maxima,* and *E. tenella*. The mRNA sequence similarity between the three species was only 66% using the Clustal Omega Sequence Alignment tool (Sievers et al., 2011). There was no similarity to the chicken genome based on a BLASTn search (Boratyn et al., 2013). Chicken ribosomal protein L4 (RPL4) and ribosomal protein lateral stalk subunit P0

(RPLP0) were used as reference genes. The geometric mean of the Ct value for RPLP0 and RPL4 was subtracted from the Ct value for the target gene to obtain the ΔCt value for each sample. The average ΔCt value of the uninfected chickens at d0 was used as the calibrator to calculate ΔΔCt and fold change using the $2^{-\Delta\Delta Ct}$ method (Schmittgen and Livak, 2008).

Visualizing Eimeria acervulina in tissue

In situ hybridization was conducted on samples collected for histological analysis using the RNAscope methodology with a singleplex Ea-SAG (XM_013394133.1) probe and the RNAscope 2.5 HD Assay–BROWN detection kit. A second set of slides were prepared as serial sections and ISH was conducted with the Ea-SAG and Muc2 (JX284122.1) singleplex probes on serial sections and detected using the RNAscope 2.5 HD Assay–BROWN detection kit. These slides were counterstained with Alcian Blue (MilliporeSigma, St. Louis, MO) and then 50% Gill's hematoxylin no. 1 (Sigma-Aldrich) to detect acidic mucus glycoproteins. Slides were sealed with VectaMount and a glass coverslip. Brightfield microscopy images were captured using a Nikon Eclipse E600 microscope with a DS-Fi1 digital camera.

Statistical Analysis

Performance data (BW, BW gain, feed intake (FI), and feed conversion ratio (FCR)) and plasma carotenoids concentration were analyzed by two factor ANOVA considering time post-infection and infection status via JMP v15.0 (SAS Institute Cary, NC, USA). Mean separation was conducted using Tukey’s Honestly Significant Difference test when significant ANOVA results were observed. Gene expression data were transformed logarithmically to conform to normality for statistical analysis and are

presented as back-transformed means (Jørgensen and Pedersen, 1998). Data were analyzed for the effect of time by infection status using a one-way ANOVA of the data subset by infection status. Additionally, data were analyzed for the effect of infection status at each timepoint by a student's t-test. Morphological data were unable to be transformed to meet conditions of normal distribution, due to unequal variances; instead, were analyzed using the nonparametric Welch's one-way test for the effect of infection status at each timepoint. Statistical significance was established at $P \leq 0.05$ for all analyses.

RESULTS

Growth Performance Measurements

There was no significant interaction of infection status and dpi for any growth performance measurements (BW, BW gain, FI, FCR) (Table 3-2). All growth performance measurements were different over dpi ($P < 0.002$). Chickens at 14 dpi had the greatest BW, BWG, and FI compared to all earlier dpi, as well as FCR worse than 3 and 5 dpi but not different from 7 and 10 dpi. BWG of infected chickens was 87g less than uninfected chickens during the study period ($P = 0.0085$). Additionally, BW ($P = 0.073$) and FI ($P = 0.067$) tended to be lower in infected chickens than uninfected chickens. Decreased BW gain and FI are hallmark signs of *E. acervulina* infection.

Plasma carotenoid concentrations in infected and uninfected chickens were evaluated throughout the study as an indirect means of assessing *E. acervulina* infection (Fig. 3-1). Infected broilers had significantly reduced plasma carotenoids on 5 and 7 dpi ($P < 0.0001$) compared to uninfected chickens. Considering that there were significant reductions in plasma carotenoid concentrations and BW gain in infected chickens

compared to uninfected chickens it seems likely that the goal of a mild *E. acervulina* infection was achieved.

Morphology Measurements

Olfm4 is a stem cell marker and thus can be used to mark the crypt. The ISH for Olfm4 revealed clear differences in CD between infected and uninfected groups starting at 3 dpi and continuing through 14 dpi (Fig 3-2A and 3-2B). To compare the measurement of CD as revealed by Olfm4 ISH with the CD determined by morphology with hematoxylin staining, a set of serial sections were compared (Table 3-3). The CD difference between infected and uninfected groups was observed again ($P < 0.0001$), with the infected group having larger CD measures than uninfected chickens. Comparing the CD measures, there was an overall difference ($P = 0.048$) between hematoxylin stained and Olfm4 stained CD measures; where hematoxylin measures were greater than the Olfm4 measures.

As expected, VH was decreased for infected chickens during the peak of infection on 5 and 7 dpi as well as 10 dpi compared to uninfected chickens (Fig 3-2C). By 14 dpi the VH of infected chickens were the same as uninfected chickens. The recovery of VH was likely supported by the combination of replacement cells produced from the elongated crypts and the completion of the *Eimeria sp*. lifecycle with no subsequent reinfection.

Intestinal gene expression

Avian beta-defensins, LEAP2, and Muc2 are part of the defensive barrier function of the intestine protecting the body from pathogens. Infected chickens had decreased AvBD1 and AvBD6 mRNA compared to uninfected chickens at 5 and 7 dpi ($P < 0.05$;

Fig. 3-3A and 3-3B). Though on 5 dpi, the difference in AvBD6 mRNA is more due to an unexplained increase in uninfected chickens rather than the decrease in infected chickens. AvBD10 mRNA was also decreased in infected chickens but only on 7 dpi ($P < 0.05$); Fig. 3-3C). Additionally, LEAP2 mRNA was decreased in infected chickens starting on 3 dpi and continuing for every timepoint except for 10 dpi where there was no difference between infected and uninfected groups ($P < 0.05$; Fig. 3-3D). Further, Muc2 mRNA was decreased in infected chickens compared to uninfected chickens at 3 and 7 dpi ($P < 0.05$; Fig. 3-3E).

Col3a1, Ki67, Olfm4 and Notch1 are genes associated with maintaining intestinal functioning and homeostasis. Collagen 3a1 mRNA was increased in infected chickens compared to uninfected chickens on 7 dpi ($P < 0.05$; Fig. 3-4A). The proliferative cell marker Ki67 mRNA was greater in infected chickens compared to uninfected chickens at 3, 5, 7, and 10 dpi ($P < 0.05$; Fig. 3-4B). The stem cell marker gene, Olfm4 mRNA was not different between infected and uninfected chickens at any timepoint (Fig. 3-4C). Notch 1 mRNA was increased in infected chickens at 7 and 10 dpi compared with uninfected chickens (Fig. 3-4D).

All 5 defensive barrier function genes followed a common pattern in infected chickens during this study (Fig 3-3): there was a decrease in mRNA abundance at peak infection that increased on 10 and 14 dpi. This pattern was significant for AvBD1, AvBD10 and LEAP2 ($P < 0.05$) and numerical trends for AvBD6 and Muc2 ($P < 0.08$). Within these defensive genes AvBD10 and Muc2 had a numerical increase on 5 dpi before decreasing to 7dpi while AvBD1, 6 and LEAP2 consistently decreased after 0 dpi. LEAP2 differed from the other four defensive genes by bottoming out on 5 dpi instead of

7 dpi, and starting to increase on 7 dpi. In contrast to the defensive barrier genes, only Ki67 significantly varied over the course of the study in infected chickens (Fig 3-4). Ki67 mRNA was increased on 3 through 10 dpi compared to 0 dpi but 14 dpi was statistically similar to both the increased dpi and 0 dpi ($P < 0.05$). Notch1 numerically increased after 3 dpi, which appeared to decrease from 0 dpi ($P < 0.05$).

Most genes varied over time in uninfected chickens during the study. Specifically, AvBD1, AvBD6, LEAP2, Ki67, and Col3a1 mRNA had significant variation over time in uninfected chickens ($P < 0.05$). Defensin genes had a general pattern in this study where there was an early increase around 3 or 5 dpi and then a decrease with the lowest value at 10 dpi. The homeostasis genes Ki67 and Col3a1 do not have the same pattern as the defensin genes. Ki67 increased over time during the study, with a significant dip on 5 dpi ($P < 0.05$). Collagen 3a1, increased from 0 dpi to 5 dpi and then decreased after 5 dpi ($P < 0.05$).

Visualizing Eimeria acervulina in situ

E. acervulina sporozoite surface antigen (Ea-SAG) mRNA was only detectable in infected chickens on 5, 7, and 10 dpi and not detected in any uninfected chickens at any timepoint based on raw qPCR Ct values of less than 40, which is the maximum number of cycles for the qPCR reaction. The raw Ct value is the number of cycles required for the fluorescent signal to exceed the background level of the reaction and is inversely proportional to the amount of RNA in the sample. On days 5 and 7 dpi, 6 out of 6 infected chickens had Ct values lower than 40 (5 dpi average Ct = 19 and 7 dpi average Ct = 26); whereas on 10 dpi only 2 of 6 infected chickens had Ct values lower than 40 (10 dpi average Ct = 37). Due to the absence of detection of Ea-SAG in any uninfected

chickens and during days 0, 3, and 14 dpi in infected chickens no quantitative statistics were used to analyze the difference.

In situ hybridization with an Ea-SAG probe was conducted for all timepoints and treatments in this study (n = 3 chickens per treatment for 0, 3, 10 and 14 dpi, n=6 per treatment for 5 and 7 dpi). Presence of Ea-SAG mRNA was observed only in infected chickens on 5 and 7 dpi (Fig. 3-5), confirming the qPCR results. Infected chickens on 10 dpi did not have positive Ea-SAG ISH signals, though it is important to point out that the samples for ISH were collected from different individual chickens from the same cage than were used for qPCR. Therefore, it seems as though the presence of Ea-SAG at 10 dpi that was detected by qPCR is more of an individual chicken response than a general response since only 2 out of 6 chickens had any signal. On 5 dpi Ea-SAG expression in situ was present along the villi and in the crypt. (Fig. 3-5). By 7 dpi the Ea-SAG signals were restricted to a few contained regions along the villi.

To better understand where *Eimeria acervulina* invades within the duodenum we compared the location of Ea-SAG mRNA signal with the location of goblet cells. Using serial sections, the Muc2 mRNA signal was reduced in the same locations that the Ea-SAG mRNA signal was present (Fig. 3-6; see regions outlined in dashed red lines). At the same time there is no discernable decrease in number of blue-stained cells in proximity to the Ea-SAG signal.

DISCUSSION

Defensive barrier functions suppressed following infection.

The intestine maintains multiple layers of defensive barriers to protect from infection. The first defensive layer is the mucus layer composed of Muc2 and other

mucin proteins secreted from goblet cells and resident commensal microbial species. The mucus layer physically restricts access to the epithelial cells (Moran, 2014). Should a pathogen make it through the mucus layer, the epithelial cells are equipped to resist invasion attempts. All epithelial cells lining the villi express host defense peptides such as LEAP2 and AvBDs, which harm invading organisms. *Eimeria* sp. are capable of invading epithelial cells and are able to shape the cellular environment to promote their longevity and to resist attacks by host defenses (Lang et al., 2009; Zhang et al., 2015).

Previous studies have shown downregulation of defensive functions and specifically LEAP2 mRNA as a consequence of *Eimeria sp.* infection (Paris and Wong, 2013; Su et al., 2014; 2017). Paris and Wong (2013) hypothesized that *Eimeria sp.* invade epithelial cells and downregulate LEAP2 to prevent their own death. In response the invaded cell downregulates amino acid transporters lowering resources available to the parasite. Essentially, once the *Eimeria sp*. blocks the defensive capabilities of the epithelial cell, the cell attempts to starve and destroy the invading parasite as a way to limit the infection. Along with LEAP2, AvBDs have been reported to be downregulated on 7 dpi perhaps by the same mechanism (Su et al., 2017). It is worth noting that timepoints other than 7 dpi have not been investigated in many studies so direct comparisons are limited. It is likely that the downregulation of defense barrier functions causes a loss in protective function of the intestine, which explains the intensity of symptoms experienced by infected chickens around peak infection. Our results agree with this hypothesis as infected chickens had decreased mRNA abundance of AvBD1, AvBD6, LEAP2, and Muc2 on 7 dpi which coincided with the lowest relative BW gain and feed intake change over time between infected and uninfected chickens.

Five and 7 dpi are considered peak infection in solo challenge studies because the lifecycle of *E. acervulina* is fixed so that after each sporozoite undergoes 2-3 rounds of asexual reproduction it transitions to sexual reproduction (Warren and Ball, 1967). If there is no re-infection then the parasite in the intestine will exhaust its reproductive potential around 7 dpi when oocyst shedding typically peaks (Allen and Fetterer, 2002). Following peak infection then, the intestine begins to recover. In this study, a pattern of increasing AvBD1 and AvBD10 mRNA was observed after 7dpi, while LEAP2 mRNA began increasing after 5 dpi. We have no explanation for why LEAP2 reached its lowest value on 5 dpi rather than 7 dpi, but it stayed significantly decreased compared to the uninfected group on 7 and 14 dpi unlike the AvBDs. In addition to being a sign of recovery the increase in defensins post-peak may be a sign of immunity developing, as it has been well established that chickens develop immunity to *Eimeria sp.* infections following 3-4 reinfection cycles (Rose, 1987). Though an explicit study tracking molecular intestinal responses over the course of reinfections or multiple challenges have not been done.

In this study there were multiple instances of significant gene expression changes over time in uninfected chickens, for both defense and homeostasis genes. There is no clear explanation for this result. Infected and uninfected chickens were housed on opposite sides of the same room and there was no obvious environmental condition or stressor that impacted the uninfected chickens during this study. Considering the similar management and performance metrics, and that both defensive and homeostasis genes varied in uninfected chickens, it is likely that the intestine is not static and gene expression changes in healthy chickens is part of maintaining intestinal homeostasis.

Very few studies have reported the mRNA abundance of genes in healthy broilers over time so no comparisons can be made with established literature.

Morphological changes ensure intestinal recovery.

Crypt elongation following *Eimeria sp,* infection has been reported previously. Following infection with *E. acervulina,* duodenal crypt elongation was observed from 3 to 12 dpi compared with uninfected chickens (Fernando and McCraw, 1973). In a follow up study, the elongation was attributed to increased duodenal crypt cell proliferation rate starting at 2 dpi in infected chickens preceding the observed crypt elongation (Fernando and McCraw, 1977). Crypt depth increases are considered to be a result of damage to villi epithelial cells or increased epithelial cell turnover requiring replacement cells from the crypt to prevent loss of absorptive surface area. Crypt elongation associated with regenerating villi can be seen following bacterial diseases in chickens (Cao et al., 2013) and generally following inflammation in the intestine (Sprinz, 1962). The bacterium, *Lawsonia intracellularis* caused increased cell proliferation and crypt elongation without increasing intestinal stem cells; likely stimulating precursor cell proliferation outside of the crypt (Huan et al., 2017). Olfactomedin 4 expression has been previously shown to be restricted to cells within the intestinal crypt in chickens (Zhang and Wong, 2018). It may be that during *Eimeria* infection, Olfm4 is being retained in cells migrating out of the crypt due to the increased proliferation rates. This has been described in mice following radiation damage, where Olfm4 is thought to play a special role in crypt proliferation after a disruption to intestinal homeostasis (Itzkovitz et al., 2012).

Olfactomedin 4 mRNA abundance was not significantly different between infection groups at any timepoint, nor did it change over time in the infected group. In

contrast, Ki67 mRNA abundance increased after infection coinciding with and likely supporting the increased CD. At first this may seem contradictory due to the ISH results in Fig. 3-2; however, qPCR and ISH do not always match as qPCR assesses the whole tissue level, or whatever specific parts of the tissue are used for RNA extraction, while ISH localizes gene expression to specific cells. Perhaps laser microdissection to isolate the crypt would yield more specific gene expression results.

Homeostasis gene expression changes reinforce the villi recovery observed in this study. Following peak-infection, the villi growth rate of infected chickens increased rapidly; at the same time, Col3a1 mRNA abundance increased, likely supporting recovery. Collagen mRNA abundance increases coinciding with VH increases have been reported previously (Brautigan et al., 2017). Also, the Notch1 expression increase during the rapid growth period is likely a consequence of that growth as the villus requires mature enterocytes to replace damaged surface area (Tian et al., 2016). The Notch pathway controls the differentiation of epithelial cells migrating up the villi. Specifically, Notch1 is expressed within precursors committed to the absorptive lineage (Fre et al., 2005). As evidenced by the increased CD, recovering VH and increased Ki67 mRNA, it seems that cell proliferation was increased following *E. acervulina* infection.

Eimeria acervulina infection corresponds to changes in localized gene expression.

When visualizing *E. acervulina* in situ, Ea-SAG, sporozoite antigen was only detected later in infection (5, 7 and 10 dpi). This sporozoite antigen was expected to be detectable on 3 dpi. It is likely that with mild challenge and low sporozoite numbers associated with the challenge dose, it took longer for the *Eimeria* to reach detectable level. When viewing the Ea-SAG signal at higher magnifications (images not shown), the

positive signal detected in 5 and 7 dpi does not account for all of the parasites, identified by morphology. The gene selected was specifically a sporozoite surface antigen so it is possible that only the sporozoite stage of *E. acervulina* produced this mRNA and was highlighted. If this is the case, alternative marker genes could be developed with this strategy to highlight stage-specific progression of infection.

The signal reduction in Muc2 mRNA seen near Ea-SAG ISH signals corresponded to the reported decrease in Muc2 mRNA in infected chickens compared to uninfected chickens. Previous research has reported a decrease in Muc2 mRNA in the intestine of challenged chickens following *E. acervulina* (Wickramasuriya et al., 2021) or mixed *Eimeria* species challenges (Cox et al., 2010; Tan et al., 2014; Chen et al., 2015). Based on the images collected in this study, it may be that the decreased Muc2 mRNA abundance detected by qPCR is from the localized reductions near where *Eimeria* has invaded the tissue.

Mucin-2 is a mucus protein secreted by goblet cells lining the villi, and is a robust marker for visualizing goblet cells by ISH (Reynolds et al., 2020). Though traditionally, goblet cells are identified using the histology stains Alcian blue in combination with Periodic acid- Schiff reagent stain (AB-PAS) to identify blue stained acidic mucin cells and magenta stained neutral mucin cells. Reynolds et al., (2020) showed that ISH for Muc2 mRNA produced more stained cells than when stained with AB-PAS. This was also seen in the current study, though only Alcian blue was used. Additionally, the acidic mucin-stained cells did not appear to decrease in regions of Muc2 mRNA reduction. The Ea-SAG signal did not appear to overlap any of the blue acidic mucin-stained regions, suggesting that there was no sporozoite invasion of goblet cells. Deplancke and Gaskins

(2001) suggested that acidic mucins have stronger defensive barrier functions than neutral mucins, preventing sporozoite access to the epithelial cell. Therefore, the decrease in Muc2 mRNA signals may be the result of the parasite manipulating expression of defensive genes of the bird. This likely would not be able to affect the existing secretory vesicles within the goblet cell, as seen in these images.

Conclusions

Following an *E. acervulina* challenge at 21 days of age, infected chickens showed elongated crypts, decreased villi heights, and decreases in LEAP2 and Muc2 mRNA starting at 3 dpi. During peak infection (5 and 7 dpi) LEAP2, AvBD1, 6, 10, and Muc2 mRNA were decreased in infected chickens compared to uninfected chickens. After peak infection villi height of infected chickens rapidly increased compared to uninfected chickens to be equivalent at 14 dpi. The villi height increase was likely supported by increases in Col3a1 and Notch1 mRNA on 7 and 10 dpi; while the crypt elongation was supported by increased Ki67 mRNA following infection though no changes in Olfm4 mRNA were detected.

A specific marker for *E. acervulina* surface antigen gene was used to visualize *Eimeria* invading epithelial cells in duodenal tissue. The Ea-SAG probe was only clearly detected at 5 and 7 dpi but that may be due to the low challenge oocyst dose. There was a pattern of suppressed Muc2 mRNA in regions of the duodenal tissue where the Ea-SAG signal was present.

REFERENCES

Allen, P.C. 1987. Physiological responses of chicken gut tissue to coccidial infection: comparative effects of *Eimeria acervulina* and *Eimeria mitis* on mucosal mass, carotenoid content, and brush border enzyme activity. Poult. Sci. 66:1306-1315.

Allen, P. C., and R. Fetterer. 2002. Recent advances in biology and immunobiology of *Eimeria species* and in diagnosis and control of infection with these coccidian parasites of poultry. Clin. Microbiol. Rev. 15:58-65.

Blake, D. P., and F.M. Tomley. 2014. Securing poultry production from the ever-present *Eimeria* challenge. Trends Parasitol. 30:12-19.

Boratyn G.M., C. Camacho, P.S. Cooper, G. Coulouris, A. Fong, N. Ma, T.L. Madden, W.T. Matten, S.D. McGinnis, Y. Merezhuk, Y. Raytselis, E.W. Sayers, T. Tao, J. Ye, and I. Zaretskaya. 2013. BLAST: a more efficient report with usability improvements. Nucleic Acids Res. 41:W29-W33.

Brautigan, D.L., R. Li, E. Kubicka, S.D. Turner, J.S. Garcia, M.L. Weintraut, E.A. Wong. 2017. Lysolecithin as feed additive enhances collagen expression and villus length in the jejunum of broiler chickens. Poult. Sci. 96:2889-2898.

Cao, G. T., X. F. Zeng, A.G. Chen, L. Zhou, L. Zhang, Y.P. Xiao, and C.M. Yang, C. M. 2013. Effects of a probiotic, *Enterococcus faecium*, on growth performance, intestinal morphology, immune response, and cecal microflora in broiler chickens challenged with *Escherichia coli K88*. Poult. Sci. 92:2949-2955.

Carvalho, F. S., A.A. Wenceslau, M. Teixeira, J.A.M. Carneiro, A.D.B. Melo, and G.R. Albuquerque. 2011. Diagnosis of *Eimeria* species using traditional and molecular methods in field studies. Vet. Parasitol. 176:95-100.

Conway, D.P. and M.E. Mckenzie. 2007. Examination of lesions and lesion scoring. Pg. 17-40 in Poultry Coccidiosis: Diagnostic and Testing Procedures. 3rd ed. Blackwell Publishing Ltd, Oxford, UK

Chen, J., G. Tellez, J.D. Richards, and J. Escobar. 2015. Identification of potential biomarkers for gut barrier failure in broiler chickens. Front. Vet. Sci. 2:14.

Cox, C. M., L.H. Sumners, S., Kim, A.P. McElroy, M.R. Bedford, and R.A. Dalloul. 2010. Immune responses to dietary β-glucan in broiler chicks during an *Eimeria* challenge. Poult. Sci. 89:2597-2607.

Del Cacho, E., M. Gallego, C. Montes, F. López-Bernad, J. Quılez, and C. Sanchez-Acedo. 2001. *Eimeria necatrix* virus: intracellular localisation of viral particles and proteins. Int. J. Parasitol. 31:1269-1274.

Deplancke, B., and H.R. Gaskins. 2001. Microbial modulation of innate defense: goblet cells and the intestinal mucus layer. Am. J. Clin. Nutr. 73:1131S-1141S.

Fernando, M. A., and B.M. McCraw. 1973. Mucosal morphology and cellular renewal in the intestine of chickens following a single infection of *Eimeria acervulina*. J. Parasitol. 59:493-501.

Fernando, M. A., and B.M. McCraw. 1977. Changes in the generation cycle of duodenal crypt cells in chickens infected with *Eimeria acervulina*. Z. Parasitenkd. 52:213-218.

Fre, S., M. Huyghe, P. Mourikis, S. Robine, D. Louvard, and S. Artavanis-Tsakonas. 2005. Notch signals control the fate of immature progenitor cells in the intestine. Nature. 435:964-968.

Huan YW, R.J. Bengtsson, N. MacIntyre, J. Guthrie, H. Finlayson, S.H. Smith, A.L. Archibald, and T. Ait-Ali. 2017. *Lawsonia intracellularis* exploits β-catenin/Wnt and Notch signalling pathways during infection of intestinal crypt to alter cell homeostasis and promote cell proliferation. PloS ONE 12:e0173782.

Itzkovitz, S., A. Lyubimova, I.C. Blat, M. Maynard, J. Van Es, J. Lees, T. Jacks, H. Clevers and A. Van Oudenaarden. 2012. Single-molecule transcript counting of stem-cell markers in the mouse intestine. Nat. Cell Biol. 14:106-114.

Jørgensen, E., and A.R. Pedersen. 1998. How to obtain those nasty standard errors from transformed data-and why they should not be used. (Aarhus Univ, DetJordbrugsvidenskabelige Fakultet, Aarhus, Denmark), International Report 7.

Lang, M., M.Kann, H.Zahner, A.Taubert, and C. Hermosilla. 2009. Inhibition of host cell apoptosis by *Eimeria bovis* sporozoites. Vet. Parasitol. 160:25–33.

Lee, S., and M.A. Fernando. 1998. Intracellular localization of viral RNA in *Eimeria necatrix* of the domestic fowl. Parasitol. Res. 84:601-606.

Liebhart, D., H. Weissenböck, and M. Hess, M. 2006. In-situ hybridization for the detection and identification of *Histomonas meleagridis* in tissues. J. Comp. Path. 135:237-242.

Liu, K., M. Jia, and E.A. Wong. 2020. Delayed access to feed affects broiler small intestinal morphology and goblet cell ontogeny. Poult. Sci. 99:5275-5285.

Miska, K. B., and R.H. Fetterer. 2017. The mRNA expression of amino acid and sugar transporters, aminopeptidase, as well as the di-and tri-peptide transporter PepT1 in the intestines of *Eimeria* infected broiler chickens. Poult. Sci. 96:465-473.

Moran Jr, E.T. 2014. Intestinal events and nutritional dynamics predispose *Clostridium perfringens* virulence in broilers. Poult. Sci. 93:3028-3036.

National Research Council. 1994. Nutrient Requirements of Poultry. 9th rev. ed. Natl. Acad. Press, Washington, DC.

Reynolds, K., Cloft, S.E., and E.A. Wong. 2020. Changes with age in density of goblet cells in the small intestine of broiler chicks. Poult. Sci. 99:2342-2348.

Rose, M. E. 1987. Immunity to *Eimeria* infections. Vet. Immunol. Immunopathol. 17: 333-343.

Schmittgen T. D. and K. J. Livak. 2008. Analyzing real-time PCR data by the comparative C(T) method. Nat. Protoc. 3:1101–1108.

Sievers, F., A. Wilm, D. Dineen, T.J. Gibson, K. Karplus, W. Li, R. Lopez, H. McWilliam, M. Remmert, J. Soding, J. D. Thompson, and D. G. Higgins. 2011. Fast, scalable generation of high-quality protein multiple sequence alignments using Clustal Omega. Mol. Syst. Biol. 7:539.

Sprinz, H. 1967. Morphological response of intestinal mucosa to enteric bacteria and its implication for sprue and Asiatic cholera. Fed. Proc. 21:57-64.

Su, S., K.B. Miska, R.H. Fetterer, M.C. Jenkins, and E.A. Wong. 2014. Expression of digestive enzymes and nutrient transporters in *Eimeria acervulina*-challenged layers and broilers. Poult. Sci. 93:1217-1226.

Su, S., D.M. Dwyer, K.B. Miska, R.H. Fetterer, M.C. Jenkins, and E.A. Wong. 2017. Expression of host defense peptides in the intestine of *Eimeria*-challenged chickens. Poult. Sci. 96:2421-2427.

Tan, J., T.J. Applegate, S. Liu, Y. Guo, and S.D. Eicher. 2014. Supplemental dietary L-arginine attenuates intestinal mucosal disruption during a coccidial vaccine challenge in broiler chickens. Br. J. Nutr. 112:1098-1109.

Tian, H., B. Biehs, C. Chiu, C.W. Siebel, Y. Wu, M. Costa, F.J. de Sauvage, and O.D. Klein. 2015. Opposing activities of Notch and Wnt signaling regulate intestinal stem cells and gut homeostasis. Cell Rep. 11:33-42.

Warren, E. W., and S.J. Ball. 1967. Schizogonous stages of *Eimeria acervulina* Tyzzer, 1929. Nature. 214:829-830.

Wickramasuriya, S. S., I. Park, Y. Lee, W.H. Kim, C. Przybyszewski, C.G. Gay, J.G. van Oosterwijk and H.S. Lillehoj. 2021. Oral delivery of *Bacillus subtilis* expressing chicken nk-2 peptide protects against *Eimeria acervulina* infection in broiler chickens. Front. Vet. Sci. 8:562.

Zhang, H. and E.A. Wong, 2018. Identification of cells expressing *OLFM4* and *LGR5* mRNA by in situ hybridization in the yolk sac and small intestine of embryonic and early post-hatch chicks. Poult. Sci. 97:628-633.

Zhang, Z., S. Wang, J. Huang, L. Liu, M. Lu, M. Li, Y. Sui, L. Xu, R. Yan, X. Song, and X. Li. 2015. Proteomic analysis of *Eimeria acervulina* sporozoite proteins interaction with duodenal epithelial cells by shotgun LC-MS/MS. Mol. Biochem. Parasitol. 202:29–33.

FIGURE CAPTIONS

Figure 3-1. Plasma carotenoids concentration in uninfected and *Eimeria acervulina* infected chickens. Chickens were infected with 100,000 *Eimeria acervulina* oocysts (Infected) or sterile water (Uninfected) at 21 d of age on 0 day post infection (dpi). All values are means ± SEM. * Indicates the infected value was different ($P < 0.0001$) from the corresponding uninfected value at that timepoint.

Figure 3-2. Crypt elongation following infection with *Eimeria acervulina*. A. Expression of Olfm4 mRNA by in situ hybridization in the duodenum of broiler chickens that were infected at 21 days of age with either 100,000 *Eimeria acervulina* oocysts (Infected) or sterile water (Uninfected) and sampled at 3, 7, and 14 days post infection (dpi). All tissues were counterstained with 50% hematoxylin. Images were captured at 40X magnification (n=6). B. Crypt Depth (CD) and C. Villus Height (VH) were measured on sections that had been stained for Olfm4 by in situ hybridization. Measures were analyzed by infection status using the nonparametric Welch's one-way test significances are indicated by asterisks (*) along the x-axis.

Figure 3-3. Avian beta defensins (AvBD), Liver enriched antimicrobial peptide 2 (LEAP2), and Mucin 2 (Muc2) mRNA profiles following infection with *Eimeria acervulina.* Chickens were infected at 21 days of age with either 100,000 *Eimeria acervulina* oocysts (Infected) or sterile water (Uninfected) and sampled at 0, 3, 5, 7, 10 and 14 days post infection (dpi). RNA from duodenal tissue were analyzed by relative qPCR (n = 6) for expression of AvBD1 (A), AvBD6 (B) and AvBD10 (C), LEAP2 (D),

and Muc2 (E) mRNA. A one-way ANOVA was used to analyze Infected and Uninfected data separately and when significant, Tukey HSD was used for mean separation. Significant mean separations ($P < 0.05$) are indicated by "abc" for Uninfected means and "xyz" for Infected means. Additionally, a t-test was conducted for each dpi to assess the effect of infection. Significances ($P < 0.05$) are indicated by asterisks (*) along the x-axis.

Figure 3-4. Collagen 3a1 (Col3a1), Marker of proliferation Ki67, Olfactomedin 4 (Olfm4) and Notch 1 mRNA profiles following infection with *Eimeria acervulina.* Chickens were infected at 21 days of age with either 100,000 *Eimeria acervulina* oocysts (Infected) or sterile water (Uninfected) and sampled at 0, 3, 5, 7, and 14 days post infection (dpi). RNA from duodenal tissue were analyzed by relative qPCR ($n = 6$) for expression of Col3a1 (A), Ki67 (B), Olfm4 (C), and Notch 1 (D) mRNA. A one-way ANOVA was used to analyze Infected and Uninfected data separately and when significant Tukey HSD was used for mean separation. Significant mean separations ($P < 0.05$) are indicated by "abc" for Uninfected means and "xyz" for Infected means. Additionally, a t-test was conducted for each DPI to assess the effect of infection. Significances ($P < 0.05$) are indicated by asterisks (*) along the x-axis.

Figure 3-5. In situ hybridization analysis of *Eimeria acervulina* sporozoite surface antigen (Ea-SAG) mRNA following infection with *E. acervulina.* Chickens were infected at 21 days of age with either 100,000 *E. acervulina* oocysts (Infected) or sterile water (Uninfected) and sampled at 5 and 7 days post infection (dpi). Cells in the duodenum expressing Ea-SAG mRNA were detected using the RNAscope 2.5 HD kit (Brown) in

situ hybridization method. All tissues were counterstained with 50% hematoxylin. Images were captured at 40X magnification (n=6).

Figure 3-6. In situ hybridization analysis of *Eimeria acervulina* sporozoite surface antigen (Ea-SAG) and Mucin 2 (Muc2) mRNA following infection with *E. acervulina*. Chickens were infected at 21 days of age with either 100,000 *E. acervulina* oocysts (Infected) or sterile water (Uninfected) and sampled at 5 and 7 days post infection (dpi). Serial sections of the duodenum were analyzed by in situ hybridization using RNAscope 2.5 HD kit (Brown). On the left, stained cells expressing Ea-SAG mRNA appear brown; whereas on the right, cells expressing Muc2 mRNA appear brown. All tissues were counterstained with Alcian Blue and 50% hematoxylin to detect the mucin glycoprotein (cells appearing blue on all images). Images were captured at 100X magnification (n = 3). Red dashed ovals on infected images point out areas of decreased Muc2 mRNA in the same regions where Ea-SAG mRNA signal is present.

TABLES

Table 3-1. Primers for quantitative PCR

Gene name	Forward/Reverse Primers (5' to 3')	Amplicon Size (bp)	Accession no.[1]
Avian β-defensin 1 (AvBD1)	GAGTGGCTTCTGTGCATTTCTG/ TTGAGCATTTCCCACTGATGAG	62	NM_204993.1
Avian β-defensin 6 (AvBD6)	GCCCTACTTTTCCAGCCCTATT/ GGCCCAGGAATGCAGACA	63	NM_001001193.1
Avian β-defensin 10 (AvBD10)	CAGACCCACTTTTCCCTGACA/ CCCAGCACGGCAGAAATT	64	NM_001001609.2
Liver Enriched Antimicrobial Peptide 2 (LEAP2)	CTCAGCCAGGTGTACTGTGCTT/ CGTCATCCGCTTCAGTCTCA	66	NM_001001606.1
Mucin 2 (Muc2)	CTGATTGTCACTCACGCCTTAATC/ GCCGGCCACCTGCAT	147	JX284122.1
Olfactomedin 4 (Olfm4)	TTGCCGGATACCACCTTTCC/ TTTCTGCAAGAGCGTTGTGG	72	NM_001040463.1
Marker of Proliferation mKi67 (Ki67)	CACAGGCAAAGGCTGTCAAA/ TCCGTGCAATTTTCCTTGCT	63	XM_015289038.4
Notch homolog-1 (Notch1)	GAGGATCCATCGTCTACTTGGAA/ ATCGGTTGCGCTCTGGAA	81	NM_001030295.1
Collagen 3a1 (Col3a1)	GGCATTCCTCCGCATCCT/ TTGCAGTGGTAGGTGATGTTCTG	57	NM_205380.2
Eimeria acervulina sporozoite surface antigen (EA-SAG)	TGAGTTCCGCACGAAGA/ TCGATGTCTCGGCAACGAA	56	XM_013394133.1
Ribosomal protein large subunit P0 (RPLP0)	GCGATTGCTCCCTGTGATG/ TCTCAGGTCCGAGACCAGTGT	58	NM_204987.2
Ribosomal protein large subunit 4 (RPL4)	TCAAGGCGCCCATTCG/ TGCGCAGGTTGGTGTGAA	63	NM_001007479.1

[1]Note that the primer sequences were designed for regions of consensus between all published variants.

Table 3-2. Growth Performance Data of Infected and Uninfected broiler chickens.[1]

Day post-infection × Infection Status		Body Weight (kg)	Body Weight Gain (kg)	Feed Intake (kg)	Feed Conversion Ratio
3 dpi	Uninfected	1.05	0.27	0.30	1.11
	Infected	1.03	0.21	0.20	0.96
5 dpi	Uninfected	1.21	0.44	0.42	1.02
	Infected	1.20	0.36	0.40	1.15
7 dpi	Uninfected	1.36	0.55	0.66	1.19
	Infected	1.30	0.49	0.61	1.25
10 dpi	Uninfected	1.68	0.85	1.14	1.34
	Infected	1.58	0.76	1.05	1.38
14 dpi	Uninfected	1.99	1.16	1.64	1.43
	Infected	1.85	1.02	1.65	1.83
SEM[2]		0.06	0.05	0.04	0.15
Day post-infection					
	3 dpi	1.04[d]	0.24[d]	0.25[e]	1.04[b]
	5 dpi	1.20[cd]	0.40[c]	0.41[d]	1.08[b]
	7 dpi	1.33[c]	0.52[c]	0.63[c]	1.22[ab]
	10 dpi	1.63[b]	0.81[b]	1.09[b]	1.36[ab]
	14 dpi	1.92[a]	1.09[a]	1.64[a]	1.63[a]
SEM[2]		0.04	0.04	0.03	0.11
Infection Status					
	Uninfected	1.46	0.65[a]	0.83	1.22
	Infected	1.39	0.57[b]	0.78	1.31
SEM[2]		0.03	0.02	0.02	0.07
Analysis of Variance		***Probabilities***			
Day post-infection × Infection Status		0.79	0.91	0.67	0.47
Day post-infection		*<0.0001*	*<0.0001*	*<0.0001*	*0.0015*
Infection Status		0.073	*0.0085*	0.067	0.31

[1]Each value represents the least-square means 6 replicate cages with each having 4 naïve chickens (Body weight at 0 dpi = 0.845 kg) during 14 days post-infection (dpi) with 100,000 *Eimeria acervulina* oocysts (Infected) or sterile water (Uninfected) at 21 days of age kept in battery cages.

[2]SEM = pooled standard error

[a,b,c,d,e]Means in the same column with different superscripts are statistically different ($P < 0.05$) based on Tukey HSD mean separation.

Table 3-3. Comparison of Crypt Depth Measures between Olfm4-stained crypts and Hematoxylin and Eosin-stained crypts[1].

Day post-infection	Stain	Uninfected (µm)	Infected (µm)
0	Olfm4	95.8	70.8
	Hematoxylin	121.4	91.4
3	Olfm4	78.6	146.4
	Hematoxylin	103.8	168.0
5	Olfm4	86.0	172.5
	Hematoxylin	101.1	231.8
7	Olfm4	130.6	223.7
	Hematoxylin	145.3	256.6
10	Olfm4	81.5	146.0
	Hematoxylin	109.8	182.6
14	Olfm4	77.1	128.7
	Hematoxylin	105.2	129.5
SEM[2]		69.3	52.4

Welch's unequal variance test	***Probabilities***
Stain	0.048
Infection Status	< 0.0001
Day post-infection	0.0027

[1]Measures following Olfm4 in situ hybridization using RNAscope 2.5 HD kit (Brown) or Hematoxylin and Eosin staining in broiler chickens that were infected at 21 days of age with 100,000 *Eimeria acervulina* oocysts (Infected) or sterile water (Uninfected) and sampled at 0 (3 hours post-infection), 3, 5, 7, 10, and 14 days post infection (dpi). Measurements were taken at 40 X magnification (n=6) using ImageJ. Measurements were analyzed using Welch's unequal variance test using JMP.

[2]SEM = pooled standard error

FIGURES

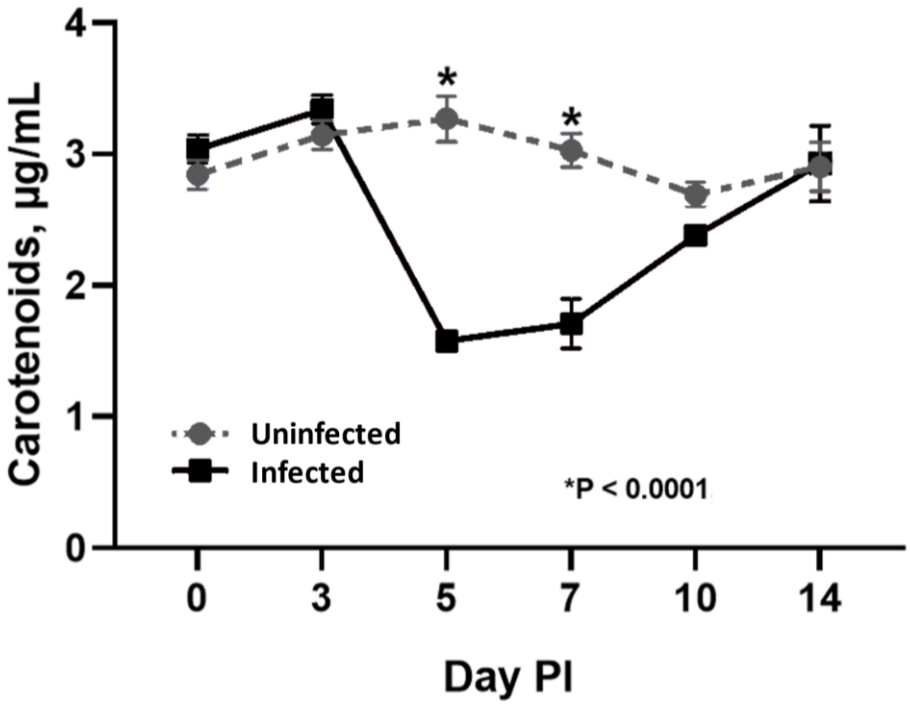

Figure 3-1

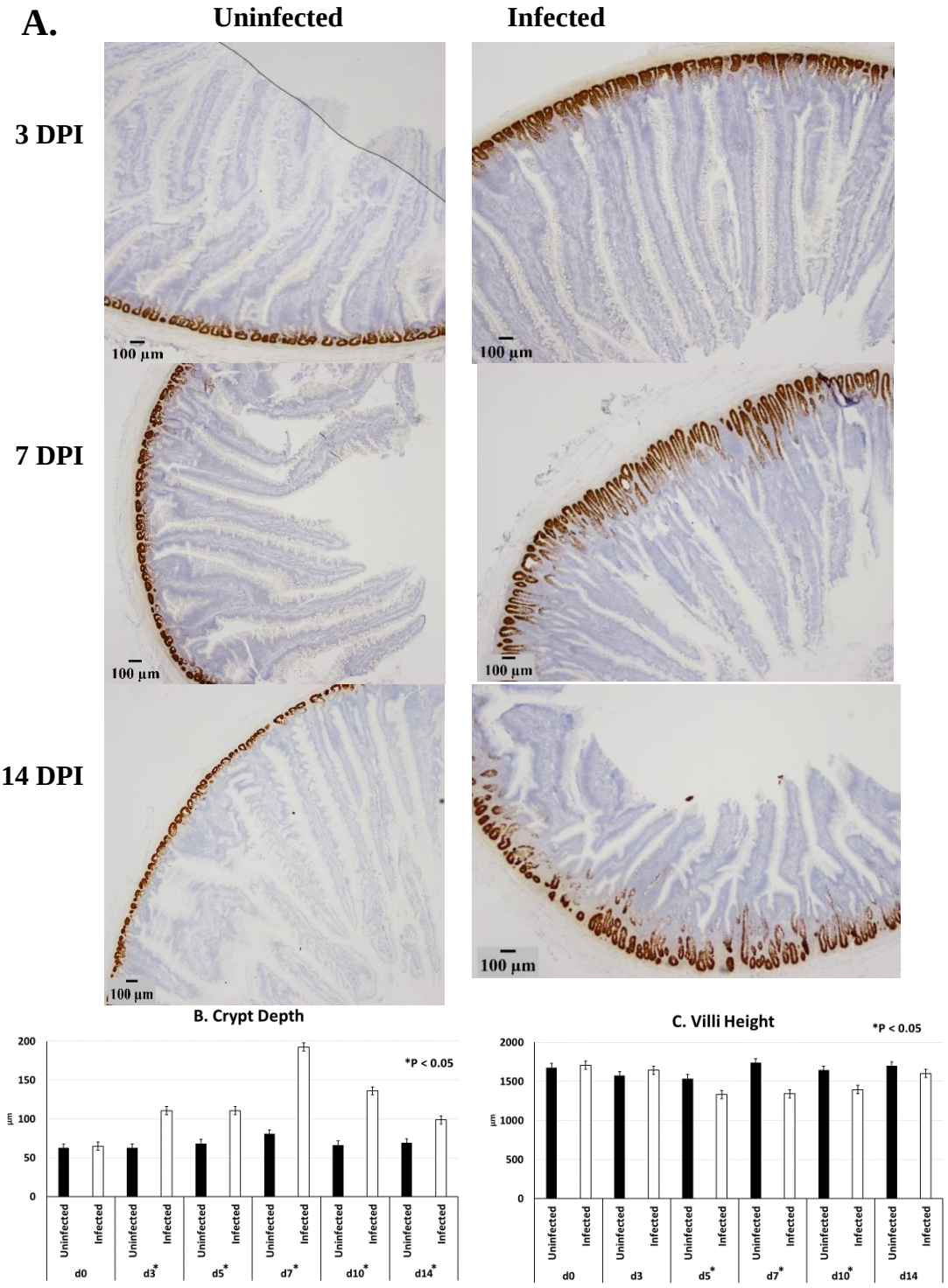
A.
Uninfected
Infected
3 DPI
7 DPI
14 DPI
100 µm
B. Crypt Depth
*P < 0.05
µm
Uninfected
Infected
d0
d3*
d5*
d7*
d10*
d14*
C. Villi Height
*P < 0.05
d0
d3
d5*
d7*
d10*
d14

Figure 3-2.

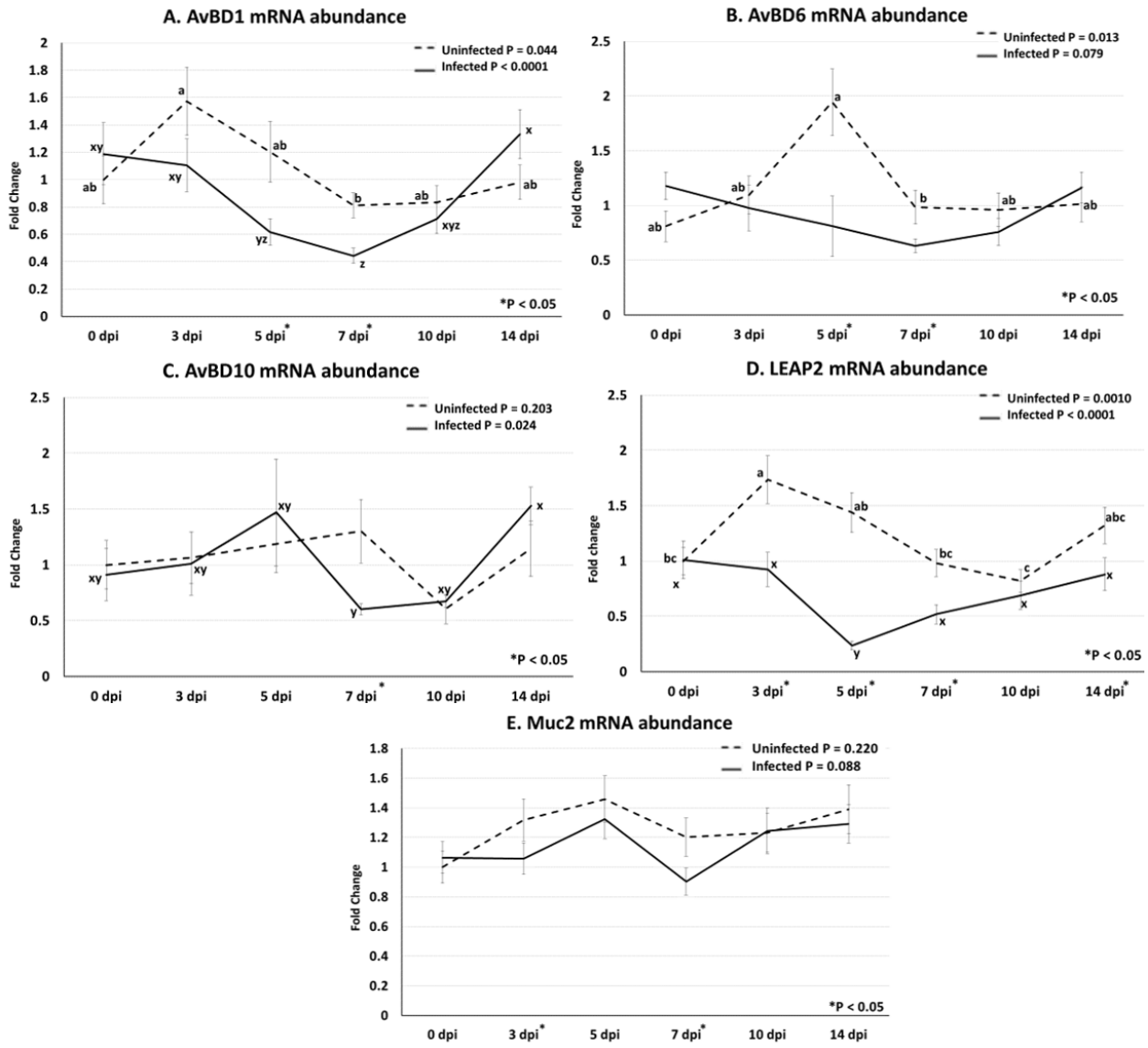
A. AvBD1 mRNA abundance
Uninfected P = 0.044
Infected P < 0.0001
Fold Change
*P < 0.05
0 dpi
3 dpi
5 dpi*
7 dpi*
10 dpi
14 dpi
B. AvBD6 mRNA abundance
Uninfected P = 0.013
Infected P = 0.079
Fold Change
*P < 0.05
C. AvBD10 mRNA abundance
Uninfected P = 0.203
Infected P = 0.024
Fold Change
*P < 0.05
D. LEAP2 mRNA abundance
Uninfected P = 0.0010
Infected P < 0.0001
Fold change
*P < 0.05
E. Muc2 mRNA abundance
Uninfected P = 0.220
Infected P = 0.088
Fold Change
*P < 0.05

Figure 3-3.

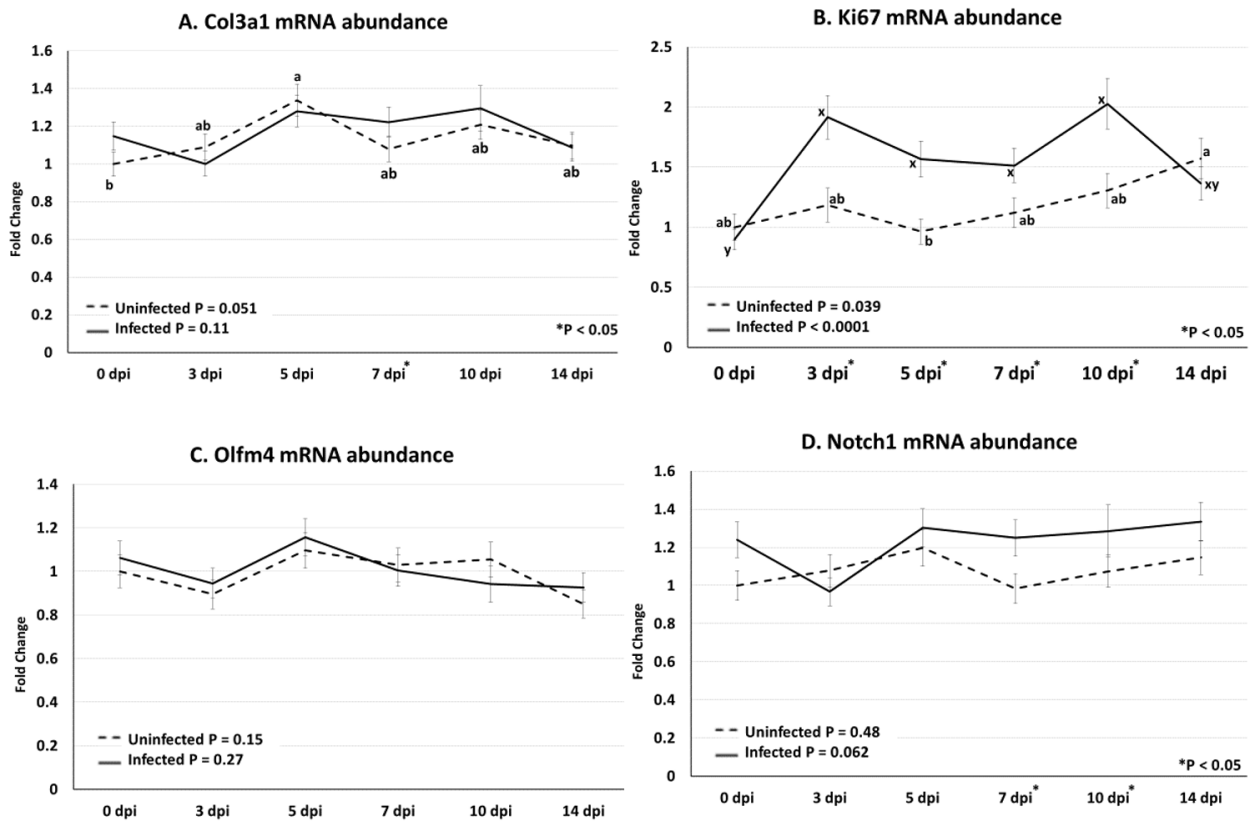
A. Col3a1 mRNA abundance
Fold Change
Uninfected P = 0.051
Infected P = 0.11
*P < 0.05
0 dpi
3 dpi
5 dpi
7 dpi*
10 dpi
14 dpi
B. Ki67 mRNA abundance
Uninfected P = 0.039
Infected P < 0.0001
*P < 0.05
C. Olfm4 mRNA abundance
Uninfected P = 0.15
Infected P = 0.27
D. Notch1 mRNA abundance
Uninfected P = 0.48
Infected P = 0.062

Figure 3-4.

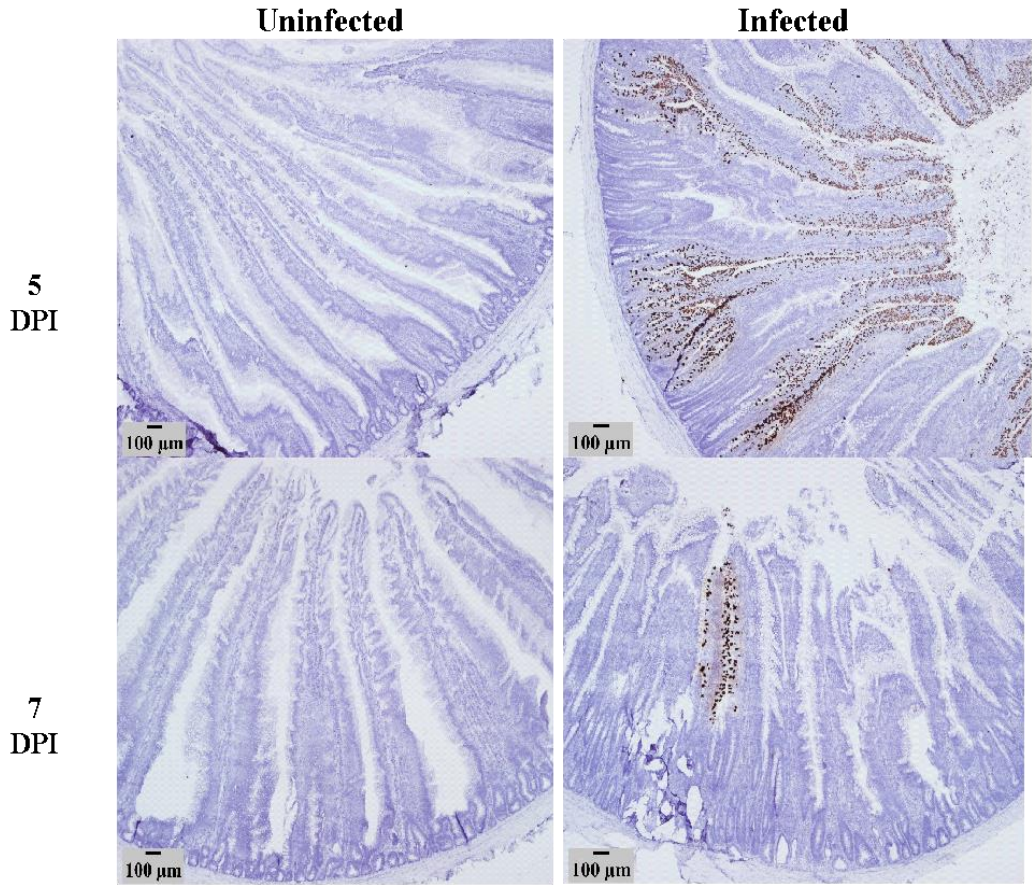

Figure 3-5

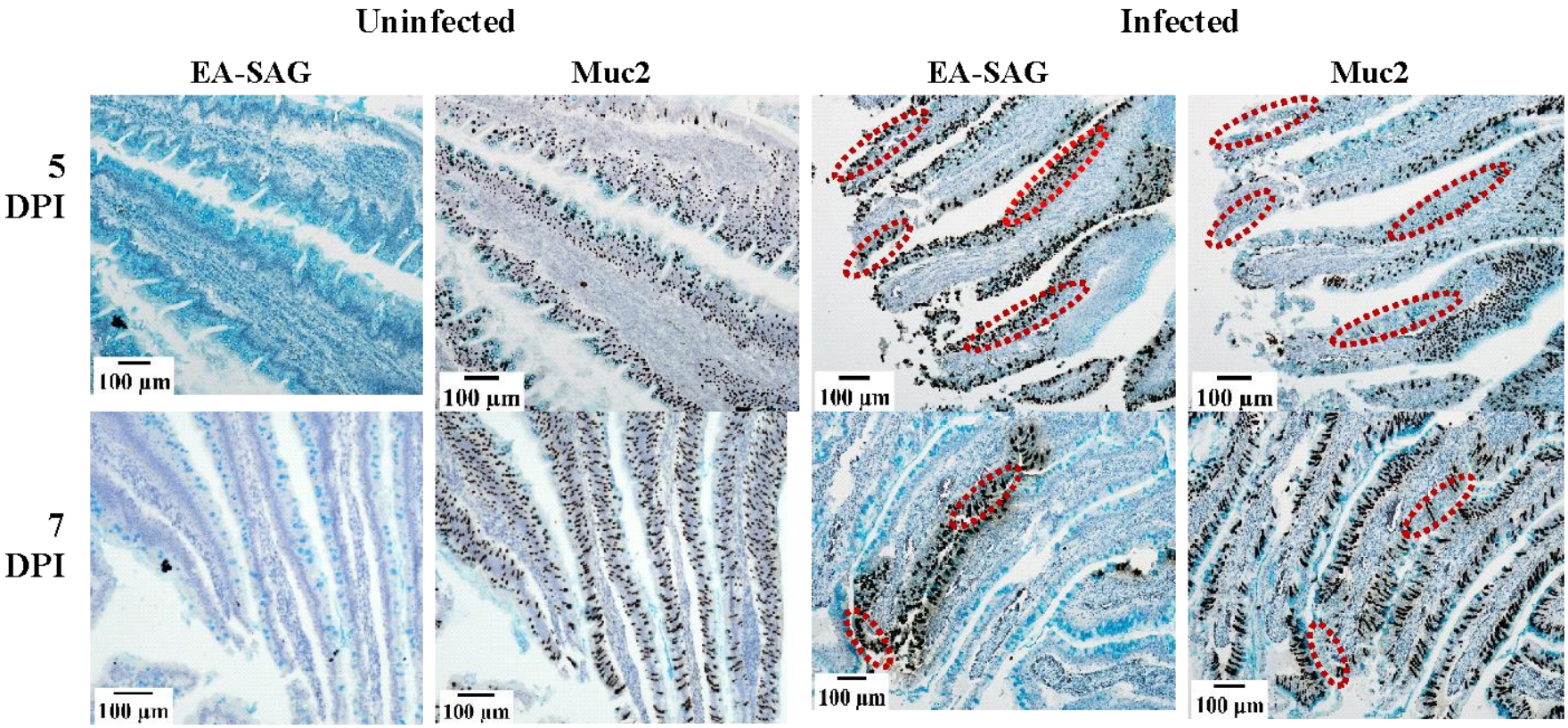

Figure 3-6.

Chapter 4: Profiling intestinal proliferative cells in the small intestine of broiler chickens via in situ hybridization during the peri-hatch period*

ABSTRACT Chickens hatch ready to consume feed without parental intervention. Mature small intestines have crypts populated by stem cells producing replacement cells to maintain the absorptive villus surface area. The embryonic crypt is rudimentary and cells along the villi are capable of proliferation. By 7 days post-hatch (d) the crypts are developed, where proliferation primarily occurs. The objective of this study was to profile the changes of genes that are markers of stem cells and proliferation: Olfactomedin 4 (Olfm4), Leucine-rich repeat containing G protein-coupled receptor 5 (Lgr5), and Ki67, a marker of stem cell proliferation during the peri-hatch period using quantitative PCR and in situ hybridization (ISH). The expression of the stem cell marker genes differed; Olfm4 increased post-hatch while Lgr5 decreased. The proliferation marker Ki67 did not change with time but ileal Ki67 mRNA was generally the greatest. The ISH was consistent with the quantitative PCR results. Olfm4 was only seen in the crypts and increased with morphological development of the crypts. In contrast Lgr5 was expressed in the crypt and the villi in the embryonic periods but became restricted to the intestinal crypt during the post-hatch period. Ki67 was expressed throughout the intestine pre-hatch, but then expression became restricted to the crypt and the center of the villi. The ontogeny of Olfm4, Lgr5 and Ki67 expressing cells showed different patterns in the small intestine during the peri-hatch period.

Keywords: In situ hybridization, Peri-hatch. Lgr5, Olfm4, Ki67

INTRODUCTION

As a precocial species the chicken hatches from the egg ready to consume and utilize complex feed-stuffs. During development, chicken embryos rely on nutrients deposited by the hen inside the albumen and the yolk (van der Wagt et al., 2020). In order to successfully survive, post-hatch embryos need to transition from primarily lipid and lipo-protein metabolism to carbohydrate heavy metabolism within the first days post-hatch (Moran, 2007). During the final embryonic days the embryo initiates small intestine functioning by swallowing the amniotic fluid that surrounds the embryo. This action coincides with the internalization of the yolk and is likely important for utilization of the yolk (van der Wagt et al., 2020).

Prior to amnion consumption, the small intestine at embryonic day (e) 15 is rudimentary and has minimal functional capability to digest complex feedstuffs (Uni et al., 2003) as the yolk sac has been the primary nutrient absorption mechanism (Wong and Uni, 2021). By day of hatch, the intestine has activated and is functional enough to support consumption of exogenous feedstuff, though not efficiently (Uni et al., 2003; Geyra et al., 2001; Reicher et al., 2020; Reicher and Uni, 2021). By 7 days post-hatch the small intestine is morphologically mature, comparable in development to older broilers (Van Leeuwen et al., 2004). After 7d the small intestine adapts to the diet by increasing enzyme secretions and interactions with the establishing microbiome population (Noy and Sklan, 1997; Bohórquez et al., 2011).

The small intestine is composed of two major structural components. The villi, finger-like projections that extend into the lumen of the intestine, are responsible for nutrient absorption. The crypts, invaginations of intestinal tissue into the lamina propria, are populated with stem cells that produce replacement cells for the villi (Uni et al.,

2000). The intestine is under constant cellular turn-over as functional epithelial cells undergo apoptosis or are sloughed off near the villi tip (Hall et al., 1994). In order to prevent loss of absorptive surface area, sufficient numbers of replacement cells must be produced by the crypt and migrate up the villi.

The late-term embryo and hatchling have cells capable of proliferation along the villi rather than restricted to the crypt as in mature intestines (Uni et al., 1998; Reicher et al., 2020). As part of the small intestinal maturation process the proliferative capabilities are restricted to the crypt (Uni et al., 2000). Reicher et al. (2020; 2022 have categorized cells as stem, progenitor, proliferative, and differentiated using immunofluorescence in chicks subjected to early, delayed feeding or in ovo feeding and have described population changes within the crypt and villi during e17 to 10d. Other studies have looked at the in situ hybridization (ISH) of stem cell marker genes Olfactomedin 4 (Olfm4) and Leucine-rich repeat containing G protein coupled receptor 5 (Lgr5) in chickens during e19-7d (Zhang and Wong, 2018). No study has combined quantitative gene expression and qualitative visualization to investigate proliferation in the small intestine during the peri-hatch period. Therefore, the objective of this study was to profile the changes in proliferative cells across the small intestine focusing on the development of the intestinal crypt during the last 4 days in ovo and first 7 days post-hatch using in situ hybridization and quantitative PCR analysis of stem and proliferative cell marker genes.

MATERIALS AND METHODS

Animals and Tissue Collection

All procedures were reviewed and approved by the Institutional Animal Care and Use Committee at Virginia Tech. Cobb 500 fertile eggs were received from a local hatchery and incubated in a Natureform 1080 incubator unit at 37.5 ˚C and 55% relative humidity. Chicks were pulled on day 21.5 of incubation and placed into battery cages (n = 20/cage) with ad libitum access to water and feed that met their nutritional requirements (NRC, 1994).

On e17 and e20, 6 eggs per treatment were randomly selected for sampling. Eggs were opened and embryos were euthanized by cervical dislocation. The entire small intestine was removed intact and rinsed with cold 1% PBS. The duodenal loop, jejunum and ileum were separated and cut into three equal pieces, the middle piece was placed into formalin for fixation and later histological analysis while the other two pieces were diced and snap frozen in liquid nitrogen for subsequent gene expression assays. This process was repeated with post-hatch chicks on 1, 3, and 7d.

Gene Expression

Frozen diced samples were homogenized with TriReagent using a tissue lyser and total RNA was extracted using Directzol RNA mini prep columns (Zymo Research, Irvine, CA). Using the Applied Biosystems high capacity cDNA reverse transcription kit (Thermo-Fisher Scientific) complementary DNA was synthesized. Gene expression was determined by quantitative PCR (qPCR) utilizing Fast SYBR Green Master Mix (Applied Biosystems) on an Applied Biosystems 7500 Fast Real-time PCR system (Thermo Fisher Scientific). qPCR reactions were run in duplicate. Gene primers were designed using Primer Express 3.0 (Applied Biosystems) and are listed in Table 4-1. Chicken ribosomal protein L4 (RPL4) and ribosomal protein lateral stalk subunit P1 (RPLP1) were used as

reference genes as they were the most stable as assessed by NormFinder (Andersen et al., 2004). The geometric mean of RPLP1 and RPL4 was subtracted from the Ct value to obtain the ΔCt value for each sample. The average ΔCt value of the Punch group at e20 was used as the calibrator to calculate ΔΔCt and fold change using the $2^{-\Delta\Delta Ct}$ method (Schmittgen and Livack, 2008). To conform to normality requirements for statistical analysis, data were logarithmically transformed. Data are presented as back transformed means and approximated standard errors (Jørgensen and Pedersen, 1998). Gene expression data were analyzed using a factorial ANOVA considering day of age, intestinal segment and the interaction of Day × Segment using JMP v15.0 (SAS Institute Cary, NC, USA) When ANOVA results were statistically significant ($P \leq 0.05$) mean separation was conducted with Tukey's Honestly Significant Difference Test.

In situ Hybridization

The intestinal segments were placed in formalin for approximately 16 hours, 70% ethanol for 24 hours and then stored in fresh 70% ethanol at 4 ˚C. The fixed segments were embedded in paraffin (StageBio, Mount Jackson, VA). Formalin fixed paraffin embedded tissues of 3 individuals per timepoint were sectioned (5 µm) using a microtome and mounted on Superfrost-Plus glass slides (Electron Microscopy Sciences, Hatfield, PA). In situ hybridization was conducted using the RNAscope (Advanced Cell Diagnostics, Newark, CA) method using single plex probes for Olfm4, Lgr5 and Ki67 (Table 1) and the RNAscope 2.5 HD Assay–BROWN detection kit (Advanced Cell Diagnostics) or RNAscope 2.5 HD Assay- RED detection kit (Advanced Cell Diagnostics). Slides were counterstained with 50% Gill's hematoxylin no. 1 (Sigma-Aldrich, St. Louis, MO), rinsed in distilled water, and placed in 0.02% ammonia water to

turn the purple stain to blue. Slides were sealed with VectaMount (Vector Lab, Burlingame, CA) for the brown kit or EcoMount (Biocare Medical, LLC, Pacheco, CA) for the red kit and a glass coverslip. All ISH was conducted in sets of up to 20 slides containing each timepoint selected randomly for each gene. Brightfield microscopy images were captured using a Nikon Eclipse 80i microscope with a DS-Ri1 digital camera.

RESULTS

Gene Expression by qPCR

The stem cell marker Olfm4 was affected by the interaction of Day × Segment ($P = 0.043$; Fig. 4-1A). In the duodenum Olfm4 mRNA did not change with age; whereas in the jejunum Olfm4 mRNA increased from e17 to 3d and 7d. In the ileum Olfm4 mRNA increased from e17 to 1d and then remained elevated from 1d to 7d. When considering the main effect of age Olfm4 mRNA expression increased over time ($P < 0.0001$).

The other stem cell marker gene Lgr5 also varied by the interaction of Day × Segment ($P = 0.0094$; Fig. 4-1B). In the duodenum, Lgr5 mRNA declined from e17 to 3d and 7d. In the jejunum, Lgr5 mRNA declined from e17 to 7d. In the ileum, Lgr5 mRNA declined from e17 to 3d. The ileum had the greatest Lgr5 mRNA abundance ($P = 0.0069$) compared to the jejunum.

The proliferative marker gene Ki67 was affected by the interaction of Day × Segment ($P = 0.046$; Fig. 4-1C). In the duodenum, Ki67 mRNA was unchanged from e17 to 1d and then declined from 1d to 7d. In the jejunum and ileum, Ki67 mRNA did not change over time. Overall Ki67 mRNA followed a quadratic pattern with a peak at 1d ($P = 0.0099$).

Gene Expression by In situ Hybridization

The small intestine showed morphological changes from the embryonic period (e17 and e20) to the post-hatch period (1d, 3d, 7d). Olfactomedin 4 expression was restricted to the crypts (Fig. 4-2), as such it is useful for highlighting crypt development. The villi developed from their initial pear-shaped structure pre-hatch to long, straight narrow structures post-hatch resulting in an increased available surface area for nutrient absorption. The crypts had a two-stage development process: first they deepened into the lamina propria during the embryonic period and then post-hatch they began to increase in number by crypt fission, where a single crypt splits into two or three crypts. This can be seen in the inset of the jejunum on 7d of Fig. 4-2. By 7d the intestine is structurally the same as a mature broiler, though proportionally smaller. During the embryonic days (e17 and e20), the Olfm4 signal was less intense than at post-hatch ages, making the crypt appear speckled instead of solid brown as observed in the post-hatch samples. The Olfm4 signal had consistent intensity across all intestinal segments.

In contrast, the Lgr5 signal was much fainter than Olfm4, appearing as single dots on the tissue rather than staining the entire region and was observed in both the crypts and the villi (Fig. 4-3). The red chromogen was used for Lgr5 due to its lower expression level, as it has a higher sensitivity than the brown chromogen. During the embryonic period, numerous areas of Lgr5 staining were observed along the villi, giving the villi a pinkish color. However, post-hatch only a few scattered Lgr5 signals were seen outside of the crypt and only in the lower villus region. Notably the jejunum on 7d showed extremely low expression of Lgr5 mRNA. There are only a few solitary dots visible within the crypt.

Proliferative cells express the gene Ki67. During the embryonic period Ki67 staining appeared ubiquitous as proliferative cells were expressed in the crypt, villi, and the underlying mucosal tissue (Fig. 4-4). Generally, post-hatch the expression was confined to mainly the crypt and along the center of the villi where the central lacteal and capillary bed resided. There were no visual differences in Ki67 expression between intestinal segments.

DISCUSSION

Olfactomedin 4 and Lgr5 are stem cell marker genes which are involved in different signaling pathways that maintain the stem cell niche. Olfm4 responds to Notch signals while Lgr5 responds to Wnt signals (Demitrack and Samuelson, 2016). In mammals Lgr5 and Olfm4 are interchangeable for marking stem cells within the crypt (Koo and Clevers, 2014). The qPCR results showed contrasting temporal patterns. Olfm4 mRNA increased post-hatch while Lgr5 mRNA decreased post-hatch, which matches the ISH results seen in this study and previously in Zhang and Wong (2018). Olfm4 is a more robust intestinal stem cell marker for chickens as it highlights the entire intestinal crypt, whereas, Lgr5 marks cells within the crypt but also some along the villi. The Lgr5 staining was different from the staining with Olfm4 which covered the entire cell. Lgr5 signals were light and punctate. Each signal dot represents a single mRNA molecule according to the manufacturer of the RNAscope procedure (Wang et al., 2012). These differences indicate that stem cells express Olfm4 mRNA to a greater extent than Lgr5 mRNA.

It is unclear functionally what role Olfm4 plays within the stem cell. Studies have shown that Olfm4 is a secreted glycoprotein that has a regulatory role for cell

proliferation and apoptosis implicating the gene in innate immunity, inflammation, and cancer (Kobayashi et al., 2007; Liu and Rodgers, 2016). It is clear that Olfm4 requires Notch signaling and that Notch signaling is required for maintaining the stem cell niche (Carulli et al., 2015; Diemtrack and Samuelson, 2016). Though in previous research from our lab, Olfm4-expressing cells were absent in some cases of chickens showing symptoms of Runting Stunting Syndrome (Cloft et al., 2022). Interestingly, the crypt cells continued to express nutrient transporter, Ki67 and mucin-2 genes suggesting that it remained functional in the absence of Olfm4 expression. It seems that while Notch signaling is required, Olfm4 may not be, further raising questions about its role within the crypt.

In contrast, the essential role of Lgr5 within the crypt is clearly established. Lgr5 is a receptor that responds to Wnt signals that in mammals construct and maintain the crypt stem cell niche (Sato et al., 2011). In chickens, Zhang and Wong (2018) showed that the Lgr5 signal was also present in vascular endothelial cells of the yolk sac of chick embryos, leading them to suggest that Lgr5 is a general stem cell marker gene rather than an intestinal stem cell marker gene. The expression pattern of Lgr5 in the crypt of the current study was much lighter than Olfm4. In the jejunum on 7d especially, the Lgr5 signal was very faint. This expression pattern has been seen in our lab previously in studies with broiler chickens at varying ages (images not shown) and in one study of broiler chicks (Zhang and Wong, 2018). We have no explanation why the expression in these instances is so much lower than at other points of the study and why Lgr5 expression generally is lower than Olfm4 in chickens.

The expression pattern of Ki67 in the chicken intestine has never before been described in the chicken. Ki67 expressing cells were observed in the crypt and along the central lacteal of the villus. The mRNA abundance as quantified by qPCR did not change greatly over time in this study but was generally increased in the ileum, as seen with Lgr5. The observed expression along the center of the villus is reminiscent of the lymphatic capillaries described in mammals, though such capillaries have been described as non-existent in the chicken (Moran, 1984). Instead underlying the epithelial cell layer is a bed of capillaries for transport of nutrients to the liver (Turk, 1982). In mammals, proliferation is essential for maintaining intestinal lacteals and thus would explain the presence of Ki67-expressing cells (Bernier-Latmani et al., 2015). The observed Ki67 mRNA in the center of the villi in chickens is likely also for proliferation of cells of the capillary bed underlying the epithelial layer.

Utilizing proliferating cell nuclear antigen (PCNA) and SRY-box transcription factor 9 (Sox9) immunofluorescence, Reicher et al. (2020; 2022) showed that stem cells within the crypt were positive for Sox9 but negative for PCNA, progenitor cells were positive for both genes, and proliferating cells were negative for Sox9 but positive for PCNA. It is unclear exactly how Sox9, PCNA, and Ki67 overlap in the chicken, in mammals they are described as somewhat overlapping and can be used interchangeably in intestinal tissue. Further research is needed in the chicken to understand the relationship between Sox9, Ki67, and PCNA expressing stem cells.

The combination of quantitative gene expression and visualization in this study enabled further conclusions to be drawn from the collected data. The methods utilized in this study give different types of results; qPCR provides tissue-level mRNA

quantification data while ISH provides cell-level mRNA expression patterns. When used in concert the ISH helps discern the cause of any changes in qPCR results. For example, the observed decrease in Lgr5 mRNA post-hatch using qPCR and ISH allowed us to determine that it was most likely due to the loss of expression outside of the crypt. The synergy between these two methods could be used in other gene expression studies to delve deeper into the responses from treatments or over time and generally enhance qPCR data.

Conclusions

This study profiles the stem cell marker genes Olfm4 and Lgr5 along with the proliferative cell marker gene Ki67 in the small intestine of peri-hatch broiler chickens. During the peri-hatch period the small intestine undergoes rapid development to facilitate the transition to life post-hatching. Olfm4 mRNA increased post-hatch while Lgr5 mRNA decreased post-hatch. The ISH expression patterns of Olfm4 and Lgr5 were consistent with the qPCR results. Olfm4-expressing cells were only seen in the crypts and the expression paralleled the morphological development of the crypt. Lgr5-expressing cells changed from being expressed along the villi, in the crypt and in the lamina propria during late embryogenesis to being restricted to the intestinal crypt. The mRNA expression proliferation marker Ki67 decreased in the duodenum from 1d to 7d. Ki67-expressing cells appeared throughout the intestine during the pre-hatch period but became restricted to the crypts and along the center of the villi post-hatch. The ontogeny of Olfm4, Lgr5 and Ki67 expressing cells show different patterns in the small intestine during the peri-hatch period.

REFERENCES

Andersen C., J. Jensen, T. Orntoft. 2004. Normalization of real - time quantitative reverse transcription -PCR data: A model - based variance estimation approach to identify genes suited for normalization, applied to bladder and colon cancer data sets. Cancer Res. 64:5245.

Basak, O., M. van de Born, J. Korving, J. Beumer, S. van der Elst, J.H. van Es, and H. Clevers. 2014. Mapping early fate determination in Lgr5+ crypt stem cells using a novel Ki67-RFP allele. EMBO J. 33:2057-2068.

Bernier-Latmani, J., Cisarovsky, C., Demir, C.S., Bruand, M., Jaquet, M., Davanture, S., Ragusa, S., Siegert, S., Dormond, O., Benedito, R. and Radtke, F., 2015. DLL4 promotes continuous adult intestinal lacteal regeneration and dietary fat transport. J. Clin. Investig. 125:4572-4586.

Bohórquez, D.V., N.E. Bohórquez and P.R. Ferket. 2011. Ultrastructural development of the small intestinal mucosa in the embryo and turkey poult: A light and electron microscopy study. Poult. Sci. 90:842-855.

Carulli A.J., T.M. Keeley, E.S. Demitrack, J. Chung, I. Maillard, and L.C. Samuelson. 2015. Notch receptor regulation of intestinal stem cell homeostasis and crypt regeneration. Develop Biol. 402:98–108.

Cloft, S.E., S.K. Kinstler, K. Reno, H.S. Sellers, M. Franca, R. Ecco, M.D. Lee, J.J. Maurer, and E.A. Wong. 2022. Runting stunting syndrome in broiler chickens is associated with altered intestinal stem cell expression of Olfm4. Avian Dis. 10.1637/21-00109.

Demitrack E.S., and L.C. Samuelson. 2016. Notch regulation of gastrointestinal stem cells. J Physiol. 594:4791–4803.

Garcia H, D. Fleyshman, K. Kolesnikova, A. Safina, M. Commane, G. Paszkiewicz, A. Omelian, C. Morrison, and K. Gurova. 2011. Expression of FACT in mammalian tissues suggests its role in maintaining of undifferentiated state of cells. Oncotarget 2:783–796.

Geyra, A., Z. Uni and D. Sklan. 2001. Enterocyte dynamics and mucosal development in the posthatch chick. Poult. Sci. 80:776-782.

Hall, P. A., P.J. Coates, B. Ansari, and D. Hopwood. 1994. Regulation of cell number in the mammalian gastrointestinal tract: the importance of apoptosis. J. Cell Sci. 107:3569-3577.

Jørgensen, E., and A.R. Pedersen. 1998. How to obtain those nasty standard errors from transformed data-and why they should not be used. Aarhus Univ. DetJordbrugsvidenskabelige Fakultet, Aarhus, Denmark. International Report 7.

Kobayashi D, S. Koshida, R. Moriai, N. Tsuji, and N. Watanabe. 2007. Olfactomedin 4 promotes S-phase transition in proliferation of pancreatic cancer cells. Cancer Sci. 98:334–340.

Koo, B. K., and H. Clevers. 2014. Stem cells marked by the R-spondin receptor LGR5. Gastroenterology 147:289-302.

Liu, W. and G.P. Rodgers. 2016. Olfactomedin 4 expression and functions in innate immunity, inflammation, and cancer. Cancer Metastasis Rev. 35:201-212.

Moran, E.T. 1984. Comparative Nutrition of Fowl and Swine: The Gastrointestinal Systems, University of Guelph, Canada. ISBN 0–88955-010–7.

Moran, E.T. 2007. Nutrition of the developing embryo and hatchling. Poult. Sci. 86:1043-1049.

National Research Council. 1994. Nutrient Requirements of Poultry. 9th rev. ed. Natl. Acad. Press, Washington, DC.

Noy, Y., and D. Sklan. 1997. Posthatch development in poultry. J. Appl. Poult. Res. 6:344-354.

Reicher, N., and Z. Uni. 2021. Intestinal brush border assembly during the peri-hatch period and its contribution to surface area expansion. Poult. Sci. 100:101401.

Reicher, N., T. Melkman-Zehavi, J. Dayan, and Z. Uni. 2020. It's all about timing: early feeding promotes intestinal maturation by shifting the ratios of specialized epithelial cells in chicks. Front. Physiol. 1677.

Reicher, N., T. Melkman-Zehavi, J. Dayan, E.A. Wong, and Z. Uni. 2022. Nutritional stimulation by in-ovo feeding modulates cellular proliferation and differentiation in the small intestinal epithelium of chicks. Anim. Nutr. 8:91-101.

Sato, T., J.H. van Es, H.J. Snippert, D.E. Stange, R.G. Vries, and M. van den Born. 2011. Paneth cells constitute the niche for Lgr5 stem cells in intestinal crypts. Nature 469:415-419.

Schmittgen T. D. and K.J. Livak. 2008. Analyzing real-time PCR data by the comparative C(T) method. Nat. Protoc. 3:1101–1108.

Scholzen, T. and J. Gerdes. 2000. The Ki-67 protein: from the known and the unknown. J. Cell. Physiol. 182:311–322

Turk, D. E. 1982. Symposium: The avian gastrointestinal tract and digestion. Poult. Sci. 61:1225-1244.

Uni, Z., R. Platin, and D. Sklan. 1998. Cell proliferation in chicken intestinal epithelium occurs both in the crypt and along the villus. J. Comp. Physiol. B 168:241-247.

Uni, Z., A. Geyra, H. Ben-Hur, and D. Sklan. 2000. Small intestinal development in the young chick: crypt formation and enterocyte proliferation and migration. Br. Poult. Sci. 41:544-551.

van der Wagt, I., I.C. de Jong, M.A. Mitchell, R. Molenaar, and H. van den Brand. 2020. A review on yolk sac utilization in poultry. Poult. Sci. 99:2162-2175.

Van Leeuwen, P., J.M. Mouwen, J.D van der Klis, and M.W. Verstegen. 2004. Morphology of the small intestinal mucosal surface of broilers in relation to age, diet formulation, small intestinal microflora and performance. Br. Poult. Sci. 45:41-48

Wang, F., J. Flanagan, N. Su, L.C. Wang, S. Bui, A. Nielson, X. Wu, H.T. Vo, X.J. Ma, and Y. Luo. 2012. RNAscope: a novel in situ RNA analysis platform for formalin-fixed, paraffin-embedded tissues. J. Mol. Diagn. 14:22-29.

Zhang, H. and E.A. Wong, 2018. Identification of cells expressing *OLFM4* and *LGR5* mRNA by in situ hybridization in the yolk sac and small intestine of embryonic and early post-hatch chicks. Poult. Sci. 97:628-633.

ACKNOWLEDGMENTS

This research was supported by Research Grant No. US-5074-18CR from the United States – Israel Binational Agricultural Research and Development (BARD) Fund.

FIGURE CAPTIONS

Figure 4-1. Relative mRNA abundance of Olfm4, Lgr5, and Ki67 mRNA in the small intestine during the peri-hatch period. Tissue samples (n=6) were collected from duodenum (Duo), jejunum (Jej), and ileum (Ile) at embryonic days 17 (e17) and 20 (e20) and 1(1d), 3 (3d), and 7 (7d) days post-hatch. Relative mRNA abundance of olfactomedin 4 (A, Olfm4), leucine-rich repeat containing G protein-coupled receptor 5 (B, Lgr5), and marker of proliferation Ki67 (C) was determined by qPCR. The e17 duodenum was used as the calibrator for calculation of the fold change. A factorial ANOVA was used to analyze for differences. Bars with differing letters are significantly different ($P \leq 0.05$).

Figure 4-2. Expression of Olfm4 mRNA in the intestine from late embryogenesis to early post hatch using in situ hybridization. Tissue samples were collected from duodenum (Duo), jejunum (Jej), and ileum (Ile) at embryonic days 17 (e17) and 20 (e20) and 1(1d), 3 (3d), and 7 (7d) days post-hatch (n = 3). Formalin-fixed, paraffin-embedded tissues were analyzed by in situ hybridization. Cells expressing Olfm4 mRNA (brown staining) were detected using the RNAscope 2.5 HD Assay-BROWN kit. The tissues were counterstained with 50% hematoxylin. Images were captured using 200x magnification and insets included were captured at 400x magnification.

Figure 4-3. Expression of Lgr5 mRNA in the intestine from late embryogenesis to early post hatch using in situ hybridization. Tissue samples were collected from duodenum (Duo), jejunum (Jej), and ileum (Ile) at embryonic days 17 (e17) and 20 (e20) and 1(1d), 3 (3d), and 7 (7d) days post-hatch (n = 3). Formalin-fixed, paraffin-embedded tissues

were analyzed by in situ hybridization. Cells expressing Lgr5 mRNA (red staining) were detected using the RNAscope 2.5 HD Assay-RED kit. The tissues were counterstained with 50% hematoxylin. Images were captured using 200x magnification and insets included were captured at 400x magnification.

Figure 4-4. Expression of Ki67 mRNA in the intestine from late embryogenesis to early post hatch using in situ hybridization. Tissue samples were collected from duodenum (Duo), jejunum (Jej), and ileum (Ile) at embryonic days 17 (e17) and 20 (e20) and 1(1d), 3 (3d), and 7 (7d) days post-hatch (n = 3). Formalin-fixed, paraffin-embedded tissues were analyzed by in situ hybridization. Cells expressing Ki67 mRNA (brown staining) were detected using the RNAscope 2.5 HD Assay-BROWN kit. The tissues were counterstained with 50% hematoxylin. Images were captured using 200x magnification.

TABLES

Table 4-1. Primers for quantitative PCR

Gene name	Forward/Reverse Primers (5' to 3')	Amplicon Size (bp)	Accession no.
Leucine rich repeat containing G protein-coupled receptor 5 (Lgr5)	TGGTTTGACCTTCGTTTGCA/ GGACATATACAATGGAGATCTGAAAACT	67	XM_425441.7[1]
Olfactomedin 4 (Olfm4)	TTGCCGGATACCACCTTTCC/ TTTCTGCAAGAGCGTTGTGG	72	NM_001040463.1
Marker of Proliferation mKi67 (Ki67)	CACAGGCAAAGGCTGTCAAA/ TCCGTGCAATTTTCCTTGCT	63	XM_015289038.4[1]
Ribosomal protein large subunit P1 (RPLP1)	TCTCCACGACGACGAAGTCA/ CCGCCGCCTTGATGAG	55	NM_205322.1
Ribosomal protein large subunit 4 (RPL4)	TCAAGGCGCCCATTCG/ TGCGCAGGTTGGTGTGAA	63	NM_001007479.1

[1]The primer sequences were designed for regions of consensus between all published variants.

FIGURES

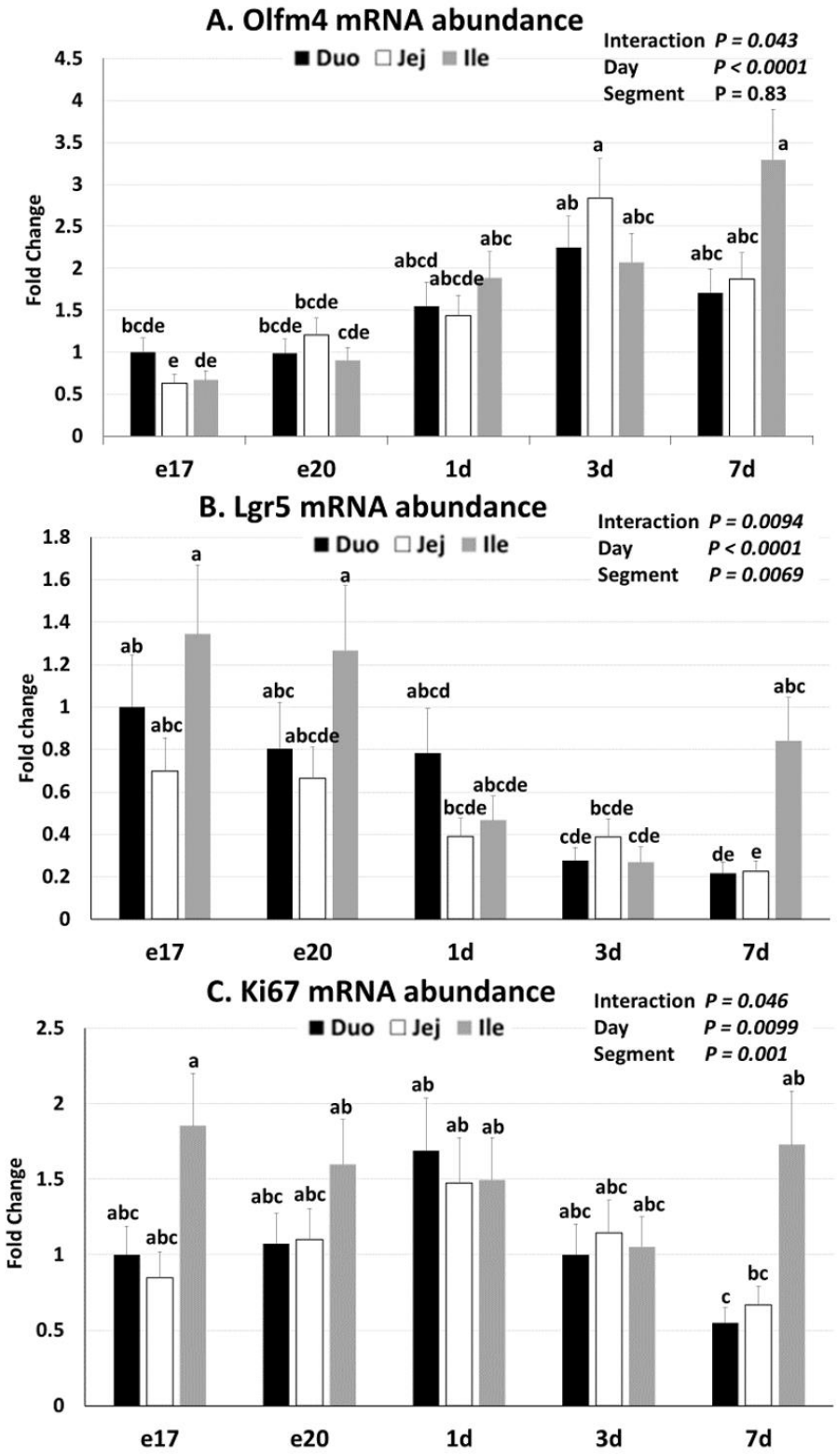

Figure 4-1.

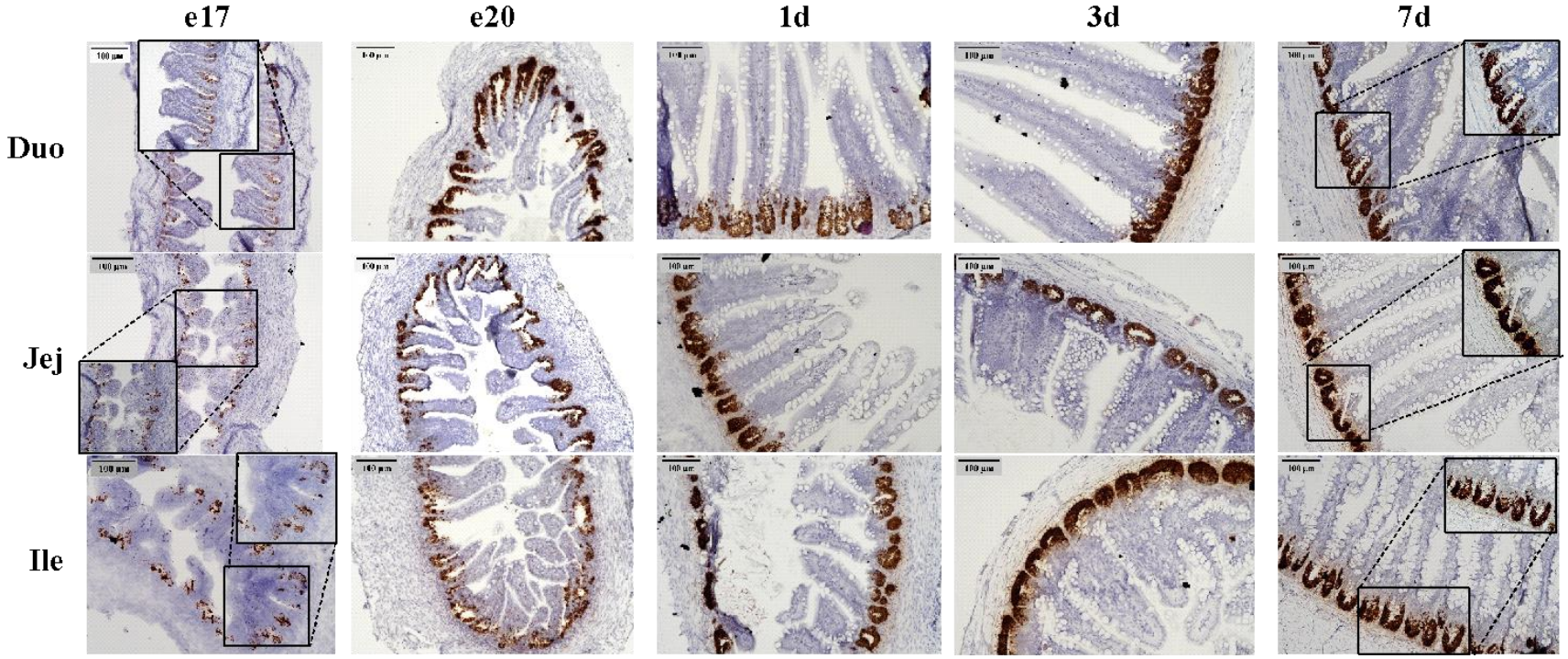

Figure 4-2.

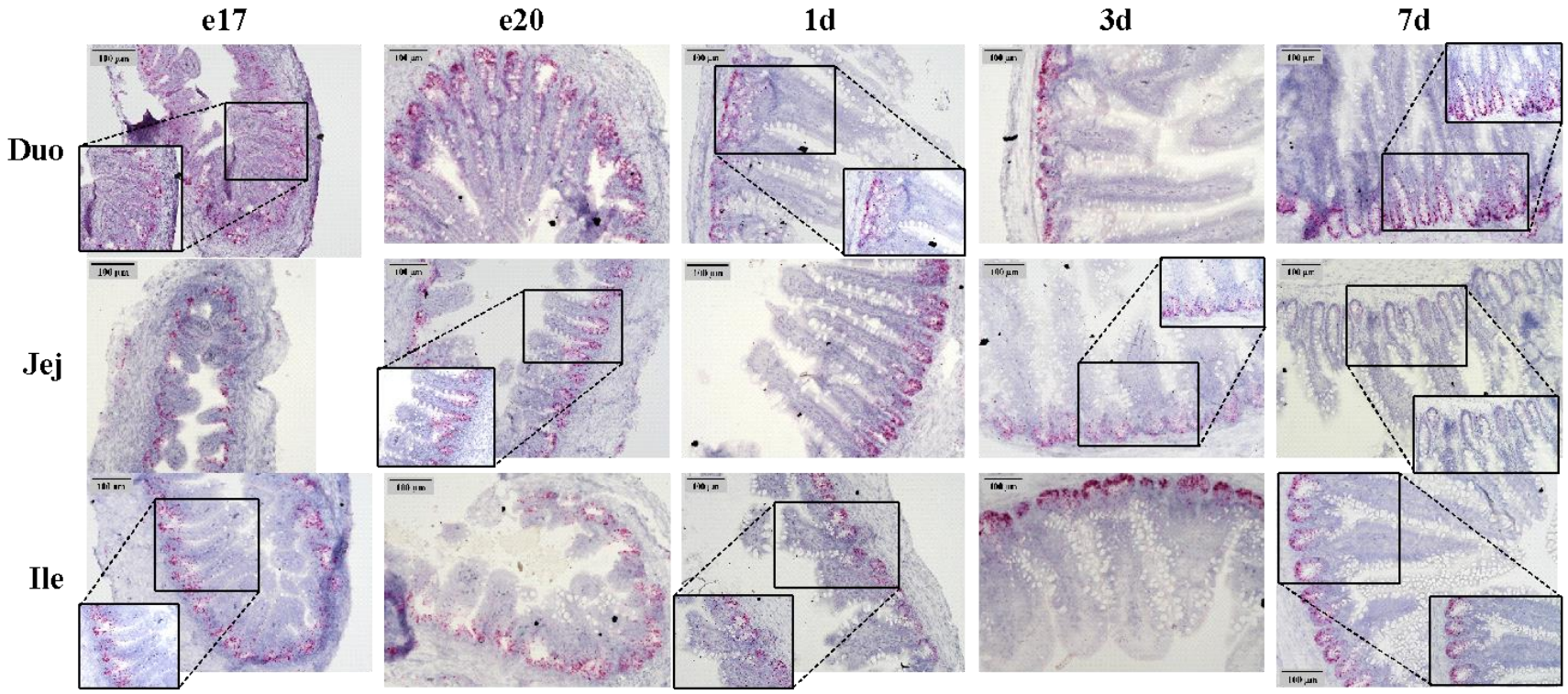

Figure 4-3.

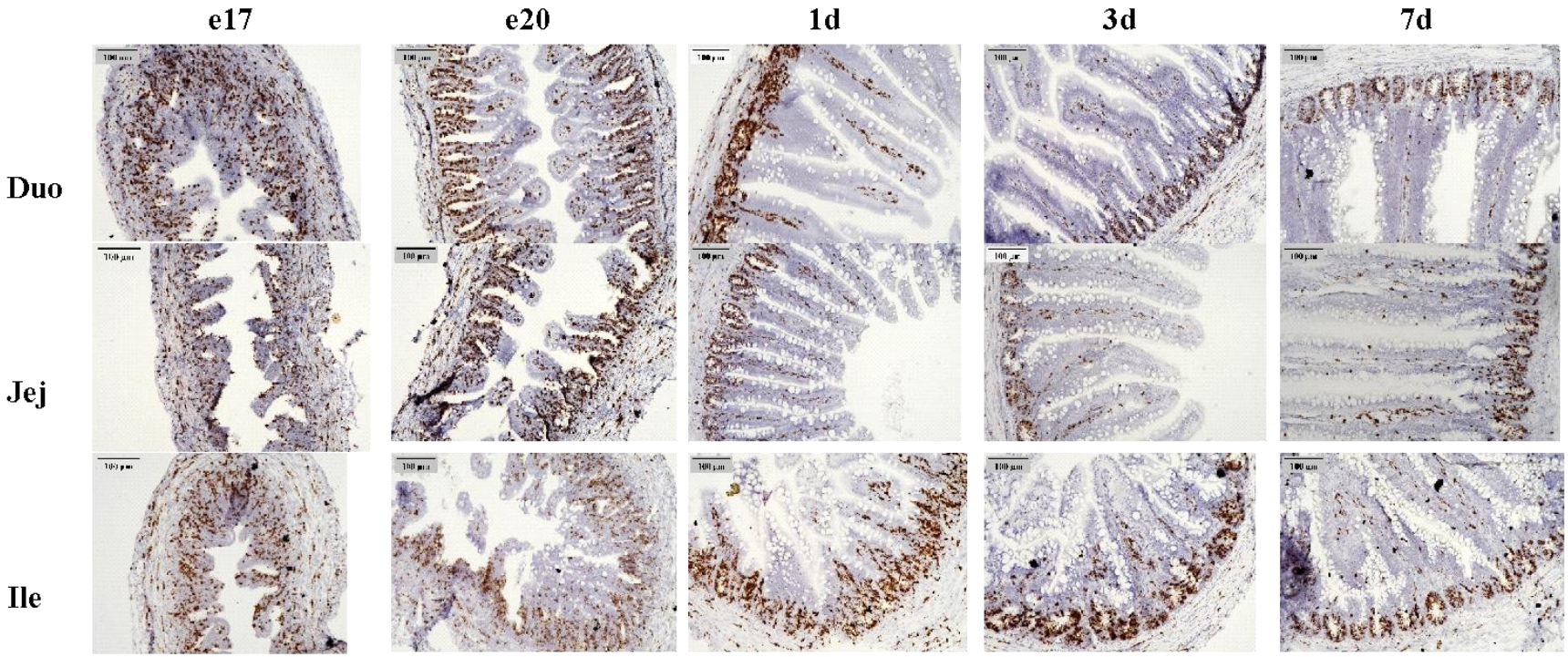

Figure 4-4.

Chapter 5: In ovo feeding of probiotics alters gene expression patterns in the small intestine during the first week post-hatch in broiler chicks*

ABSTRACT In ovo feeding into the amnion supplements the chick during the hatching process and fosters the transition to feed post-hatch. Previous research has established that in ovo injection of nutrients hastens the maturation of the small intestine and the injection of probiotics promotes immunocompetence. This study aimed to clarify the effect probiotics have on the small intestinal maturation at the molecular level. On embryonic day 17.5 eggs were injected with 0.3 ml of 10^6 CFU of Primalac® probiotic in 0.75% saline (Probiotic), saline alone (Saline), or non-injected but punched (Punch). On e20 the mRNA abundance of Mucin-2 (Muc2) and Peptide transporter 1 (PepT1) in the ileum of the Probiotic group were increased above the Punch group, but were similar to the Saline group. The Saline group on e20 had numerically increased Muc2 and PepT1 mRNA in all intestinal segments, as well as increased expression of Notch pathway genes compared to the Punch group. The fact that the Probiotic group response was confined to the ileum while the Saline group had increases in all segments suggests different mechanisms of stimulation likely consistent with the nature of the solutions themselves. After e20 no major effects of in ovo injection were observed and the Punch group had significant increases in Muc2 and PepT1 mRNA on 3 and 7d, respectively. Taken together these results imply that in ovo feeding caused a transient early expression of markers for absorptive (PepT1) and goblet (Muc2) cells.

Keywords: In ovo feeding, Probiotics, Saline, Muc2, PepT1

INTRODUCTION

The modern broiler chicken has been genetically selected for the efficient conversion of feed to body weight, reaching a marketable weight (2.2 kg/5 lbs) as early as 35 days post-hatch. At the same time the embryonic developmental period is biologically fixed at 21 days, accounting for approximately 38% of their life. During the incubation period embryos rely on protein and lipoproteins contained within the albumen and yolk for energy to support their growth and development (reviewed by van der Wagt, 2020). In the final days of incubation embryos swallow the amnion fluid surrounding them, which activates the rapid intestinal maturation process in time for the internalization of the yolk (Uni et al., 1998; 2000; Moran, 2007). The hatching process of chicks is perfectly timed for the introduction of additional nutrients into the amnion via in ovo feeding (Uni and Ferket, 2003). After consuming the amnion fluid, during hatching embryos rely exclusively on glycogen reserves in the yolk sac membrane and liver (reviewed by Givisiez et al., 2020).

In ovo feeding of nutrients and probiotics promotes intestinal development during the peri-hatch period. Initial functioning of intestinal villi starts at embryonic (e) day 17 while the embryo is swallowing the amnion fluid. By hatch (e20-21.5) intestinal villi length increases along with the formation of crypts. By 7 days post-hatch the initial intestinal structural development is laid, resulting in long straight villi with multiple crypts supplying each villus (Uni, 2006). The small intestine on 7d is almost fully mature though functionally it is still not enzymatically efficient until 14-16d (Moran, 2007). A number of studies have shown that providing nutrients, carbohydrates and amino acids via in ovo feeding increases villi height and crypt depth as well as the expression of

nutrient transporters along the intestine during the first 7d (Givisiez et al., 2020). Providing probiotics via in ovo feeding has been reported to foster development of the gastrointestinal microbiome by supplying pioneer colonizers and inducing competitive exclusion of pathogenic species as well as improve immunocompetence in post-hatch chicks (reviewed by Das et al., 2021). Despite the interest in probiotic in ovo feeding on immunocompetence and the microbiome, few studies have investigated the impacts on small intestinal maturation during the first week of life. The objective of the current study was to determine the ability of a commercial, mixed species probiotic provided via in ovo feeding on e17.5 to modulate the small intestinal maturation process during the final days of incubation and the first week post-hatch.

The mature small intestine is composed of villi and crypt structures lined with epithelial cells which are responsible for the unique functions of the intestine. The crypt contains stem cells expressing Leucine rich repeat containing G protein-coupled receptor 5 (Lgr5) and Olfactomedin 4 (Olfm4), that continuously divide due to niche factors localized within the crypt (Zhang and Wong, 2018; Hou et al., 2017). Achaete-scute complex homolog 2 (Ascl2) serves as a master regulator of stem cells and maintains the crypt niche by interacting with Lgr5, working in concert with the Wnt family member 3a (Wnt3a) (Schuijers et al., 2015). Daughter cells migrate away from the crypt niche and retain limited proliferative capability, indicated by marker of proliferation Ki67 expression, and begin to differentiate as they move up the villi.

There are two differentiation cell lineages: absorptive and secretory. Notch signals direct precursor cells along the differentiation lineages. Absorptive precursors express the Delta-Like Ligand 1 (DLL1) which binds Notch 1 and triggers the expression

of Hairy and enhancer of split-1 (Hes1) (Fre et al., 2005). Terminally differentiated absorptive cells are termed enterocytes and can be characterized by high expression of peptide transporter 1 (PepT1; Zhang and Wong, 2017). Secretory precursors express Atonal BHLH Transcription Factor 1 (Atoh1) and based on signals received differentiate into goblet, enteroendocrine, tuft or Paneth cells (Hou et al., 2017). Goblet cells can be characterized by expression of Mucin 2 (Muc2) (Reynolds et al., 2020) and enteroendocrine cells by Chromogranin A (Zhao et al., 2022).

MATERIALS AND METHODS

Animal Husbandry

All procedures were reviewed and approved by the Institutional Animal Care and Use Committee at Virginia Tech. Approximately 325 Cobb 500 fertile eggs were received from a local hatchery and incubated in a Natureform 1080 incubator unit at 37.5 ˚C and 55% relative humidity. On the 12th day of incubation all eggs were candled to assess viability, 6 eggs (1.8%) were removed due to embryo death or infertility.

On e17.5 in ovo feeding treatments were applied to all eggs, with approximately 100 eggs per treatment in the following manner. Egg flats were removed from the incubator and sprayed with 70% ethanol. After allowing a moment to dry, eggs were punched with a plastic egg piercer device creating a hole approximately the same size as a 20-gauge needle. Then eggs were manually injected with 0.3 ml of either 0.75% saline (Saline) or 10^6 CFU of commercially available Primalac W/S probiotic (Star-Labs Inc., Clarksdale, MO) containing *Lactobacillus acidophilus, Lactobacillus casei, Bifidobacterium bifidum and Enterococcus faecium* dissolved in 0.75% saline (Probiotic). One group of eggs had a hole punched but were not injected with anything to serve as

non-injected controls (Punch). After treatment application, eggs were sprayed again with 70% ethanol and transferred into a hatcher basket by treatment.

The hatch was pulled on e21.5 (DOH) by treatment. Chicks were individually weighed and placed in 3 battery cages (n = 20/cage) per treatment. Each cage was provided ad libitum access to water and a corn-soybean meal crumble starter diet that was formulated to meet the nutritional requirements as described by the National Research Council (NRC, 1994). On 1, 3, 5, and 7 days (d) post-hatch, each individual chick was weighed. No mortalities occurred during this study.

Tissue Collection

On e20, 6 eggs per treatment were randomly selected from hatcher baskets for sampling. Eggs were opened and embryos were euthanized by cervical dislocation. The entire small intestine was removed intact and rinsed with cold 1% PBS. The duodenal loop (with the pancreas removed), jejunum (spanning from the end of the duodenal loop to Meckel's diverticulum), and ileum (spanning from Meckel's to the ileocecal junction) were separated. The segments were diced and snap frozen in liquid nitrogen before being placed at -80 ˚C for storage. Additionally, on 1, 3, and 7 d, 2 chicks per cage (n = 6/treatment) were randomly selected and euthanized by cervical dislocation. Due to the larger size of the intestine post-hatch, approximately 5 cm from the middle of each segment was diced, and snap frozen.

RNA extraction and Quantitative PCR

Collected samples were homogenized with TriReagent using a tissue lyser and processed with the Directzol RNA mini prep columns (Zymo Research, Irvine, CA) to extract total RNA. Complementary DNA was synthesized using the Applied Biosystems

high capacity cDNA reverse transcription kit (Thermo-Fisher Scientific). Gene expression was determined by quantitative PCR (qPCR) utilizing Fast SYBR Green Master Mix (Applied Biosystems) in duplicate on an Applied Biosystems 7500 Fast Real-time PCR system (Thermo Fisher Scientific). All gene primers were designed using Primer Express 3.0 (Applied Biosystems) and are listed in Table 5-1. Chicken ribosomal protein L4 (RPL4) and ribosomal protein lateral stalk subunit P1 (RPLP1) were used as reference genes as they were the most stable as assessed by NormFinder (Andersen et al., 2004). The geometric mean of RPLP1 and RPL4 was subtracted from the Ct value to obtain the ΔCt value for each sample. The average ΔCt value of the Punch group at e20 was used as the calibrator to calculate ΔΔCt and fold change using the $2^{-\Delta\Delta Ct}$ method (Schmittgen and Livak, 2008).

Statistical Analysis

Body weight data were analyzed by two factor ANOVA considering age and treatment via JMP v15.0 (SAS Institute Cary, NC, USA). Mean separation was conducted using Tukey's Honestly Significant Difference test when significant ANOVA results were observed. Gene expression data were transformed logarithmically to conform to normality for statistical analysis and are presented as back-transformed means (Jørgensen and Pedersen, 1998). Due to the complexity of interpreting a three factor ANOVA, data were subset by intestinal segment for analysis using a two factor ANOVA by day and treatment, and in instances of significant ANOVA results Tukey's Honestly Significant Difference test was used for mean separation. In addition, data were subset by day for analysis using a two factor ANOVA by segment treatment. As before, Tukey's Honestly

Significant Difference test was used for mean separation when appropriate. Statistical significance was established at $P \leq 0.05$ for all analyses.

RESULTS

Growth Performance

The overall hatch rate at e21.5 was 72.6% (Table 5-2). Chicks were actively hatching for 24 hours prior to the pull on e21.5. Statistical analysis was not conducted on hatch rates due to a lack of replicates, but the percentages were reported to verify that in ovo injection did not affect hatchability (Uni et al., 2005). The individual group hatch rates were Probiotic (68.1%), Saline (75.5%), and Punch (75.0%). To assess any possible negative effects of in ovo feeding and due to the large number of remaining eggs at hatch pull, residual breakouts were conducted. During the breakouts, 26 additional chicks hatched out of their eggs, but they were not placed as part of the study. Inclusion of the late hatched chicks increased the overall hatch rate to 81.9% and the Probiotic and Saline group hatch rates increased to 85.7%. It is likely that the Punch group did not have any chicks hatched out as they were the last group pulled because they were in the lowest hatcher basket and the first group to undergo the breakout of their eggs following placement. Treatments were randomly assigned to the hatcher baskets where unfortunately there was a minor (half a degree) decrease in temperature at the bottom of the hatcher where the Punch group was placed, which may account for the reduced hatchability. There was no obvious evidence of mortality due to the in ovo feeding on e17.5 as the overall percent of live eggs was 93.1%. The number of live eggs following in ovo feeding were Probiotic (90.1%), Saline (97.0%) and Punch (92.0%).

Though this study was not designed to evaluate growth performance, individual body weights were collected throughout the study to generally assess growth (Table 5-3). At hatch there was a significant difference in hatchling body weights ($P = 0.012$) where Probiotic chicks were approximately 1.4g heavier than Saline and Punch chicks. This increase was not maintained through the post-hatch period; instead, the Saline group fell behind the other two groups at 7d ($P = 0.0052$). During the post-hatch period chicks were raised in 3 replicate battery cages, there was no difference in body weights between the cages (data not shown).

Effect of Probiotics on Gene Expression

Stem cell marker genes. For analysis of Treatment × Day, qPCR data were calibrated to the average of the Punch group e20 value for analysis by intestinal segment using a two factor ANOVA considering day, treatment and the interaction of day and treatment. There were no Treatment × Day interactions and no main effects of treatment but there were main effects of day. The mRNA abundance for the stem cell regulatory gene, Ascl2 decreased on 7d compared with all other timepoints in the duodenal and jejunal segments (Fig. 5-1A; $P \leq 0.0003$). In the ileum Ascl2 was greatest at 7d and lowest at 3d ($P = 0.003$). The stem cell gene Lgr5 mRNA was greatest at e20 in all intestinal segments ($P < 0.0001$; Fig. 5-1B). The mRNA for the stem cell marker gene Olfm4 increased after e20 in the duodenum, jejunum and ileum ($P < 0.003$; Fig 5-1C). Wnt3A, a stem cell niche gene, mRNA was greatest at 1d and lowest at 3d ($P = 0.027$) in the duodenum (Fig. 5-1D).

For analysis of Treatment × Segment, data were calibrated to the average of the Punch group e20 duodenum value and subset by day for analysis by a two-factor

ANOVA considering intestinal segment, treatment and the interaction of segment and treatment. There were no Treatment × Segment interactions, but there were main effects of Treatment or Segment. On e20 and 3d Ascl2 mRNA was decreased in the ileum compared to the duodenum and jejunum (P = 0.0006; Fig. 5-2A). There were no differences on 1d. Though on 7d, the ileal Ascl2 mRNA was increased compared to the jejunum but similar to the duodenum (P = 0.013). There was no treatment effect on Ascl2 mRNA. The stem cell gene Lgr5 mRNA was increased on e20 and 7d in the ileum compared to both duodenum and jejunum, but on 1d Lgr5 mRNA was decreased in the jejunum compared to the ileum and duodenum (P = 0.018; Fig. 5-2B). There were no segment differences on 3d for Lgr5 mRNA but there was an increase in the Probiotic group compared to the Saline group but it was similar to the Punch group (P = 0.042). The other stem cell gene, Olfm4 mRNA did not differ (Fig. 5-2C). Wnt3a was increased in the duodenum compared to the ileum on e20 and increased compared to the jejunum and ileum on 1d (P ≤ 0.011; Fig 5-2D). There was no treatment effect on Wnt3a or Olfm4 mRNA.

Cellular differentiation and proliferation genes. Analysis of Treatment x Day for Ki67, PepT1, Muc2, and Chromogranin A are shown in Figure 3. Ki67 is expressed in proliferating cells. For Ki67, there was no Treatment x Day interaction but there were main effects of day (Fig 5-3A). The mRNA of Ki67 was decreased on 7d in the duodenum (P = 0.0008). The jejunal Ki67 mRNA had significant p-value for the main effect of day but there was no mean separation. In the ileum, Ki67 mRNA was greater on e20 compared to 1d and 3d (P = 0.010).

Differentiated enterocytes express the Peptide transporter 1 (PepT1). PepT1 mRNA was affected by the interaction of day × treatment in the jejunum and ileum ($P \leq 0.013$; Fig. 5-3B) and a main effect of day in the duodenum. In the jejunum, for the Punch group PepT1 mRNA was greater at d3 than any other time point. By contrast in the Saline group, there was no difference in PepT1 mRNA at any day. For the Probiotic group, PepT1 mRNA was the lowest at e20 compared to d1, d3 and d7. In the ileum, PepT1 mRNA for the Punch group was greater at 7d than e20, whereas, in the Saline group PepT1 mRNA was greater at d3 than e20. For the Probiotic group there was no difference in mRNA on any day. All three intestinal segments had significant main effects of day ($P < 0.0001$). In all three segments mRNA was lowest on e20 in all intestinal segments. There was a main effect of treatment in the ileum where the Probiotic group had increased mRNA compared to the Saline group ($P = 0.023$).

Mucin-2 (Muc2) is a component of the mucus secreted by goblet cells. There was no Treatment x Day interaction for Muc2, but there were main effects of Day. All 3 intestinal segments had increased Muc2 mRNA after e20 ($P < 0.0001$; Fig. 5-3C). There was no effect of treatment on Muc2 mRNA.

Chromogranin A is a marker gene for enteroendocrine cells of the intestine. There was not a Treatment x Day interaction or a main effect of Day in any intestinal segment, but there was a main effect of treatment in the ileum. The Punch group had increased Chromogranin A mRNA above the Saline group though it was similar to the Probiotic group ($P = 0.017$; Fig. 5-3D).

Analysis of Treatment x Segment for Ki67, PepT1, Muc2, and Chromogranin A mRNA are shown in Figure 5-4. The proliferation marker Ki67 mRNA had no significant

Treatment x Segment interaction (Fig 5-4A). On e20, Ki67 was decreased in the Probiotic group compared to the Saline group but similar to the Punch group ($P = 0.018$). Also, on e20, the ileal Ki67 mRNA was increased compared to the duodenum and jejunum ($P = 0.0004$). There were no differences on 1d or 3d. On 7d, the ileal Ki67 mRNA was increased compared to the duodenum and jejunum ($P = 0.001$), but there was no main effect of treatment on this day.

PepT1 mRNA had a Treatment × Segment interaction on e20 ($P = 0.0069$) and 7d ($P \leq 0.042$; Fig 5-4B). On e20 PepT1 mRNA of the Probiotic group was greater in the ileum than the duodenum and jejunum, but the same between intestinal segments of the Punch and Saline groups. On 7d, in the Punch group PepT1 mRNA in the ileum was greater than the duodenum and jejunum, whereas there was no difference among intestinal segments for the Saline and Probiotic groups. There were a main effects of segment on e20 ($P = 0.051$), 1d ($P = 0.001$), and 7d ($P < 0.001$) where PepT1 mRNA was increased in the ileum compared to the jejunum. There were no significant differences on 3d. There was no main effect of treatment for PepT1 mRNA on any day.

There was an interaction of Treatment × Segment for Muc2 mRNA on e20 ($P = 0.047$) and 3d ($P = 0.046$; Fig. 5-4B). At e20, Muc2 mRNA in the ileum was greater than the duodenum; whereas there was no difference between intestinal segments for Punch and Saline groups. At 3d, Muc2 mRNA was greater in the jejunum and ileum than the duodenum for the Punch group, greater in the ileum than the duodenum in the Saline group and not different among intestinal segments in the Probiotic group. Each day had a significant main effect of segment where the ileum had greater Muc2 mRNA than the duodenum ($P \leq 0.033$). There was no significant main effect of treatment on Muc2.

Chromogranin A had a Treatment × Segment interaction on e20 ($P = 0.001$) and 7d ($P = 0.018$; Fig 5-4D). On e20, Chromogranin A mRNA in the Punch group was greater in the ileum than the duodenum and jejunum, and greater in the ileum than jejunum for the Probiotic group but not different among intestinal segments for the Saline group. On 7d, in the Punch and Probiotic groups, chromogranin A mRNA was greater in the ileum than the duodenum; whereas in the Saline group there was no difference between intestinal segments. Additionally, on e20 and 7d there were significant effects of segment where the ileum mRNA was greater than the duodenum ($P < 0.006$). There were no significant effects on 1d and 3d nor were there any significant main effects of treatment on any day.

Analysis of Treatment x Day for Notch 1, DLL1, Hes1, and Atoh1 mRNA are shown in Figure 5-5. There was no significant interaction of Treatment x Day nor significant main effect of treatment for any of the Notch cell differentiation signaling genes. Notch 1 is a niche factor involved in enterocyte differentiation as cells move away from the crypt. Notch 1 mRNA in the ileum was decreased on 1d and 3d compared with e20 ($P = 0.003$; Fig. 5-5A). Notch 1 interacts with DLL1 expressed on the absorptive precursor cells. DLL1 mRNA in the duodenum was increased on 1d compared to 3d and 7d ($P = 0.002$; Fig. 5-5B). In the jejunum and ileum, DLL1 mRNA decreased on 3d compared to e20 ($P \leq 0.048$). Binding of Notch1 to DLL1 triggers expression of Hes1 within absorptive precursor cells. In the duodenum Hes1 mRNA increased on 1d compared to 7d ($P = 0.001$; Fig 5-5C). There were no differences between days in the jejunum. In the ileum, Hes1 mRNA was greatest on e20 and lowest on 3d ($P = 0.037$).

Secretory precursor cells express Atoh1 instead of Notch1. In all 3 intestinal segments Atoh1 mRNA increased after e20 ($P \leq 0.0003$; Fig 5-5D).

Analysis of Treatment x Segment for Notch 1, DLL1, Hes1, and Atoh1 mRNA are shown in Figure 5-6. There were no significant interactions of Treatment x Segment for any of these Notch signaling genes. Notch 1 mRNA, which is expressed in absorptive lineage cells was increased in the ileum compared to the duodenum on e20 but the pattern reversed on 1d where the duodenum was greater than the ileum ($P \leq 0.042$; Fig. 5-6A). DLL1, the Notch ligand mRNA was increased in the ileum compared to the duodenum on e20 ($P = 0.001$) and 7d ($P = 0.003$; Fig 5-6B). The transcription factor Hes1 mRNA was similarly increased in the ileum compared to the duodenum on e20 ($P = 0.006$; Fig 5-6C). Also, on e20 DLL1 and Hes1 mRNA were increased in the Saline group compared to the Punch group, but similar to the Probiotic group ($P < 0.02$). Atoh1 mRNA did not differ between segments or by treatments at any timepoint (Fig. 5-6D).

DISCUSSION

Effect on stem cells

The functioning and development of the intestinal crypts was not seemingly altered by in ovo feeding in this study. Previous research supports this conclusion, as significant increases in villi height have been reported but increases in crypt depth have not been described, though few studies have ever investigated stem cell expression following in ovo feeding (reviewed by Das et al., 2021). Recently Reicher et al. (2022a) showed by in situ hybridization that in ovo feeding of L-glutamine, L-leucine, or saline caused an increase in Lgr5 expression in the lower villus area and decrease in the upper villus area on e19 compared to non-injected embryos. That study did not assess gene

expression via qPCR, and the correlation between in situ expression and qPCR for Lgr5 is unclear. Additionally, there were no differences post-hatch (Reicher et al., 2022a). Thus, the comparability between the current study and previous research is limited.

The intestinal crypt maintains stem cell populations through local expression of Wnt family proteins and other niche factors. Ascl2 and Wnt3a directly regulate Lgr5-expressing stem cells but Ascl2 is also responsible for the formation and maintenance of crypt structures in the intestine (van der Flier et al., 2009). In this study both Ascl2 and Wnt3a mRNA were lower on 3d and 7d than earlier timepoints, perhaps suggesting that once the crypt niche is established a lower expression level is required to sustain the stem cell population despite the increased expression of stem cell genes. The population of stem cells within the crypt has been described as stable in mature mammals (Itzkovitz et al., 2012), and in post-hatch chicks (Reicher et al., 2022a) supporting this hypothesis.

Effect on cellular differentiation

Optimal intestinal functioning requires a balance of absorptive enterocytes and secretory lineage cells, apoptotic-epithelial cells and migrating precursor cells, as well as sufficient absorptive surface area and secreted mucin proteins. In the peri-hatch period the intestine rapidly changes from embryonic cells to mature cells in response to stimuli in the intestine (Moran, 2007). The major functional cell-type of the intestine are the absorptive enterocytes, which have been previously shown to be well marked in situ by PepT1 (Zhang and Wong, 2017). Two secretory lineage cell types in chickens, goblet cells and enteroendocrine cells, have been shown to be marked by Muc2 and Chromogranin A, respectively (Reynolds et al., 2020; Zhao et al., 2022). Evaluating the

gene expression of cell marker genes provides a sense of the different cell-type populations in the intestine.

Chromogranin A mRNA has never been characterized in the peri-hatch chick, and enteroendocrine cells make up a very small percentage of the epithelial cell population so it is unclear what the observed mRNA patterns means for the population of enteroendocrine cells within the intestine. A recent study reported no change in glucagon-like peptide 2 expressing enteroendocrine cell numbers, following in ovo feeding though it did identify that enteroendocrine cells play a key role in promoting the enhancement of the small intestinal maturation process following in ovo feeding (Reicher et al., 2022b).

The current study observed significant interactions of treatment and segment or treatment and day in mRNA abundance of PepT1 on e20 and 7d and Muc2 on e20 and 3d. Both genes had increases on e20 in the ileum of the Probiotic group and in all three segments of the Saline group compared to the duodenum of the Punch group. In ovo feeding resulted in early expression of marker genes for enterocytes (PepT1) and goblet cells (Muc2) which may indicate greater quantities of the differentiated cell types. The increases for the Probiotic group at e20 were confined to the ileum which is likely associated with the colonization by the probiotic species.

Notch family proteins are the main signals used to direct cell differentiation in the intestine. Absorptive lineage precursor cells express Notch1 and Hes1 while secretory lineage precursors express DLL1 and Atoh1 (Fre et al., 2005). Notch1, Hes1, and DLL1 mRNA were increased on e20 in the ileum. Additionally, on e20 the Saline group had increased Hes1 and DLL1 mRNA compared to the Punch group. Taken together these results suggest that the increased PepT1 and Muc2 mRNA seen on e20 in the Saline

group may be due to activation of the Notch signaling pathway. Recently, Reicher et al. (2022b) proposed a similar mechanism of action for the stimulation of enterocytes via Insulin-like growth factor 1 (IGF-1) stimulation, which is increased following in ovo feeding of L-glutamine. Both IGF-1 and Notch signaling proteins stimulate intestinal cells through the mammalian target of rapamycin (mTOR) pathway, though the details of their cross-talk have yet to be clarified (Kaur and Moreau, 2019). Thus, the reported increases in IGF-1 from L-glutamine in ovo feeding and the increased Notch signaling resulting from in ovo feeding of saline may work in concert to stimulate intestinal maturation.

The increases observed at e20 for the in ovo fed groups are not maintained throughout the entire study. PepT1 mRNA peaks in the jejunum of the Punch group on 3d and in the ileum on 7d while the mRNA for the Saline and Probiotic groups are similar throughout the entire study. Similarly, Muc2 mRNA was greater on 3d in the jejunum and ileum of the Punch group compared to the Probiotic group. Liu et al. (2020) showed that both PepT1 and Muc2 mRNA increase with age in post-hatch chicks provided feed.

Probiotics and Saline stimulate the intestine via different mechanisms

Previous studies have speculated that in ovo fed saline stimulates nutrient transporters by increasing the Na^+ and Cl^- ion levels, which can act as co-factors to specific nutrient transporters such expressed throughout the intestine (Reicher et al., 2022a; 2022b). In contrast, probiotics are only expected to colonize and therefore exert an effect within the ileum. This difference in location seemingly explains why the Saline and Probiotic group responses differed on e20. Only the ileum of the Probiotic group had increased PepT1, while the Saline group was somewhat elevated in all intestinal

segments, compared to the Punch group on e20. Additionally, the benefit of providing Na^+ and Cl^- ions to the intestine was likely limited as they would be used by nutrient transporters and have no means of persisting. Beyond the possible stimulatory mechanism as co-factors, the Saline group had increased Hes1 and DLL1 mRNA on e20 compared to the Punch group. It seems that saline stimulates the Notch pathway within absorptive precursor cells and enterocytes. No other study has reported on Notch signals following in ovo feeding but Reicher et al. (2022b) reported that in ovo feeding of saline enhanced enterocyte maturation compared to non-injected controls.

The effect of the in ovo probiotic was limited to increasing PepT1 and Muc2 in the ileum on e20. Proszkowiec-Weglarz et al. (2020) have suggested that Muc2 gene expression is delayed post-hatch compared to other defensive barrier function genes and may require the stimulation of antigens for upregulation of gene expression. Similarly, Liu et al. (2020) found that PepT1 and Muc2 mRNA increase in chicks upon access to feed. One previous study reported increased ileal Muc2 mRNA on e19, doh and 3d following in ovo feeding of various probiotics in agreement with the current study (Majidi-Mosleh et al., 2017). Together, this implies that in ovo fed probiotics are likely providing antigenic stimulation of the ileum.

Conclusion

The objective of the current study was to explore how in ovo feeding of a commercial probiotic impacts the small intestine maturation during the peri-hatch period. We observed the majority of changes occurring 48 hours post-injection, at e20. On e20 the Probiotic fed group had increased ileal PepT1 and Muc2 mRNA compared to non-injected control embryos. The Saline group on e20 had increased PepT1 and Muc2

mRNAs in all intestinal segments though to a lesser extent than the Probiotic group. The increased mRNA was not sustained throughout the study and the non-injected controls had later increases in Muc2 (3d) and PepT1 (7d), consistent with previous studies. The mechanisms behind the Saline group and Probiotic group mRNA increases seemed to differ slightly. The Saline group at e20 had increased mRNA of Hes1 and DLL1 which are Notch signals that trigger absorptive lineage commitment during cellular differentiation. This implies that in ovo feeding of Saline promoted the production of enterocytes within the small intestine resulting in an increase in the enterocyte marker PepT1. The Probiotic group did not enhance Notch signaling genes to the same extent as the Saline group but instead may have provided antigenic stimulation to the intestine promoting early Muc2 mRNA upregulation. Regardless, this study is one of the first to probe the underlying mechanisms for the long-reported enhancements to small intestinal maturation from in ovo feeding and provide an initial hypothesis upon which future research can expand.

REFERENCES

Andersen C., J. Jensen, T. Orntoft. 2004. Normalization of real - time quantitative reverse transcription -PCR data: A model - based variance estimation approach to identify genes suited for normalization, applied to bladder and colon cancer data sets. Cancer Res. 64:5245.

Das, R., P. Mishra, R. Jha. 2021. In ovo feeding as a tool for improving performance and gut health of poultry: a review. Front. Vet. Sci. 8:754246.

Fre, S., M. Huyghe, P. Mourikis, S. Robine, D. Louvard, and S. Artavanis-Tsakonas. 2005. Notch signals control the fate of immature progenitor cells in the intestine. Nature. 435:964-968.

Givisiez, P.E.N., A. L.B. Moreria Filho, M.R.B. Santos, H.B. Oliveria, P.R. Ferket, C.J.B. Oliveria, and R.D. Malheiros. 2020. Chicken embryo development: metabolic and morphological basis for in ovo feeding technology. Poult. Sci. 99:6774-6782.

Hou Q, Ye L, Huang L, Yu Q. 2017. The research progress on intestinal stem cells and its relationship with intestinal microbiota. Front. Immunol. 8:599.

Itzkovitz, S., Blat, I. C., Jacks, T., Clevers, H., and van Oudenaarden, A. (2012). Optimality in the development of intestinal crypts. Cell. 148:608-619.

Jørgensen, E., and A.R. Pedersen. 1998. How to obtain those nasty standard errors from transformed data-and why they should not be used. Aarhus Univ. DetJordbrugsvidenskabelige Fakultet, Aarhus, Denmark. International Report 7.

Kaur, H. and R. Moreau. 2019. Role of mTORC1 in intestinal epithelial repair and tumorigenesis. Cell. Mol. Life Sci. 76:2525-2546.

Liu, K., M. Jia, and E.A. Wong. 2020. Delayed access to feed affects broiler small intestinal morphology and goblet cell ontogeny. Poult. Sci. 99:5275-5285.

Majidi-Mosleh, A., A.A. Sadeghi, S.N. Mousavi, M. Chamani and A. Zarei. 2017. Ileal MUC2 gene expression and microbial population, but not growth performance and immune response, are influenced by in ovo injection of probiotics in broiler chickens. Br. Poult. Sci. 58:40-45.

Moran, E.T. 2007. Nutrition of the developing embryo and hatchling. Poult. Sci. 86: 1043-1049.

National Research Council. 1994. Nutrient Requirements of Poultry. 9th rev. ed. Natl. Acad. Press, Washington, DC.

Proszkowiec-Weglarz, M., L.L. Schreier, S. Kahl, K.B. Miska, B. Russell, B. and T.H. Elsasser. 2020. Effect of delayed feeding post-hatch on expression of tight junction–and gut barrier–related genes in the small intestine of broiler chickens during neonatal development. Poult. Sci. 99:4714-4729.

Reicher, N., T. Melkman-Zehavi, J. Dayan, E.A. Wong, and Z. Uni. 2022a. Nutritional stimulation by in-ovo feeding modulates cellular proliferation and differentiation in the small intestinal epithelium of chicks. Anim Nutr. 8:91-101.

Reicher, N., T. Melkman-Zehavi, J. Dayan, E.A. Wong, and Z. Uni. 2022b. Intra-amniotic administration of l-glutamine promotes intestinal maturation and enteroendocrine stimulation in chick embryos. Sci. Rep. 12:1-13.

Reynolds, K.L., S.E. Cloft, and E.A. Wong. 2020. Changes with age in density of goblet cells in the small intestine of broiler chicks. Poult. Sci. 99:2342-2348.

Schmittgen T. D. and K. J. Livak. 2008. Analyzing real-time PCR data by the comparative C(T) method. Nat. Protoc. 3:1101–1108.

Schuijers, J., J.P. Junker, M. Mokry, P. Hatzis, B.K. Koo, V. Sasselli, L.G. van der Flier, E. Cuppen, A. van Oudenaarden and H. Clevers. 2015. Ascl2 acts as an R-spondin/Wnt-responsive switch to control stemness in intestinal crypts. Cell stem cell. 16:158-170.

Uni, Z. 2006. Early development of small intestinal function. Pages 29-43 in G.C. Perry (Ed.), Avian Gut Function in Health and Disease, Carfax Publ. Co., Oxfordshire, UK.

Uni, Z. and P.R. Ferket. 2003. Enhancement of development of oviparious species by in ovo feeding. North Carolina State Univ, Raleigh, NC, Yissum Research Development Company of the Hebrew Univ of Jerusalem, Jerusalem, IL, assignees. US Pat. No. 6,592,878, Washington, DC, US Patent and Trademark Office.

Uni, Z., R. Platin, and D. Sklan. 1998. Cell proliferation in chicken intestinal epithelium occurs both in the crypt and along the villus. J. Comp. Physiol. B 168:241-247.

Uni, Z., A. Geyra, H. Ben-Hur, and D. Sklan. 2000. Small intestinal development in the young chick: crypt formation and enterocyte proliferation and migration. Br. Poult. Sci. 41:544-551.

Uni, Z., P.R. Ferket, E. Tako, and O. Kedar. 2005. In ovo feeding improves energy status of late-term chicken embryos. Poult. Sci. 84:764-770.

van der Flier, L.G., M.E. van Gijn, P. Hatzis, P. Kujala, A. Haegebarth, D.E. Stange, H. Begthel, H., M. van den Born, V. Guryev, I. Oving, I. and J.H. van Es. 2009. Transcription factor achaete scute-like 2 controls intestinal stem cell fate. Cell. 136:903-912.

van der Wagt, I., I. C. de Jong, M. A. Mitchell, R. Molenaar, and H. van den Brand. 2020. A review on yolk sac utilization in poultry. Poult. Sci. 99:2162-2175.

Zhang, H., and E.A. Wong. 2017. Spatial transcriptional profile of PepT1 mRNA in the yolk sac and small intestine in broiler chickens. Poult. Sci. 96:2871-2876.

Zhang, H. and E.A. Wong, 2018. Identification of cells expressing *OLFM4* and *LGR5* mRNA by in situ hybridization in the yolk sac and small intestine of embryonic and early post-hatch chicks. Poult. Sci. 97:628-633.

Zhao, D., M.B. Farnell, M.H. Kogut, K.J. Genovese, R.S. Chapkin, L.A. Davidson, L.R. Berghman, and Y.Z. Farnell. 2022. From crypts to enteroids: establishment and characterization of avian intestinal organoids. Poult. Sci. 101:101642.

ACKNOWLEDGMENTS

This research was supported by Research Grant No. US-5074-18CR from the United States – Israel Binational Agricultural Research and Development (BARD) Fund.

FIGURE CAPTIONS

Figure 5-1. mRNA abundance of stem cell related genes: Expression of Achaete-scute complex homolog 2 (Acsl2), Leucine rich repeat containing G protein-coupled receptor 5 (Lgr5), Olfactomedin 4 (Olfm4), and Wnt family member 3a (Wnt3a) mRNA in each intestinal segment from embryonic day (e) 20 to 7 days post-hatch (d). At e17.5 eggs received a 0.3 ml in ovo injection of probiotics in saline, saline alone, or no injection but were punched (Punch). Relative mRNA abundance from qPCR (n=6) was calibrated to the average of Punch group e20 value for each intestinal segment and subset by intestinal segment. The analysis presented is a 2-factor ANOVA considering Treatment × Day interaction (Int), Day and Treatment (Trt) main effects.

Figure 5-2. mRNA abundance of stem cell related genes: Expression of Achaete-scute complex homolog 2 (Acsl2), Leucine rich repeat containing G protein-coupled receptor 5 (Lgr5), Olfactomedin 4 (Olfm4), and Wnt family member 3a (Wnt3a) mRNA on embryonic day (e) 20 to 7 days post-hatch (d) in each intestinal segment. At e17.5 eggs received a 0.3 ml in ovo injection of probiotics in saline, saline alone, or no injection but were punched (Punch). Relative mRNA abundance from qPCR (n=6) was calibrated to the average of Punch group e20 duodenum value and subset by day. The analysis presented is a 2-factor ANOVA considering Treatment × Segment Interaction (Int), Segment (Seg), and Treatment (Trt).

Figure 5-3. mRNA abundance of differentiated cell marker genes: Expression of marker genes for precursor cells - marker of proliferation Ki67, enterocytes - Peptide transporter

1 (PepT1), goblet cells - Mucin-2 (Muc2), and enteroendocrine cells - Chromogranin A in each intestinal segment from embryonic day (e) 20 to 7 days post-hatch (d). At e17.5 eggs received a 0.3 ml in ovo injection of probiotics in saline, saline alone, or no injection but were punched (Punch). Relative mRNA abundance from qPCR (n=6) was calibrated to the average of Punch group e20 value for each intestinal segment and subset by intestinal segment. The analysis presented is a 2-factor ANOVA considering Treatment × Day interaction (Int), Day and Treatment (Trt) main effects. Bars with different letters within each intestinal segment are significantly different from each other ($P \leq 0.05$).

Figure 5-4. mRNA abundance of differentiated cell marker genes: Expression of marker genes for precursor cells - marker of proliferation Ki67, enterocytes - Peptide transporter 1 (PepT1), goblet cells - Mucin-2 (Muc2), and enteroendocrine cells - Chromogranin A on embryonic day (e) 20 to 7 days post-hatch (d) in each intestinal segment. At e17.5 eggs received a 0.3 ml in ovo injection of probiotics in saline, saline alone, or no injection but were punched (Punch). Relative mRNA abundance from qPCR (n=6) was calibrated to the average of Punch group e20 duodenum value and subset by day. The analysis presented is a 2-factor ANOVA considering Treatment × Segment Interaction (Int), Segment (Seg), and Treatment (Trt). Bars with different letters within each intestinal segment are significantly different from each other ($P \leq 0.05$).

Figure 5-5. mRNA abundance of Notch pathway genes associated with intestinal cell differentiation: Expression of Notch 1, Delta-Like Ligand 1 (DLL1), Hairy and enhancer

of split-1 (Hes1), and Atonal BHLH Transcription Factor 1 (Atoh1) in each intestinal segment from embryonic day (e) 20 to 7 days post-hatch (d). At e17.5 eggs received a 0.3 ml in ovo injection of probiotics in saline, saline alone, or no injection but were punched (Punch). Relative mRNA abundance from qPCR (n=6) was calibrated to the average of Punch group e20 value for each intestinal segment and subset by intestinal segment. The analysis presented is a 2-factor ANOVA considering Treatment × Day interaction (Int), Day and Treatment (Trt) main effects.

Figure 5-6. mRNA abundance of Notch pathway genes associated with intestinal cell differentiation: Notch 1, Delta-Like Ligand 1 (DLL1), Hairy and enhancer of split-1 (Hes1), and Atonal BHLH Transcription Factor 1 (Atoh1) on embryonic day (e) 20 to 7 days post-hatch (d) in each intestinal segment. At e17.5 eggs received a 0.3 ml in ovo injection of probiotics in saline, saline alone, or no injection but were punched (Punch). Relative mRNA abundance from qPCR (n=6) was calibrated to the average of Punch group e20 duodenum value and subset by day. The analysis presented is a 2-factor ANOVA considering Treatment × Segment Interaction (Int), Segment (Seg), and Treatment (Trt).

TABLES

Table 5-1. Primers for quantitative PCR

Gene name	Forward/Reverse Primers (5' to 3')	Amplicon Size (bp)	Accession no.[1]
Achaete-scute complex homolog 2 (Ascl2)	GGGTGGAAAAAAAGAAATGGAA/ CCCTCCCCCTGCAGAAAC	58	NM_001389502.2
Leucine rich repeat containing G protein-coupled receptor 5 (Lgr5)	TGGTTTGACCTTCGTTTGCA/ GGACATATACAATGGAGATCTGAAAACT	67	XM_425441.7
Olfactomedin 4 (Olfm4)	TTGCCGGATACCACCTTTCC/ TTTCTGCAAGAGCGTTGTGG	72	NM_001040463.1
Wnt family member 3A (WNT3a)	GACTGGTCCCCAAGCAGCTA/ TGCTACGCTGGGCATGATC	62	NM_001171601.3
Marker of Proliferation mKi67 (Ki67)	CACAGGCAAAGGCTGTCAAA/ TCCGTGCAATTTTCCTTGCT	63	XM_015289038.4
Peptide Transporter 1 (PepT1)	CCCCTGAGGAGGATCACTGTT/ CAAAAGAGCAGCAGCAACGA	66	NM_204365.2
Mucin-2 (Muc2)	CTGATTGTCACTCACGCCTTAATC/ GCCGGCCACCTGCAT	147	JX284122.1
Chromogranin A	CAGGGAGAAGTAGCTTTGGACAA/ CCTCGCTGCTGTTGCTCAT	68	XM_040673024.2
Notch homolog-1 (Notch1)	GAGGATCCATCGTCTACTTGGAA/ ATCGGTTGCGCTCTGGAA	81	NM_001030295.1
Delta like canonical Notch ligand 1 (DLL1)	GGCCGGTCATCGTTGACTT/ TCCAGGGAAACTGGCTGTTC	63	NM_204973.3
Hes family bHLH transcription factor 1 (Hes1)	TCAGCGAGTGCATGAACGA/ GCGCACCTCAGCGTTGA	68	XM_040679737.2
Atonal homolog 1 (Drosophila) (Atoh1)	AATGTCATCCCCTCCTTCAACA/ CCATCTGCAGCGTCTCGTACT	61	XM_004941130.5
Ribosomal protein large subunit P1 (RPLP1)	TCTCCACGACGACGAAGTCA/ CCGCCGCCTTGATGAG	55	NM_205322.1
Ribosomal protein large subunit 4 (RPL4)	TCAAGGCGCCCATTCG/ TGCGCAGGTTGGTGTGAA	63	NM_001007479.1

[1]Note that the primer sequences were designed for regions of consensus between all published variants.

Table 5-2. Hatch rate following in ovo feeding at embryonic day 17.5

Treatment Group[1]	Hatched[2]		Late hatching		Alive in egg	Total live eggs[4]	
Probiotic	62	68.1%	16	85.7%	13	91	90.1%
Saline	74[3]	75.5%	10	85.7%	10	98	97.0%
Punch	69	75.0%	0	75.0%	23	92	92.0%
Overall	204	72.6%	26	81.9%	46	281	93.1%

[1]Treatment groups: Punch- non-injected controls, Saline- injected with 0.3 ml of 0.75% saline solution, Probiotic- injected with 0.3 of 10^6 CFU of Primalac W/S probiotic suspended in 0.75% saline solution.
[2]Chicks were classified as hatched if they had cleared the egg shell on their own. Percentages are based on the count of live eggs after breakout not number at transfer given in the final column of the table.
[3]1 hatchling was found dead.
[4]Due to the large number of eggs remaining unhatched at pull, residual breakouts were conducted. Chicks were designated as hatching if they were alive and in the process of hatching (internal or external pip and in correct position) during residual hatch break-outs following pull at embryonic day 21.5. Percentage is based on the number of eggs: Probiotic 101, Saline 101, Punch 100.

Table 5-3. Individual body weights at hatch and post-hatch following in ovo feeding at embryonic day 17.5[1].

Treatment Group[2]	**DOH (g)**	**1d (g)**	**3d (g)**	**5d (g)**	**7d (g)**
Probiotic	50.3[a]	51.5	76.3	123.2	180.3[a]
Saline	49.1[b]	51.2	76.2	121.4	173.1[b]
Punch	48.8[b]	51.3	78.1	125.2	180.2[a]
Standard Error	0.4	0.5	0.7	1.3	1.8
Analysis of Variance			***Probabilities***		
Treatment effect	*0.012*	0.85	0.14	0.10	*0.0052*

[1]Individuals were weighed in grams (g) just after hatch pull on embryonic day 21.5 (DOH), and on 1, 3, 5, 7 day post-hatch (d). Sample size on DOH was approximately 68 per group; D1 60 per group, D3 54 per group, D5 and D7 48 per group.

[2]Treatment groups: Punch- non-injected controls, Saline- injected with 0.3 ml of 0.75% saline solution, Probiotic- injected with 0.3 of 10^6 CFU of Primalac W/S probiotic suspended in 0.75% saline solution.

[a,b]Means in the same column with different superscripts are statistically different ($P < 0.05$) based on Tukey HSD mean separation.

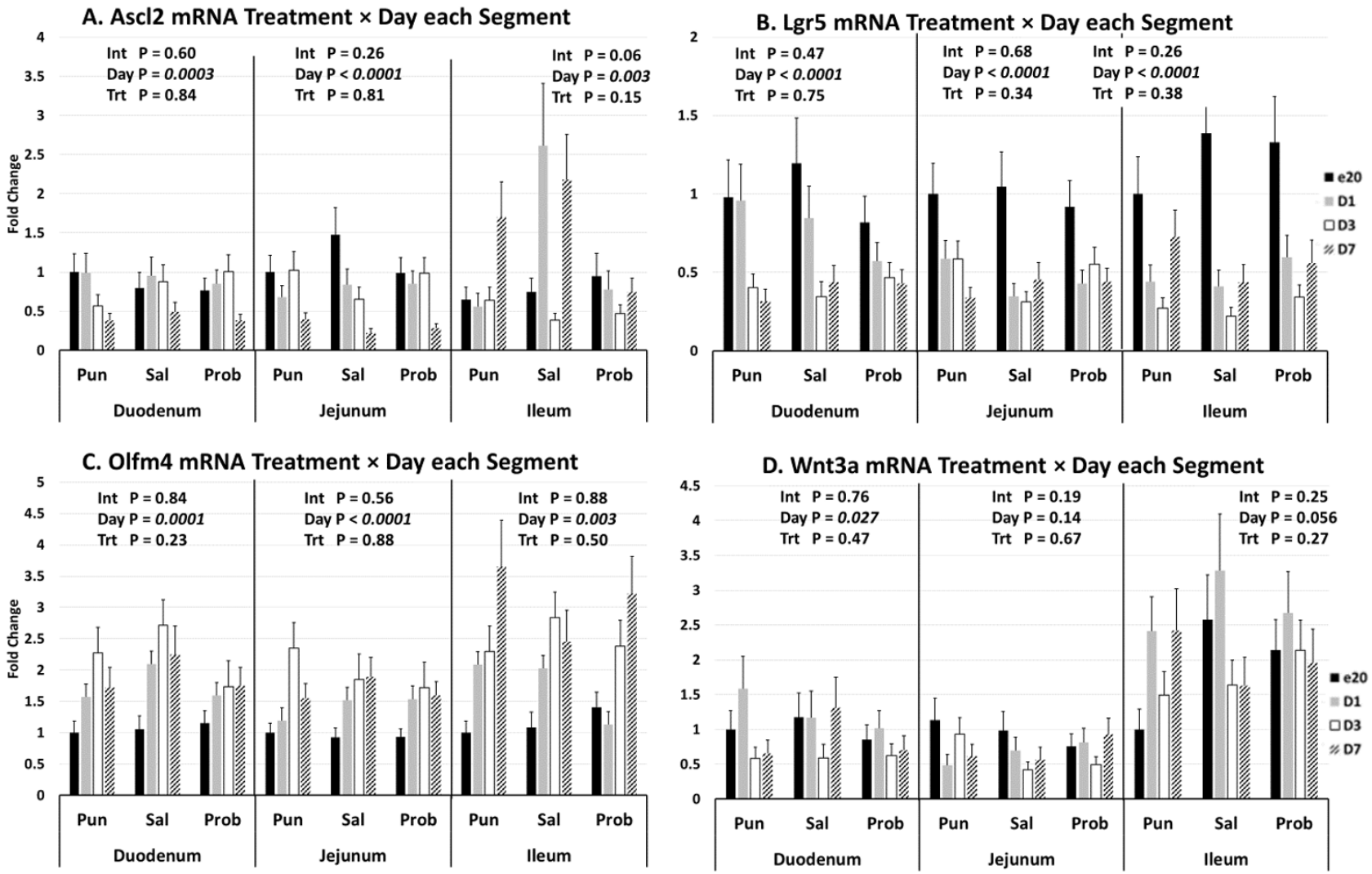
A. Ascl2 mRNA Treatment × Day each Segment
Int P = 0.60
Day P = 0.0003
Trt P = 0.84
Int P = 0.26
Day P < 0.0001
Trt P = 0.81
Int P = 0.06
Day P = 0.003
Trt P = 0.15
B. Lgr5 mRNA Treatment × Day each Segment
Int P = 0.47
Day P < 0.0001
Trt P = 0.75
Int P = 0.68
Day P < 0.0001
Trt P = 0.34
Int P = 0.26
Day P < 0.0001
Trt P = 0.38
C. Olfm4 mRNA Treatment × Day each Segment
Int P = 0.84
Day P = 0.0001
Trt P = 0.23
Int P = 0.56
Day P < 0.0001
Trt P = 0.88
Int P = 0.88
Day P = 0.003
Trt P = 0.50
D. Wnt3a mRNA Treatment × Day each Segment
Int P = 0.76
Day P = 0.027
Trt P = 0.47
Int P = 0.19
Day P = 0.14
Trt P = 0.67
Int P = 0.25
Day P = 0.056
Trt P = 0.27
Fold Change
Pun
Sal
Prob
Duodenum
Jejunum
Ileum
e20
D1
D3
D7

Figure 5-1.

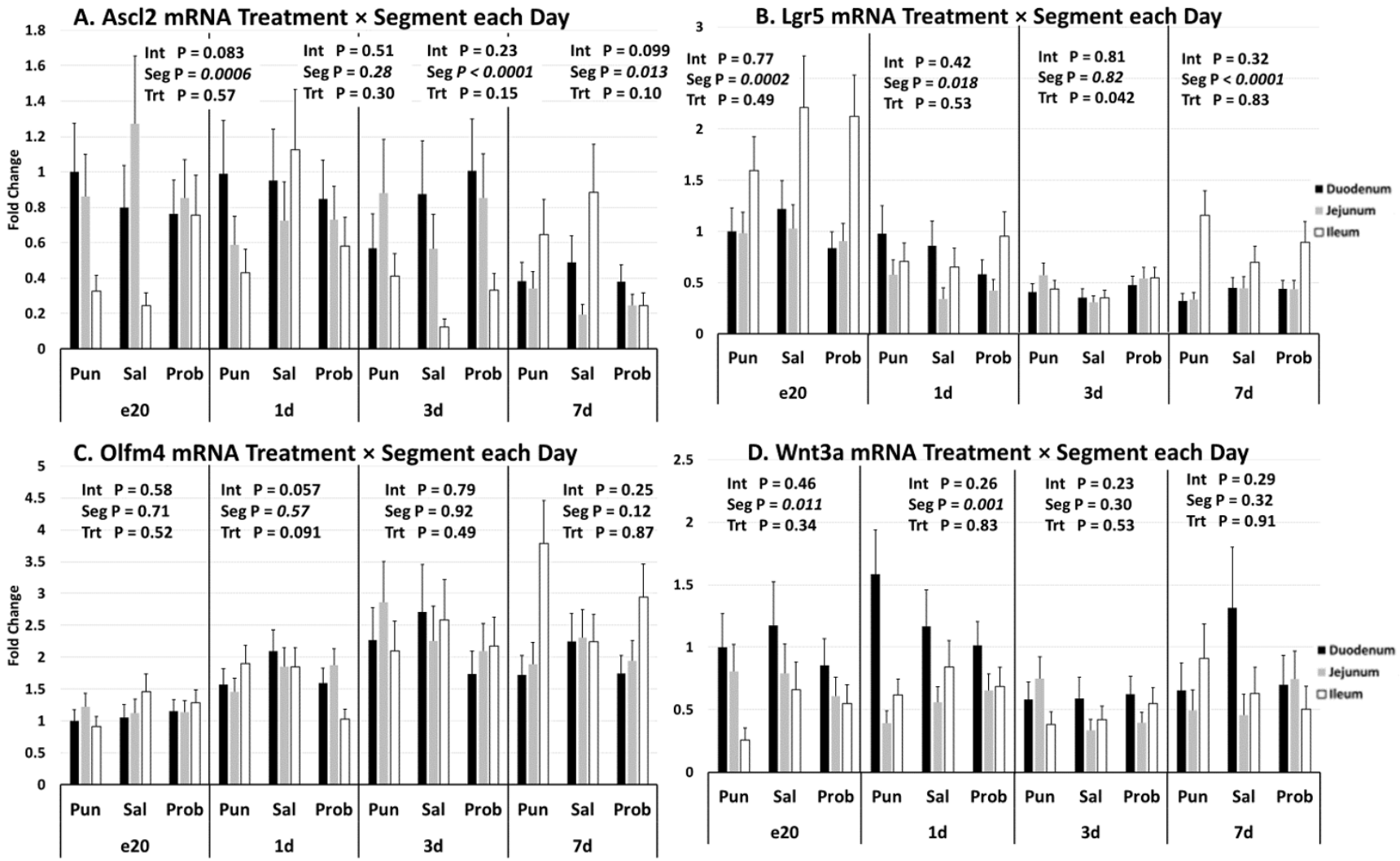
A. Ascl2 mRNA Treatment × Segment each Day
Fold Change
Int P = 0.083
Seg P = 0.0006
Trt P = 0.57
Int P = 0.51
Seg P = 0.28
Trt P = 0.30
Int P = 0.23
Seg P < 0.0001
Trt P = 0.15
Int P = 0.099
Seg P = 0.013
Trt P = 0.10
B. Lgr5 mRNA Treatment × Segment each Day
Int P = 0.77
Seg P = 0.0002
Trt P = 0.49
Int P = 0.42
Seg P = 0.018
Trt P = 0.53
Int P = 0.81
Seg P = 0.82
Trt P = 0.042
Int P = 0.32
Seg P < 0.0001
Trt P = 0.83
Duodenum
Jejunum
Ileum
C. Olfm4 mRNA Treatment × Segment each Day
Int P = 0.58
Seg P = 0.71
Trt P = 0.52
Int P = 0.057
Seg P = 0.57
Trt P = 0.091
Int P = 0.79
Seg P = 0.92
Trt P = 0.49
Int P = 0.25
Seg P = 0.12
Trt P = 0.87
D. Wnt3a mRNA Treatment × Segment each Day
Int P = 0.46
Seg P = 0.011
Trt P = 0.34
Int P = 0.26
Seg P = 0.001
Trt P = 0.83
Int P = 0.23
Seg P = 0.30
Trt P = 0.53
Int P = 0.29
Seg P = 0.32
Trt P = 0.91
Pun Sal Prob
e20
1d
3d
7d

Figure 5-2.

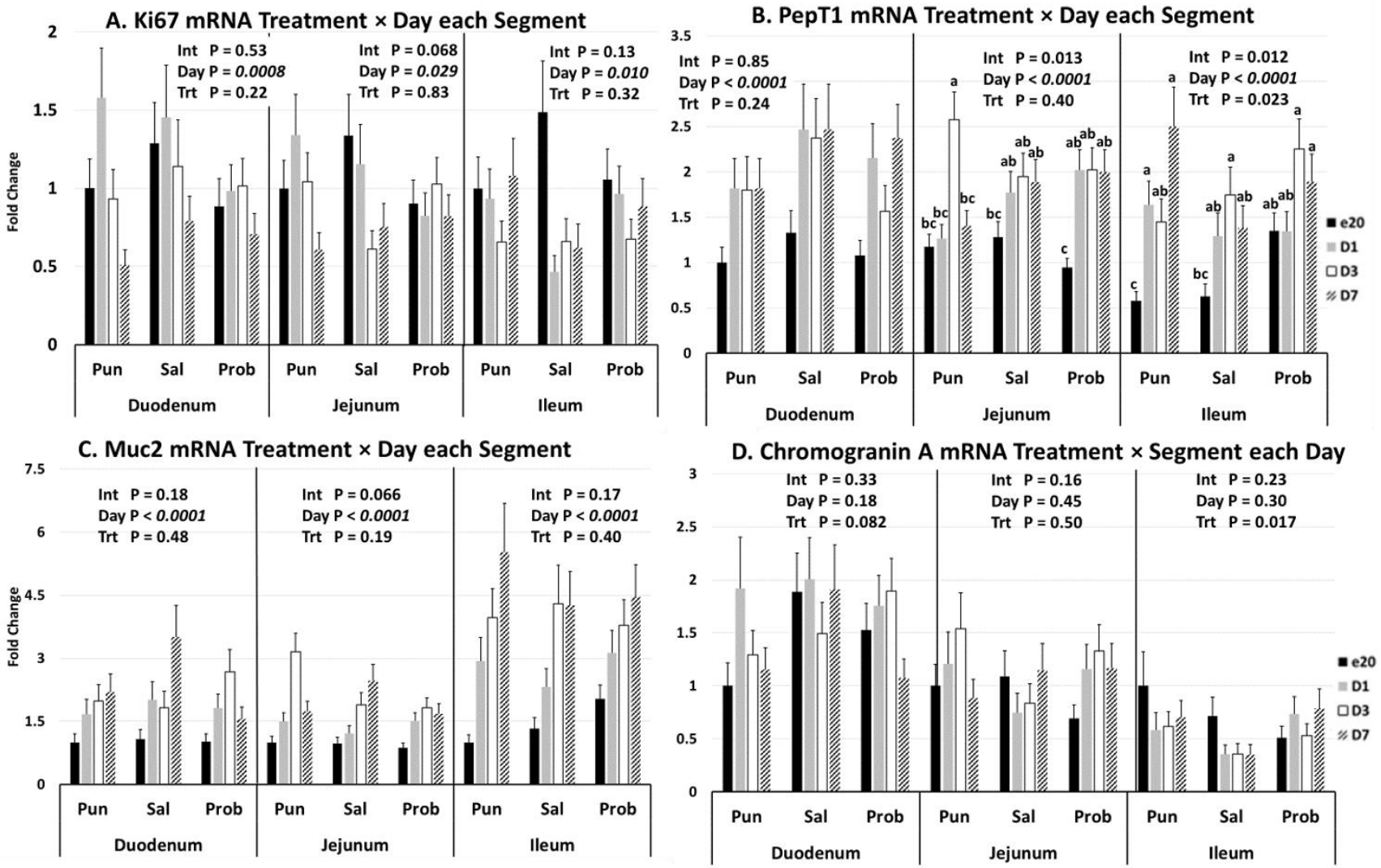
A. Ki67 mRNA Treatment × Day each Segment
Int P = 0.53
Day P = 0.0008
Trt P = 0.22
Int P = 0.068
Day P = 0.029
Trt P = 0.83
Int P = 0.13
Day P = 0.010
Trt P = 0.32
Fold Change
Pun Sal Prob Pun Sal Prob Pun Sal Prob
Duodenum Jejunum Ileum
B. PepT1 mRNA Treatment × Day each Segment
Int P = 0.85
Day P < 0.0001
Trt P = 0.24
Int P = 0.013
Day P < 0.0001
Trt P = 0.40
Int P = 0.012
Day P < 0.0001
Trt P = 0.023
e20
D1
D3
D7
C. Muc2 mRNA Treatment × Day each Segment
Int P = 0.18
Day P < 0.0001
Trt P = 0.48
Int P = 0.066
Day P < 0.0001
Trt P = 0.19
Int P = 0.17
Day P < 0.0001
Trt P = 0.40
D. Chromogranin A mRNA Treatment × Segment each Day
Int P = 0.33
Day P = 0.18
Trt P = 0.082
Int P = 0.16
Day P = 0.45
Trt P = 0.50
Int P = 0.23
Day P = 0.30
Trt P = 0.017

Figure 5-3.

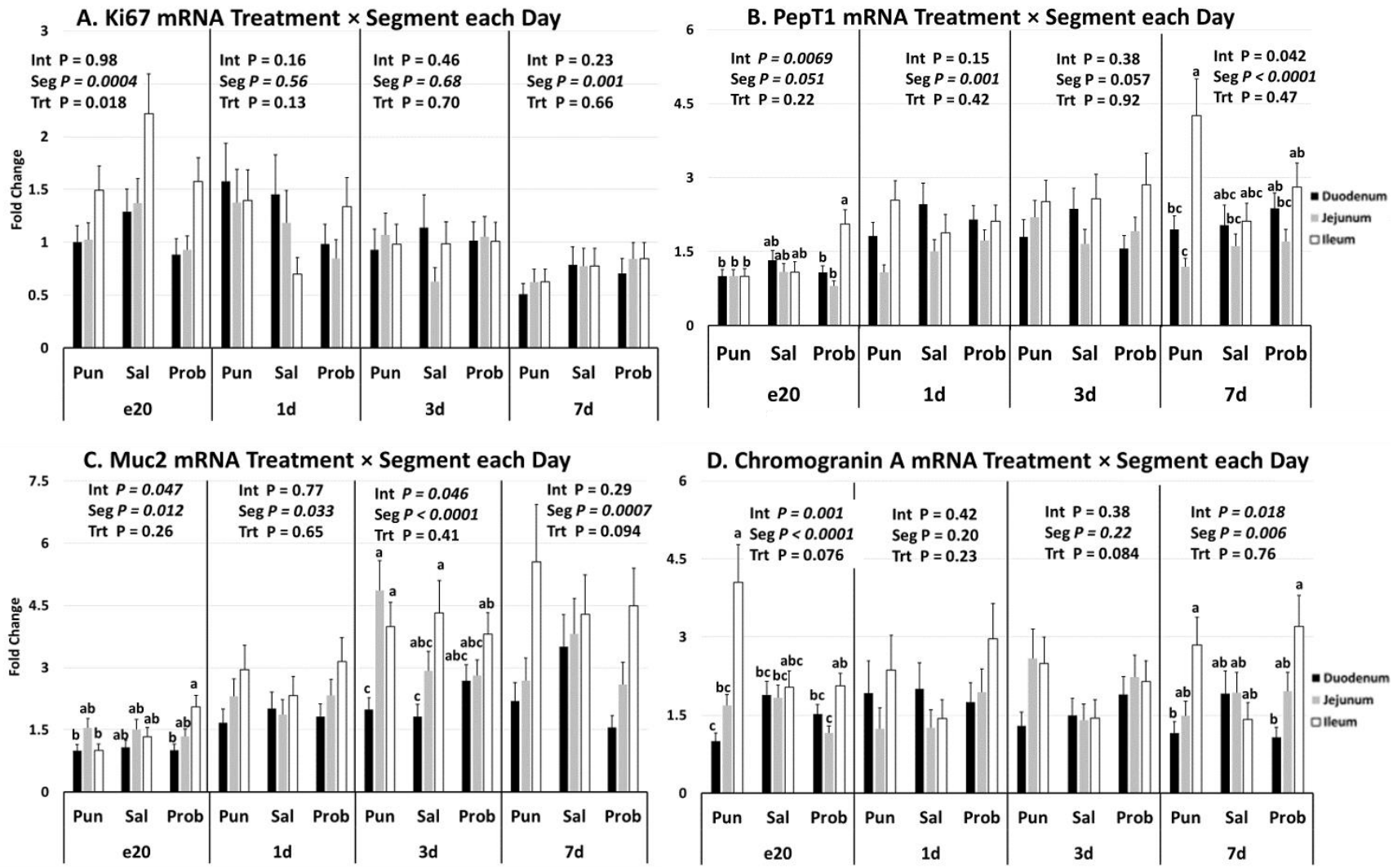
A. Ki67 mRNA Treatment × Segment each Day
Int P = 0.98
Seg P = 0.0004
Trt P = 0.018
Int P = 0.16
Seg P = 0.56
Trt P = 0.13
Int P = 0.46
Seg P = 0.68
Trt P = 0.70
Int P = 0.23
Seg P = 0.001
Trt P = 0.66
Fold Change
Pun Sal Prob Pun Sal Prob Pun Sal Prob Pun Sal Prob
e20 1d 3d 7d
B. PepT1 mRNA Treatment × Segment each Day
Int P = 0.0069
Seg P = 0.051
Trt P = 0.22
Int P = 0.15
Seg P = 0.001
Trt P = 0.42
Int P = 0.38
Seg P = 0.057
Trt P = 0.92
Int P = 0.042
Seg P < 0.0001
Trt P = 0.47
Duodenum
Jejunum
Ileum
C. Muc2 mRNA Treatment × Segment each Day
Int P = 0.047
Seg P = 0.012
Trt P = 0.26
Int P = 0.77
Seg P = 0.033
Trt P = 0.65
Int P = 0.046
Seg P < 0.0001
Trt P = 0.41
Int P = 0.29
Seg P = 0.0007
Trt P = 0.094
D. Chromogranin A mRNA Treatment × Segment each Day
Int P = 0.001
Seg P < 0.0001
Trt P = 0.076
Int P = 0.42
Seg P = 0.20
Trt P = 0.23
Int P = 0.38
Seg P = 0.22
Trt P = 0.084
Int P = 0.018
Seg P = 0.006
Trt P = 0.76

Figure 5-4.

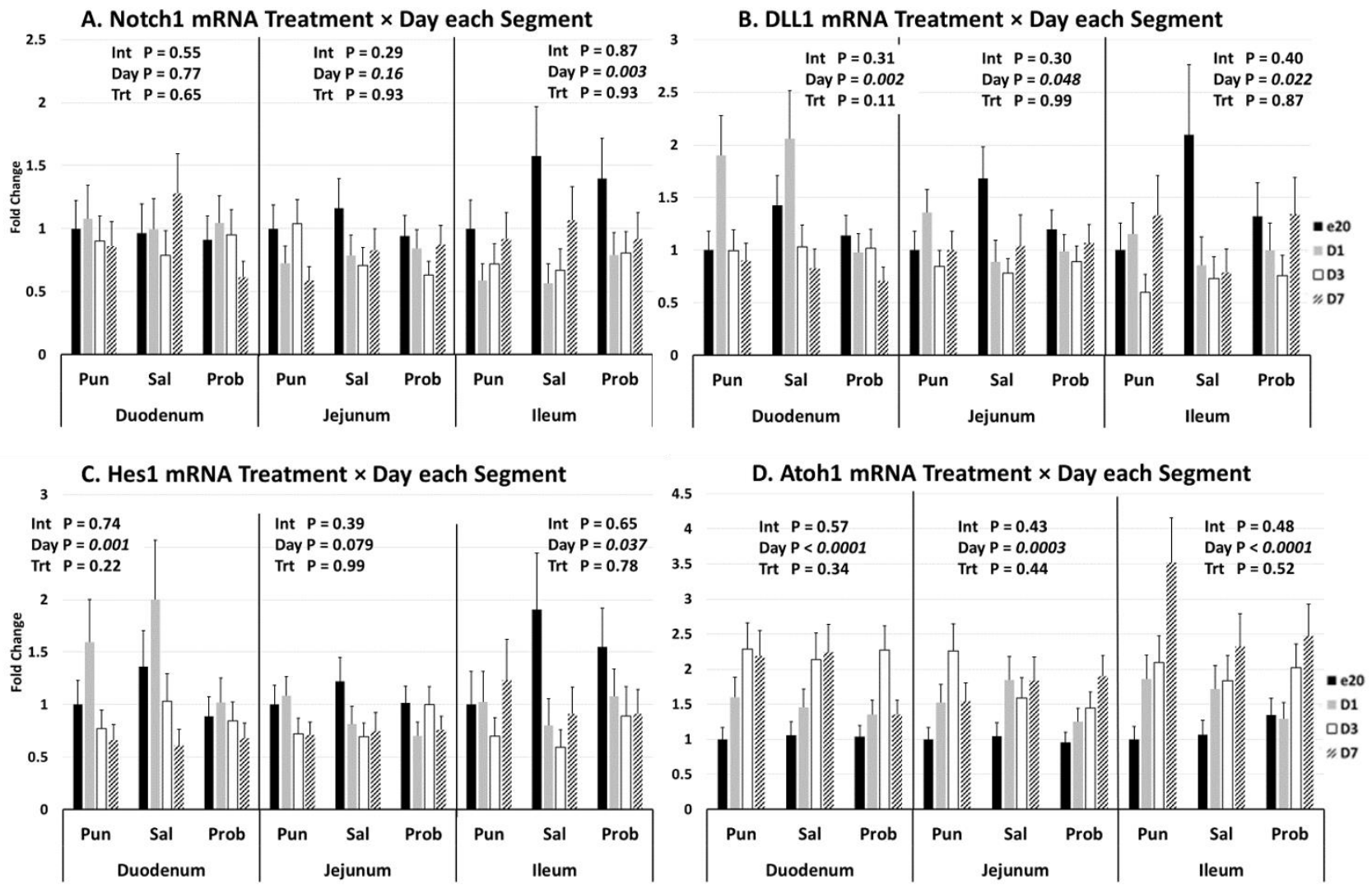
A. Notch1 mRNA Treatment × Day each Segment
Int P = 0.55
Day P = 0.77
Trt P = 0.65
Int P = 0.29
Day P = 0.16
Trt P = 0.93
Int P = 0.87
Day P = 0.003
Trt P = 0.93
B. DLL1 mRNA Treatment × Day each Segment
Int P = 0.31
Day P = 0.002
Trt P = 0.11
Int P = 0.30
Day P = 0.048
Trt P = 0.99
Int P = 0.40
Day P = 0.022
Trt P = 0.87
C. Hes1 mRNA Treatment × Day each Segment
Int P = 0.74
Day P = 0.001
Trt P = 0.22
Int P = 0.39
Day P = 0.079
Trt P = 0.99
Int P = 0.65
Day P = 0.037
Trt P = 0.78
D. Atoh1 mRNA Treatment × Day each Segment
Int P = 0.57
Day P < 0.0001
Trt P = 0.34
Int P = 0.43
Day P = 0.0003
Trt P = 0.44
Int P = 0.48
Day P < 0.0001
Trt P = 0.52
Fold Change
Pun
Sal
Prob
Duodenum
Jejunum
Ileum
e20
D1
D3
D7

Figure 5-5.

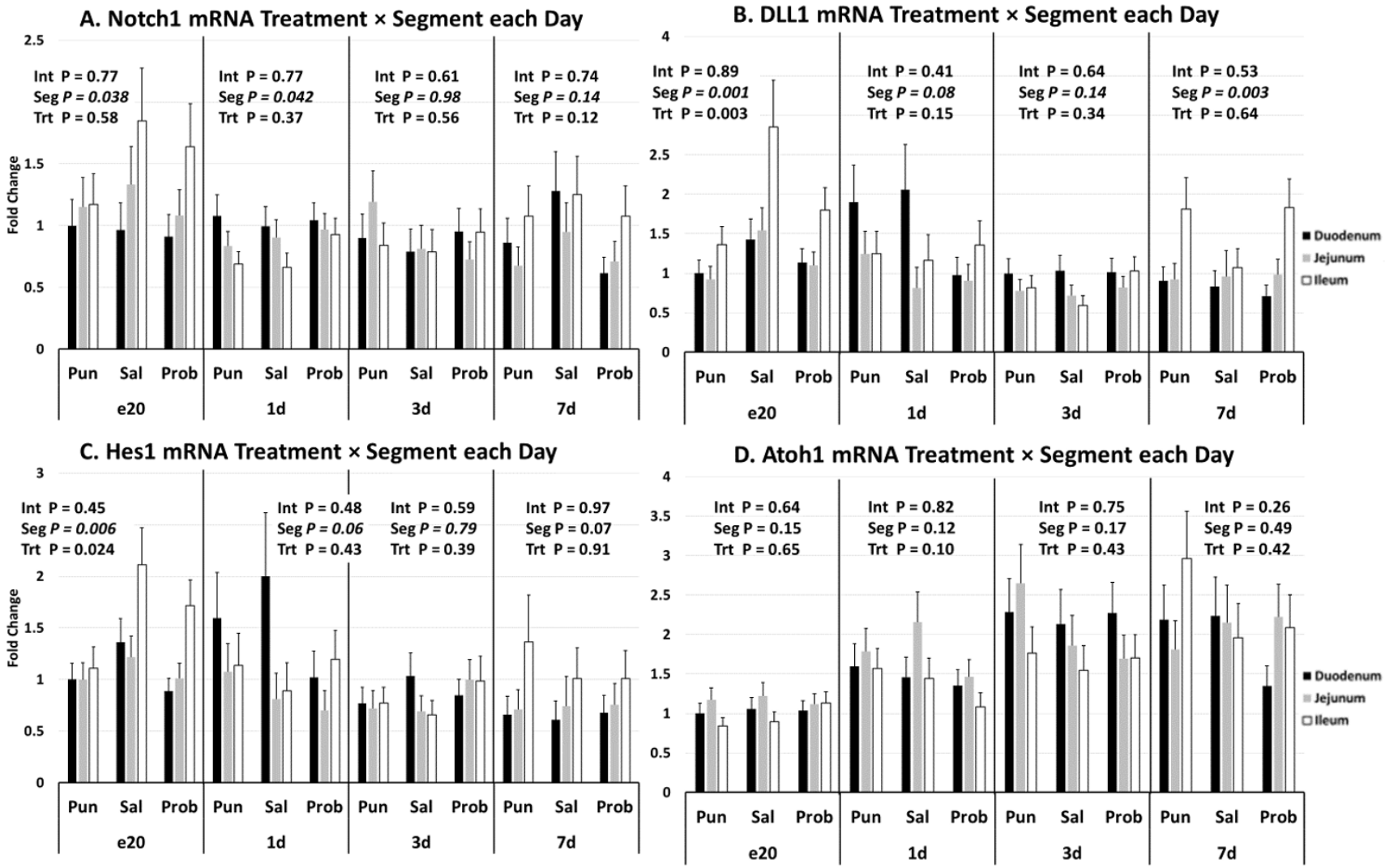
A. Notch1 mRNA Treatment × Segment each Day
Int P = 0.77
Seg P = 0.038
Trt P = 0.58
Int P = 0.77
Seg P = 0.042
Trt P = 0.37
Int P = 0.61
Seg P = 0.98
Trt P = 0.56
Int P = 0.74
Seg P = 0.14
Trt P = 0.12
B. DLL1 mRNA Treatment × Segment each Day
Int P = 0.89
Seg P = 0.001
Trt P = 0.003
Int P = 0.41
Seg P = 0.08
Trt P = 0.15
Int P = 0.64
Seg P = 0.14
Trt P = 0.34
Int P = 0.53
Seg P = 0.003
Trt P = 0.64
C. Hes1 mRNA Treatment × Segment each Day
Int P = 0.45
Seg P = 0.006
Trt P = 0.024
Int P = 0.48
Seg P = 0.06
Trt P = 0.43
Int P = 0.59
Seg P = 0.79
Trt P = 0.39
Int P = 0.97
Seg P = 0.07
Trt P = 0.91
D. Atoh1 mRNA Treatment × Segment each Day
Int P = 0.64
Seg P = 0.15
Trt P = 0.65
Int P = 0.82
Seg P = 0.12
Trt P = 0.10
Int P = 0.75
Seg P = 0.17
Trt P = 0.43
Int P = 0.26
Seg P = 0.49
Trt P = 0.42
Fold Change
Pun Sal Prob
e20
1d
3d
7d
Duodenum
Jejunum
Ileum

Figure 5-6.

Chapter 6 Discussion and Conclusion

Defining the Balance-Point Model

In the first chapter, I introduced the Balance-Point model of intestinal homeostasis as a way to evaluate the intestinal responses to disturbance events. The following principles define the Balance-Point Model.

- Homeostasis: dynamic balance between nutrient absorption and defensive barrier functions resulting in a healthy intestine sending sufficient nutrients to the body
- Allostasis: a new balance-point changed from homeostasis
- All disturbances result in a 2-phase transition in functioning as the intestine is not static
    - Disturbances cause disruption responses which aim to contain the causative agent and may cause damage in the process
    - Adaptation phase follows disruption responses to preserve critical intestinal functioning for survival
- Adaptations culminate in a changed balance (Allostasis) that includes compensatory adaptations
- Allostasis is transitory and eventually homeostasis returns once compensatory adaptations fade-away
- The characteristics of the transition are influenced by the type of disturbance
    - Inherent disturbances are essential for the proper development of the intestine
    - Novel disturbances: Any disturbance event that is not integrated into the developmental process of the intestine
        - Novel disturbances can be positive or negative

Disturbance events disrupt intestinal homeostasis and can be novel or inherent. During homeostasis the intestine optimally balances nutrient absorption with defensive barrier functions, acting synergistically with the microbiome. Disturbances disrupt intestinal homeostasis by forcing a shift from the balance-point that is homeostasis to respond to the disturbance and then to adapt to the effects that the disturbance and the response caused on the intestine (Fig. 6-1).

In response to disruptions to homeostasis the intestine changes to preserve overall functionality; but changing the balance-point results in inefficiencies. Most adaptation mechanisms are compensatory to overcome the lost production during the response period. Compensatory responses are reactions that cause the intestine to consume more nutrients than when in homoeostasis. The intestine strives to reach homeostasis so when the disturbance has been overcome the compensatory adaptations are toned down and a new balance of absorption versus defense is reached. The new balance is not as efficient as homeostasis which achieves optimal functioning at the same time as minimizing associated costs (Woods and Wilson, 2013); instead, this allostatic state includes the additional cost of the compensatory adaptations despite the disturbance being over (Ramsay and Woods, 2014). It is important to note that changes in the intestine are reflected in the whole body and have impacts on the management and productivity of the individual. Eventually the compensatory adaptations disappear as the intestine strives towards homeostasis. In short lived broiler chickens, the intestine does not always have time to return to homeostasis before processing, though the potential is there.

Disturbance events occur frequently throughout life and cause a variety of responses ranging from a minor loss of function to death of the individual. When events

occur frequently enough in the life history of a species a characteristic set of responses and adaptations occur. The responses become optimized to the point that these **inherent disturbances** appear to be important developmental stages of the intestine with no apparent long-term consequences or inefficiencies in the allostatic state. The best example of such a disturbance is the peri-hatch intestinal maturation process described in Chapters 4 and 5.

In contrast, **novel disturbances** highlight the fragility of the homeostatic state balance-point with disordered responses, usually losing barrier integrity and accruing tissue destruction. The response to novel disturbances typically perpetuates the initial harm caused by the disturbance itself. Additionally, the compensatory mechanisms cause additional costs that have long term consequences and are included in the allostatic balance-point. In this instance, "novel" refers to the individual's experience with the disturbance event, they are naive to this disturbance. Novel disturbances are common throughout the course of life but they have not evolved with the species to the point that they are crucial for its development like inherent disturbances. Novel disturbances were investigated in Chapters 2, 3, and 5.

Novel disturbances fall into two broad categories based on the degree of harm afflicted upon the intestine. **Negative disturbances** themselves result in loss of homeostasis due to damage by a causative agent or an aggressive activation of the immune system. Classic negative disturbances are diseases or toxicities where the disturbance is the introduction of the etiological agent into the intestine resulting in cell or tissue damage. In response, the immune system is activated to clear out the cause of disruption and to contain the effects to the local area. Activation of the immune system

siphons nutrients away from the bloodstream preventing them from being shared with the rest of the body (Klasing, 2007). Additionally, the immune response itself damages the intestine through incidental cellular destruction. Once the disturbing agent has been removed the production of replacement cells is overcharged, draining more nutrients from what would otherwise be sent to the rest of the body. To compensate for the loss of absorptive surface area the undamaged regions typically increase their absorptive capabilities, though this is not sufficient to fully overcome the lost absorption from the damaged region (Fernando and McCraw, 1973). Eventually, the absorptive capacity stabilizes across the entire intestine as it reaches an allostatic state.

The other category of novel disturbances is **Positive disturbances**. Compared to negative disturbances the disturbance is much milder but it still causes a shift to the allostatic state as there is a change from homeostasis. In positive disturbances the disturbance itself does not cause harm to the intestine but instead the disruption response by the intestine causes the change. A good example of this is the addition of a dietary feed additive. The chicken may show a slight decrease in feed intake or mild diarrhea as it adjusts to a new diet but often times there is no apparent response to a diet change, especially if the diet is gradually introduced. However, at a cellular level the feed additive, is disrupting homeostasis. One common result of feed additives are increases in absorptive surface area resulting from increased crypt depth and villus height. In order to accomplish this, cell proliferation would need to increase, increasing the nutrient needs of the intestine and additional structural proteins would need to be produced to support the lengthened villi. The small physiological changes that enable the villi growth push the intestine into an allostatic state that is nearly identical to the previous homeostatic

balance-point. Positive disturbances are understudied compared to negative disturbances so more research is necessary to elucidate the mechanisms involved. Inherent disturbances are neither positive nor negative in their current iteration but may have started out as either while still novel. Having defined the Balance-point Model the remainder of the chapter will be spent applying this model to the research chapters of this dissertation.

Investigating the balance point model with novel and expected disturbances

Each research chapter investigated a different disturbance event in broiler chickens. The first research chapter (Chapter 2) examined the changes in intestinal cell populations following a negative novel disturbance: Runting Stunting Syndrome (RSS) from four different incidents of infection. The second research chapter (Chapter 3) characterized the disruption using intestinal gene expression and morphological measurements following negative novel disturbance by *Eimeria acervulina*. Chapter 4 then profiled the response of proliferative cells to the inherent disturbance- the peri-hatch intestinal maturation process utilizing intestinal gene expression at a tissue and cellular level. The final research chapter (Chapter 5) assessed the effect of adding a positive novel disturbance, providing probiotics via in ovo feeding, during the peri-hatch intestinal maturation process through intestinal gene expression. Each research chapter will now be reframed by applying the Balance-Point Model and describing the transition phases.

In Chapter 2, a novel negative disturbance RSS was studied using two groups of naturally-infected (RSS-clinical-GA, RSS-clinical-BR) and two groups of experimentally infected (RSS-litter, RSS-astrovirus) chicks. The causative agent of RSS is unclear. Previous studies have induced clinical RSS by inoculating chicks with intestinal

homogenate, or by placing chicks on dirty litter. Other studies have tested infecting chicks with specific viruses, such as was done in the RSS-astrovirus group. All four groups showed clinical signs of infection and their intestines presented characteristic lesions: cystic crypts and signs of inflammation. The clinical signs are the response to the disturbance, the immune system activates to clear out the causative agent. Further, cystic crypts form as the epithelial cells degenerate to seal off the infected crypts. In the RSS-clinical-GA and RSS-litter groups there was a loss of Olfm4 mRNA in the crypt which might be an additional disruption of the Notch signaling pathway. It is unclear why only those two groups showed a loss of Olfm4 mRNA in crypt cells. Is it an effect of the causative agent or a consequence of the response mounted to overcome the infection? Beyond responding to the infection, the intestine adapts to the loss of crypt productivity as cystic crypts form by increasing crypt depth to ensure sufficient replacement cell production. There may be other compensatory mechanisms occurring but the study methodology was limited due to the nature of the samples utilized (archival samples of formalin fixed paraffin embedded intestinal tissue from a diagnostic laboratory and samples from previous research). Future studies evaluating changes in Notch signaling genes during RSS may pinpoint the cause of Olfm4 shutdown as well as clarify if the absence of Olfm4 is responsible for the continuation of the stunted appearance.

Chapter 3 investigated the disturbance event of a single challenge of *Eimeria acervulina*, a novel negative disturbance in broiler chickens. A mild coccidiosis infection was achieved as evidenced by slowed body weight gain, feed intake depression, and decreased plasma carotenoids compared to the non-infected chickens. In response to the *Eimeria* infection, mRNA for defense genes (LEAP2, AvBDs and Muc2) decreased

during 5- and 7-days post-infection, the peak of the infection. Using in situ hybridization, Muc2 mRNA was shown to be decreased in regions where the *Eimeria acervulina* was shown to be present. *Eimeria* invades epithelial cells and causes tissue destruction as the parasite lyses infected cells to perpetuate their lifecycle. To compensate for the destruction occurring along the villi, crypt proliferation increases, resulting in increased crypt depth and increased expression of the marker of proliferation Ki67 gene. Following the life cycle of the parasite, villus height increases, is accompanied by increased gene expression of Col3a1 and Notch 1 to ensure the intestine recovers and reaches an allostatic state.

The major difference between the two negative novel disturbances in Chapters 2 and 3 is the allostatic state reached. The chicks infected with RSS did not seem to have effectively adapted to their intestinal disturbance as they continue to remain stunted following clearance of the likely causative viral agents; especially compared to the *Eimeria* challenged chickens. Following the completion of the parasite life-cycle, the intestine entered a state of compensatory intestinal hyperplasia, which was supported by increased gene expression of supportive signals and in turn triggered compensatory weight gain. The stunting presented by the RSS chicks may be due to the loss of Olfm4 expression in the crypt, though this was not present in all groups despite their continuation of clinical growth depression. As detailed previously and in Chapter 2, the mechanism of disruption is still unclear but it is clear that there is an inability of the intestine to move into an effective allostatic balance state where intestinal functioning is sufficient to meet the base-line maintenance needs of the individual but not enough to

escape their stunted state. It is also possible that the persistent stunting could be due to long-term issues not related to the intestine.

One piece that is lacking in chapters 2 and 3 is identifying the return to homeostasis. This is challenging in broiler chickens due to their young processing age; though most research studies investigating the responses to RSS or *Eimeria sp*. infection have not tracked chickens to processing age and none to my knowledge have maintained chickens beyond processing age (Smyth, 2017; Soutter et al., 2020). Broilers vaccinated against *Eimeria sp*. with a live vaccine have been reported to occasionally improve their feed efficiency compared to medicated broilers (Williams, 2002), which may suggest a return to homeostasis. Future challenge studies may be able to show the return to homeostasis if they tracked infected chickens to processing age or beyond, or utilized broiler breeders instead.

Chapter 4 profiles the proliferative cells in the small intestine during the inherent disturbance, the peri-hatch intestinal maturation process. The small intestine develops from short, round pre-villi structures with rudimentary crypts during late embryogenesis (e17) to long straight villi that protrude out into the lumen of the intestine and deep crypts by the end of the first week post-hatch. The mRNA expression of the stem cell marker Olfm4 increases with age while the other stem cell marker Lgr5 mRNA expression decreases with age. Additionally, the expression pattern of Lgr5 changes over time from being expressed throughout the intestine to being restricted to the crypt. Similarly, the expression pattern of marker of proliferation gene Ki67 changes from being expressed across the entirety of the intestine to being confined to the crypt and up the center of the villi.

Unlike the previous chapters, which investigated novel disturbances, the inherent disturbance profiled in chapter 4 does not undergo clear response and adaptation phases but instead appears to transition from one homeostatic balance-point to another. In the case of the peri-hatch intestinal maturation process, the first homeostatic balance-point is amongst the embryonic epithelial cells capable of proliferation, but not specialized for the functional needs of the intestine. The second balance-point, occurring at or near the end of the first week, is epithelial cells that are capable of proliferation restricted to the crypt and separate epithelial cells responsible for the functional needs of the intestine along the villi. The transition between the two balance-points was not perceptible in the current study as mechanistic gene expression was not being investigated. In hindsight, conducting additional investigations into Notch or Wnt signaling would likely shed light on the mechanisms underlying the transition between balance-points.

The final research chapter (Chapter 5), adds a positive novel disturbance to the inherent peri-hatch intestinal maturation process by the in ovo administration of probiotics in the late stages of embryogenesis (e17.5). The effect of in ovo feeding was seen on e20 where the probiotic fed group had increased expression of PepT1 mRNA in the ileum compared to the duodenum and ileum of the non-injected (punch) group as well as Muc2 mRNA in the ileum compared to the duodenum of the punch group. At the same time the Saline fed group had numerically increased expression of Muc2 and PepT1 mRNA in all intestinal segments, though lesser than the ileum of the probiotic fed group. Also, on e20, the saline fed group had increased Notch signaling genes (Hes1 and DLL1). The probiotic fed and saline fed groups had different responses, though both had increased expression of Muc2 and PepT1 mRNA, which is associated with mature

intestines. The probiotic fed group responses were localized to the ileum where the probiotic species most likely colonized. The saline fed group likely promoted the production of enterocytes across the small intestine through some as of yet unclear mechanism. The probiotic fed group did not stimulate Notch signaling genes to the same extent as the saline, implying a different mechanism of stimulation is occurring within the ileum.

Like the previous chapter there is no clear adaptation occurring. The effects of the in ovo feeding were a short-term stimulation, mainly confined to e20. The increased gene expression in the in ovo fed groups are likely a transitory compensatory mechanism in between the two balanced states occurring during the intestinal maturation process. Compared to the damage caused by negative disturbances it is likely that this positive disturbance does not override the organized transition that is the inherent peri-hatch intestinal maturation process.

Limitations and Opportunities of the proposed model

This dissertation is a first attempt to propose the Balance-Point Model for understanding intestinal homeostasis. Further research is needed to elucidate and expand on the principles of the model outlined earlier in this chapter and the remainder of this chapter will be spent pointing out limitations and opportunities for this model.

The major limitation of this dissertation and model presently is that all the research methodologies were mRNA based rather than evaluating responses at a phenotypic level such as protein quantification and activity or bird performance and composition. The decision to utilize mRNA level techniques was rooted in the goal of

wide application for this model as poultry science mainly utilizes mRNA level techniques due to the lack of antibodies for specific proteins and cost of proteomics work.

The proposed model assumes that the molecular responses observed in these studies correspond to and predict phenotypic responses of the intestine and the whole bird. More research is needed to define the correlation between mRNA abundance and protein expression as well as to clarify the relationship between quantitative PCR and in situ hybridization expression patterns. Furthermore, research needs to connect the solitary mRNA abundances investigated in this dissertation with broader molecular pathways, metabolomics and microbiomes, which must influence gastrointestinal physiology but have yet to be characterized.

The goal for this model is to be applicable beyond poultry scientists and to gastrointestinal physiologists working with other species. First the model would need to be tested on additional species as the current work focuses solely on young broiler chickens. The foundational principles are not likely to change much though as they were developed from applying the conclusions from many mammalian (rodent and human) studies. More likely, terminology or specific definitions may change from additional research. For example, the use of homeostasis may need to be altered as the original definition of homeostasis in physiology is limited to responses that must be maintained within a set range of parameters such as blood pH or glucose levels.

This model is a first step towards holistically modeling the responses of the intestine to disturbance events. From a poultry science perspective such a model could be applied to defining the nutritional needs of poultry during different stages of life or over the course of an infection. Beyond poultry science this model can be a teaching tool for

training young scientists about gastrointestinal physiology or for researchers to establish a standard set of criteria for evaluating enteric diseases or novel feed additives.

References

Cloft, S.E., S.K. Kinstler, K. Reno, H.S. Sellers, M. Franca, R. Ecco, M.D. Lee, J.J. Maurer, and E.A. Wong. 2022. Runting stunting syndrome in broiler chickens is associated with altered intestinal stem cell expression of Olfm4. Published in Avian Diseases. 66:1-10.

Fernando, M. A., and B.M. McCraw. 1973. Mucosal morphology and cellular renewal in the intestine of chickens following a single infection of Eimeria acervulina. J. Parasitol. 59:493-501.

Klasing, K. 2007. Nutrition and the Immune System. Br. Poult. Sci. 48:525-537.

Ramsay, D.S. and S.C. Woods. 2014. Clarifying the roles of homeostasis and allostasis in physiological regulation. Psychol. Rev. 121:225-247.

Smyth, V. J. 2017. A review of the strain diversity and pathogenesis of chicken astrovirus. Viruses. 9:29.

Soutter, F., D. Werling, F.M. Tomley, and D.P. Blake. 2020. Poultry coccidiosis: design and interpretation of vaccine studies. Front. Vet. Sci. 7:101.

Williams, R.B. 2002. Anticoccidial vaccines for broiler chickens: pathways to success. Avian Pathol. 31:317-353.

Woods H. and J. Wilson. 2013. An information hypothesis for the evolution of homeostasis. Trends Ecol. Evol. 28:283-289.

Figure Captions

Figure 6-1. A graphical representation of the Balance-Point Model. I. Homeostasis- balanced nutrient absorption and defensive barrier functioning. II. Disruption Response- disturbance event disrupts defensive barrier functioning and nutrient absorption, the activation of the immune system to contain the disturbance event further disturbs the balance. III. Adaptation Phase- compensatory mechanisms initiate as the intestine begins to recover causing nutrient absorption and defensive barrier functions to rebound. IV. Allostasis- a transitory stable balance between nutrient absorption and defensive barrier functioning that includes the new costs of compensatory adaptations. Eventually, the intestine returns to homeostasis once the compensatory adaptations fall off. Figure 6-1 was created by S. Cloft

FIGURES

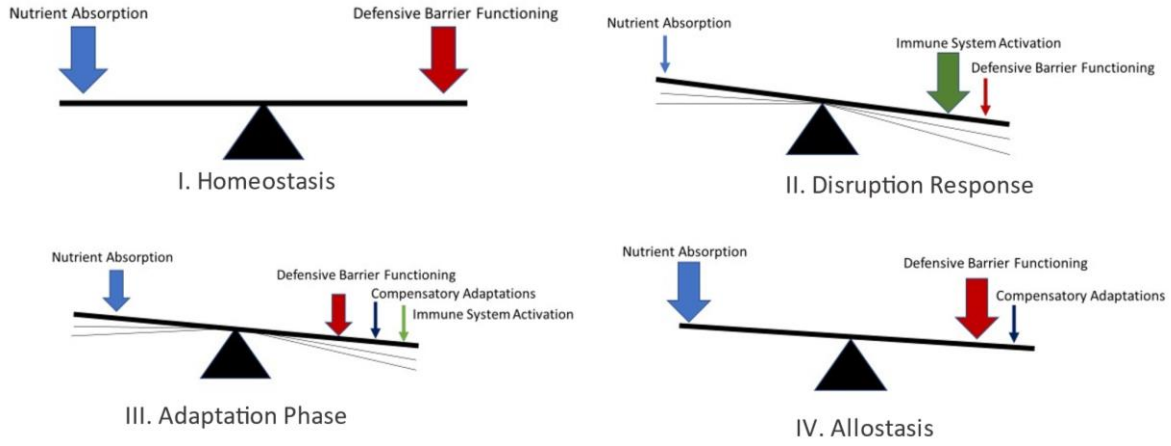

Figure 6-1.